IMPROVING THE MECHANICAL AND PHYSICAL PROPERTIES OF THERMOPLASTIC BLENDS BY PARTIAL REPLACEMENT OF INDUSTRIAL WASTE AND INCLUSIONS OF CARBON NANOMATERIALS

SITI NURASHIKIN BINTI MOHAMED YAZID

UNIVERSITI TEKNIKAL MALAYSIA MELAKA

2024

IMROVING THE MECHANICAL AND PHYSICAL PROPERTIES OF THERMOPLASTIC BLENDS BY PARTIAL REPLACEMENT OF INDUSTRIAL WASTE AND INCLUSIONS OF CARBON NANOMATERIALS

This report is submitted in accordance with requirement of the University Teknikal Malaysia Melaka (UTeM) for Bachelor Degree of Manufacturing Engineering (Hons.)

by

SITI NURASHIKIN BINTI MOHAMED YAZID

FACULTY OF INDUSTRIAL AND MANUFACTURING
TECHNOLOGY AND ENGINEERING
2024

DECLARATION

I hereby, declared this report entitled "Improving the Mechanical and Physical Properties of Thermoplastic Blends by Partial Replacement of Industrial Waste and Inclusions of Carbon Nanomaterials" is the results of my own research except as cited in reference.

Signature :

Author's Name : SITI NURASHIKIN BINTI MOHAMED YAZID

Date : 28 JUNE 2024

APPROVAL

This report is submitted to the Faculty of Industrial and Manufacturing Engineering and Engineering of Universiti Teknikal Malaysia Melaka as a partial fulfilment of the requirements for the degree of Bachelor of Manufacturing Engineering (Hons.). The members of the supervisory committee are as follow:

ASSOCIATE PROFESSOR TS. DR. JEEFFERIE BIN ABD. RAZAK
CEng IMechE ; P.Tech MBOT
Faculty of Manufacturing Engineering
Universiti Teknikal Malaysia Melaka (UTeM)
Hang Tuah Jaya,
76100 Durian Tunggal,
Melaka, Malaysia.

____

(Principal Supervisor) – Signature & Stamp

ABSTRAK

Sebagai tindak balas kepada isu pencemaran plastik yang semakin meningkat dan permintaan yang meningkat untuk produk mesra alam dan terbiodegradasi, kajian ini meneroka pembangunan bahan termaju yang mampan. Penyelidikan menggabungkan polipropilena (r-PP) kitar semula dengan polietilena berketumpatan rendah (LDPE) melalui kaedah pengadunan leburan, mengoptimumkan keadaan seperti suhu, kelajuan pemutar dan nisbah adunan menggunakan pendekatan faktorial penuh dua peringkat Reka Bentuk Eksperimen (DOE). Sebanyak 2^3 reka bentuk eksperimen digunakan untuk meneroka tiga pembolehubah dengan tiga replikasi di titik tengah. Keadaan optimum yang dikenal pasti ialah suhu 160°C, kelajuan pemutar 445.170 rpm, dan nisbah adunan 70 wt.% r-PP/LDPE. Keadaan ini telah meningkatkan sifat mekanikal dengan ketara, mencapai kekuatan tegangan 12.777 MPa, kekuatan lentur 16.504 MPa, dan kekuatan hentaman 0.305 J. Ketumpatan adunan juga lebih tinggi dengan lebih r-PP (1.17975 g/cm^3) berbanding kepada LDPE (1.0715 g/cm^3). Berikutan itu, adunan r-PP/LDPE digabungkan dengan graphene nanoplatelets (GNPs) pada muatan yang berbeza-beza (0, 1, 3, 5, dan 7 wt.%) untuk meningkatkan lagi sifat bahan tersebut. Sifat mekanikal telah diuji, dan morfologi fasa dianalisis menggunakan mikroskop elektron pengimbasan pelepasan medan (FESEM). Kajian mendapati bahawa mengoptimumkan parameter pencampuran dan nisbah campuran meningkatkan morfologi fasa kecil dan meningkatkan kebolehcampuran separa antara polimer r-PP dan LDPE. Ini membawa kepada peningkatan kekuatan tegangan, lenturan dan hentaman. Penambahan nanopengisi menghasilkan peningkatan sebanyak 16.95% dalam kekuatan tegangan, 40.82% dalam kekuatan lentur dan 22.62% dalam kekuatan hentaman, menunjukkan bahawa GNPs secara berkesan meningkatkan kedua-dua sifat mekanikal dan fizikal bagi r-PP/LDPE-GNPs nanokomposit.

ABSTRACT

In response to the escalating issue of plastic pollution and the heightened demand for environmentally friendly and biodegradable products, this study explores the development of a sustainable advanced material. The research blends recycled polypropylene (r-PP) with low-density polyethylene (LDPE) through the melt blending method, optimizing conditions such as temperature, rotor speed, and blend ratio using a Design of Experiment (DOE) two-level full factorial approach. A total of 2^3 experimental designs were used to explore three variables with three replications at the center point. The optimal conditions identified were a temperature of 160°C, a rotor speed of 445.170 rpm, and a 70 wt.% r-PP/LDPE blend ratio. These conditions significantly improved mechanical properties, achieving a tensile strength of 12.777 MPa, a flexural strength of 16.504 MPa, and an impact strength of 0.305 J. The density of the blend was also higher with more r-PP (1.17975 g/cm^3) compared to LDPE (1.0715 g/cm^3). Following this, r-PP/LDPE blends were combined with graphene nanoplatelets (GNPs) at varying loadings (0, 1, 3, 5, and 7 wt.%) to further enhance the material's properties. Mechanical properties were tested, and phase morphology was analyzed using a field emission scanning electron microscope (FESEM). The study found that optimizing mixing parameters and blend ratios improved the morphology of the minor phase and increased the partial miscibility between r-PP and LDPE polymers. This led to enhanced tensile, flexural, and impact strength. Adding GNPs nanofillers resulted in increases of 16.95% in tensile strength, 40.82% in flexural strength, and 22.62% in impact strength, demonstrating that GNPs effectively enhance both the mechanical and physical properties of the r-PP/LDPE-GNPs nanocomposite.

DEDICATION

Only

My beloved father, Mohamed Yazid bin Mohamed Saod

My appreciated mother, Mariana binti Mohd Shatar

My personal banker, Siti Nurfarahin binti Mohamed Yazid

My siblings, Debab, Kacang, Papai, Bambam, Uteh, Tibi, Gendut

For giving me moral support, cooperation, encouragement, and understandings

Specially thanks to Dr. Jeefferie bin Abd Razak and Nur Asyilah binti Awang Ngah for their encouragement, guidance and assists to finish this project.

ACKNOWLEDGEMENT

In the name of ALLAH, the most gracious, the most merciful, with the highest praise to Allah that I manage to complete this final year project successfully without difficulty. I would to express my sincere gratitude to Dr. Jeefferie bin Abd Razak for giving me a guidance and support throughout the duration of this project with valuable insights that have been instrumental in shaping this report and making it a success. I would also like to greatest thank to Nur Asyilah binti Awang Ngah for provided support and assists me with invaluable contributions. The support and encouragement throughout this project have been greatly appreciated. Also, thanks to all people who helped me in any aspect during this project. My family, and colleagues that have been a great source of motivation and support. This report would not have been possible without all their support and their guidance. I am truly grateful for their contributions.

TABLE OF CONTENTS

LIST OF TABLES

LIST OF FIGURES

LIST OF ABBREVIATIONS

UV	-	Ultraviolet
PR	-	Partial replacement
PW	-	Plastic waste
EPS	-	Expanded polystyrene
INP	-	Iranian Nano-materials Pioneers
CE	-	Circular Economy
PP	-	Polypropylene
r-PP	-	Recycle of Polypropylene
LDPE	-	Linear Density Polyethylene
HDPE	-	High Density Polyethylene
LLDPE	-	Low Linear Density Polyethylene
PE	-	Polyethylene
GNPs	-	Graphene Nanoplatelets
rHDPE	-	Recycle high density polyethylene
RSM.	-	Response surface methodology
DoE	-	Design of Experiment
RSM	-	Response Surface Morphology
FE-SEM	-	Field Emission Scanning Electron Microscope

LIST OF SYMBOLS

nm	-	Nanometre
g/cm^3	-	Gram per cubic centimetre
µm	-	Micron
S/m	-	Siemens per meter
wt.%	-	Weight percentage
mm	-	Millimetre
%	-	Percentage
°C	-	Celsius
g	-	Gram
g/cm^3	-	Gram per cubic centimetre
µm	-	Micron
S/m	-	Siemens per meter

CHAPTER 1

INTRODUCTION

1.1 Background of the Study

The circular economy (CE) is a concept aimed at minimizing environmental damage by implementing a closed-loop system throughout the entire lifecycle of industrial products. This strategy is not the same as the linear economy model, which produces goods, uses them, and then discards them as waste. On the other hand, the circular economy emphasizes resource efficiently and sustainable behaviours through an ongoing cycle of production, consumption, and restoration. To complete product lifecycle loops, turn garbage into useful goods, and achieve environmental resilience throughout economic expansion, CE transitions need eco-innovations.

Eco-innovation involves creating or implementing new products with a reduction in environmental risk, pollution, and resource effects over time compared to a linear economy. Commonly, manufacturing companies have begun applying the circular economy. For example, Nokia has a program called the e-waste reduction program, where consumers return their old mobile phones, chargers, and accessories of any brand to the company for safe disposal. Nokia then breaks down these old items and recycles their components into new materials or new products. Despite the need to buy new raw materials from supply, they are recycled and used, which leads to cost savings. This scenario not only applies to this company but commonly happened to any manufacturing sector which experienced losses due to rejection and product defects during the manufacturing process. The defected or rejected product will be scrapped and repurpose into new product innovation, which in the end, supporting the concept of CE. This situation are mainly happened in the manufacturing factory which dealing with plastic based production.

Stressing the value of plastic recycling highlights how important it is to move toward a circular economy, avoiding the use of fossil fuels and closing the circle on plastic consumption. However, after plastics have been recycled, they usually lose the properties. Among commercial type of polymers is polypropylene (PP). That is commonly known and widely used due to its affordability and ease of molding. PP is one of the most extensively used polyolefins in a range of applications owing to its multiple benefits, such as high physical and mechanical qualities, simplicity of processing, cheap cost, and recyclability. Moreover, substantial weight reduction may be accomplished when PP is utilized into goods because of its low density. PP also exhibits outstanding thermal and chemical resistance and a good moisture barrier. The industrial scrapped of PP was known as r-PP, which was commonly repurpose by the industry to fabricate the second-grade product with acceptable and reasonable value.

Other types of polymer plastic include polyethylene (PE), which is the second most common type of plastic utilized after PP. Polyethylene comes in a variety of forms, including low density (LDPE), medium density (MDPE), high density (HDPE), and linear low density (LLDPE). LDPE is characterized by a highly branched polymer structure, which gives it a lower density and strength compared to other types of polyethylene. Industries favour LDPE for its excellent flexibility, transparency, and resistance to impact and moisture. LDPE's lower tensile strength compared to HDPE is balanced by its high ductility and ease of processing, making it ideal for applications like plastic bags, film wrap, and containers. Its chemical resistance makes LDPE suitable for packaging and storing a variety of products. The ability of LDPE to be processed by methods such as extrusion and blow molding provides versatility in manufacturing. Its affordability and recyclability make LDPE a valuable material for cost-effective and sustainable production. The widespread use of LDPE in packaging, agriculture, and building can be attributed to its unique properties, flexibility in processing, and cost-effectiveness.

Polymer in single phase always suffered with the performance limitation. It was commonly modified through the blending with others phase of polymer and also through composite making. A polymer blend is a material that may be used to create a thermoplastic blend in a cost-effective way by properly blending two or more polymers. The aim is to develop a material having special or stronger mechanical and physical characteristics compared to individual polymers. In addition, the decrease in costs caused polymers to mix as the combination allowed polymer-based product manufacturers to produce materials that satisfied performance requirements at a cheaper price. Additionally, this mixture or blend can promote sustainability since its polymers can be recycled and used to make more variation of polymer characteristics and attributes. Numerous research works examine polymer blends, especially those including polypropylene (PP) and polyethylene (PE).

The main factors that decide whether PP can be compounded with different PEs are those concerning the miscibility or immiscibility between these two components. PP and LDPE are generally seen as immiscible, with these latter materials showing clear phase separation during cooling/crystallization throughout the composition range. The miscibility of PP/LDPE depends upon processing conditions, composition, and high temperatures. Whenever PP cooling a miscible mix with LDPE could lead to phase separation, resulting in an immiscible blend. Understanding these interrelationships is critical for building hybrid blends that are suitable for varied applications and improved polymer blend materials characteristics.

However, to further enhance the blend properties, the filler is generally added. Interestingly, utilizing the carbon based nanofiller such as the graphene nanoplatelets (GNPs) are hypothetically able the reinforce the polymer blend. GNPs are graphite nanocrystals in the form of platelets composed of many layers of graphene joined by the Van der Waal's forces. Recently, GNPs nanofiller have attracted substantial attention because of their multiple benefits including superior thermal, mechanical, and electrical characteristics, and inexpensive cost.

This study was conducted to see the improvement in the mechanical and physical properties of thermoplastic r-PP/LDPE blends with the inclusion of graphene nano-platelets in response to circular economics. The effects of GNPs nanofiller loadings to the thermoplastic blend r-PP/LDPE was analysed. In addition, other important support testing of physical and mechanical are also conducted to understand the roles of experimental variables in the obtained findings.

The fracture morphological characteristics of r-PP/LDPE-GNPs nanocomposites blends were examined through the Scanning Electron Microscopy (SEM), allowing for the observation of fracture morphologies. To fulfil the research objectives, a Design of Experiment (DOE) approach was employed, specifically utilizing a full factorial strategy for optimizing main respond of the tensile strength of the r-PP/LDPE thermoplastic blend. The optimization focused on key mechanical and physical properties as major responses. Finally, this work aims to promote r-PP/LDPE-GNPs as a possible advanced material, providing a greener and more efficient option for the future generation and contributing to the circular economy principles. Therefore, the r-PP/LDPE thermoplastic blends combined with GNPs nanofillers have significant potentials in a range of applications spanning electronics, aerospace, car, military to green technology.

1.2 Problem Statement

Industrial waste is becoming an important environmental and social problem. Inefficient management and disposal pollute soil, water, and air, harming ecosystems and public health. The release of toxic materials into the environment, which leads in pollution that damages both communities and natural areas. Exposure to these chemicals, especially via dirty air and water sources, poses major health consequences. Inefficient use of resources in industrial activities increases waste production. Improper enforcement of environmental standards and other regulations may induce incorrect garbage disposal by industries. A strong approach is required to solve this multifaceted challenge, involving investment, encouraging cleaner industrial practices, and strengthening rules.

Plastic waste has emerged as a major environmental concern due to the many generations of plastic produced by many companies to meet the needs of consumers. The increasing use of plastics in packaging and manufacturing, their durability and resistance to degradation have combined to create a lot of plastic waste. This presents serious environmental challenges that marine pollution, loss of wildlife and the persistence of plastic in landfills occur. This growing issue is worsened by the increasing use of single-use plastics and the need for flexible products. To address this issue, initiatives are taken to raise public awareness of the negative environmental impact of the use of plastics, develop a recycling program and support sound business practices with manufacturers recycling, using eco-friendly packaging, and using less plastic. The needs of a circular economy and environmentally friendly strategies are greater exposure to reducing single-use plastics that can reduce impact is highlighted by plastic waste.

Polypropylene (PP), a common type of plastic known for its durability and versatility, poses recycling challenges due to the complexity of the recycling processes involved. The difficulty arises because recycling PP often involves complex processes. It need high technology facilities to handle the recycling process to be effectively. Despite these challenges, there are ongoing efforts and advancements in technologies aimed at improving the recycling rates of polypropylene, promoting a more sustainable approach to managing this commonly used plastic. Recycled polypropylene (r-PP) can be blended with other polymers, and one commonly used combination is with low-density polyethylene (LDPE). This blending practice offers a way to enhance the properties and applications of recycled polypropylene.

The blending of recycled polypropylene (r-PP) with low-density polyethylene (LDPE) can encounter several challenges. One significant issue arises from the distinct chemical and physical properties of the two polymers, making it difficult to achieve a homogeneous and well-balanced blend. Ensuring proper compatibility during the blending process becomes crucial to avoid issues such as phase separation or insufficient mechanical properties in the final product. Additionally, variations in the sources and compositions of recycled materials can further complicate the blending process, affecting the overall consistency and quality of the r-PP/LDPE blend. Addressing these challenges requires careful formulation, process optimization, and quality control measures to attain a successful and economically viable blend for various applications.

Adding the graphene nanoplatelets to a thermoplastic blend of recycled polypropylene (r-PP) and low-density polyethylene (LDPE) are challenging. Because graphene nanoplatelets have a tendency to agglomerate, it is difficult to establish an equal dispersion of them inside the polymer matrix. As a result, achieving uniform distribution is crucial for utilizing graphene's advantageous qualities, such as its increased strength. The processing characteristics of the blend may be affected, requiring careful adjustments to maintain optimal processing conditions and prevent issues such as poor mold filling. Another challenge involves establishing strong interfacial adhesion between graphene nanoplatelets and the polymer matrix. Incompatibility at this interface can lead to reduced mechanical properties in the final product. Furthermore, the adding of graphene increases the overall cost of the blend, necessitating a careful balance between the enhanced properties and economic considerations. Quality control measures are essential to maintain consistent dispersion and distribution throughout the manufacturing process. Addressing these challenges requires a combination of meticulous formulation, process optimization, and potential modifications, such as using compatibilizers, to enhance the interaction between graphene nanoplatelets and the r-PP/LDPE blend.

1.3 Objective

The objectives refer to the study field that are:

i. To optimize the r-PP/LDPE thermoplastic blend formulation using extrusion process via two level full factorial DOE method.
ii. To evaluate the effect of graphene nanoplatelets (GNPs) loadings in enhancing the mechanical properties of r-PP/LDPE thermoplastic nanocomposites hybrid blends.
iii. To observe the fracture surface morphology of r-PP/LDPE-GNPs thermoplastic nano composites hybrid blends by using the Scanning Electron Microscope (SEM) observation.

1.4 Scope of Study

The following are the scope of this study:

i. The mechanical strength of r-PP/LDPE thermoplastic blends formulation that was produced using a single screw extrusion technique was systematically optimized by using a two-level full factorial design approach via Design of Experiment (DOE).
ii. Tensile strength was selected as a main response and is utilized to investigate the optimum mechanical properties depending on independent variables such as temperature, extrusion speed, and r-PP/LDPE ratio.
iii. Correlate the mechanical characteristics of r-PP/LDPE-GNPs for three different samples (control, best, and worst) depending to the effects of GNPs nanofiller loading at 0, 1, 3, 5 and 7 wt.%.
iv. Scanning Electron Microscope (SEM) is being used to examine the fracture surface morphology of r-PP/LDPE-GNPs thermoplastic nano composites hybrid blend.

1.5 Project significance

This study is significant because it addresses the environmental effect of plastic waste created by the manufacturing sector that uses the linear economy model. Plastic may be reused and changed into new goods using a circular economic method by combining with others polymer and reinforcing it with nanomaterials which then improves both mechanical and physical qualities of the resulting good. As a result, industrial plastic waste not only acts as a possible source of cash, but also as a great resource for developing solutions with specialized features that satisfy demands in a more sustainable way.

1.6 Thesis Organization

This thesis is divided into five sections: introduction, literature review, methodology, results and discussion, and conclusion. The background study, problem statement, goals, research scope, project importance, thesis arrangement, and research summary are all covered in Chapter ONE. Continuing with Chapter TWO, in which the research of thermoplastic blends of r-PP/LDPE, the mechanical and physical characteristics of thermoplastic blend r-PP/LDPE, and Graphene Nanoplatelets (GNPs) nanofiller is broadly discussed. In addition, information on the circular economy was provided in this part. The experimental approach is presented using a flow chart and a basic illustration in Chapter THREE. The approach encompasses the overarching study framework, the r-PP/LDPE technique, and all testing procedures and phases. For further discussion, the data acquired from all relevant trials will be provided in Chapter FOUR. Finally, in Chapter FIVE, the general conclusions of this investigation will be summarized.

CHAPTER 2

LITERATURE REVIEW

2.1 Thermoplastic Blends

A thermoplastic blend refers to the combination of thread polymers that can be heated and cooled over again without chemical reaction. The process involves melting and fusion of the polymers, known as melt blending technique. This method can offer specialized qualities, mechanical characteristics, processability, economic benefits and unique functionality features. Thermoplastic blends generally find application in automotive, packaging, construction, and consumer products (Morris, 2022). Polypropylene PP and low-density polythene (LDPE) are the most popular type of thermoplastics. The structure of thermoplastics is shown by long polymer chains made of monomer units that repeat, which can also be branched or linear as shown in the Figure 2.1. These chains can be assembled to form either an amorphous or semi- crystalline structure. Thermoplastics have weak intermolecular forces between polymer chains such as dipole-dipole interactions, hydrogen bonds, and van der Waals' forces (Ketema & Worku, 2020). The weak bonds make the thermoplastics soften when they are heated, giving the polymer chains some room to move around. When they condense and get cold again, the chains of polymer harden.

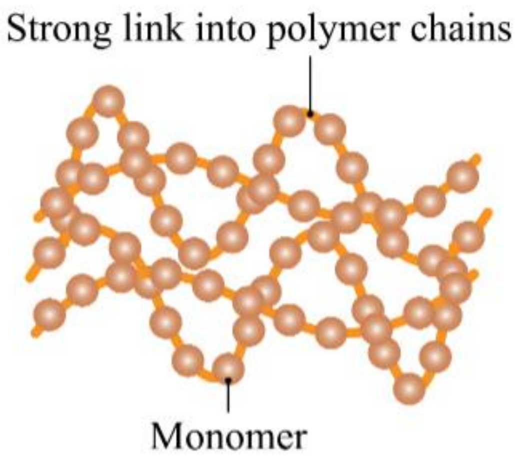

Figure 2.1: Thermoplastic Structure (Anandvijay Karuppiah,2016)

2.2 Polypropylene (PP)

Polypropylene (PP) is a versatile and flexible material made by polymerizing propylene monomers. With its numerous favourable properties, PP finds uses in many different industries. Its excellent chemical resistance lets it to withstand corrosive substances including acids, alkalis, and solvents (Maddah, H.A., 2016). The lightweight nature of PP is helpful for items requiring lower weight, and its ability to tolerate high temperatures makes it acceptable for application in high temperature scenarios. The straight-line arrangement of its components contributes to the material's hardness and strength, particularly in its pure state. Known for its strength and stiffness (QUAN & TAKAYAMA, 2022).

The structure of polypropylene includes joining propylene units in a polymerization process, generating long, straight-line chains. Propylene, a three-carbon alkene with the basic formula C_3H_6, acts as the essential building component. The repetitive pattern in each unit ($-CH_2-CH(CH_3)-$) leads in a long-chain structure shown in the Figure 2.2. This straight-line arrangement contributes to the material's strength and is responsible for its high chemical resistance, thermal resistance, and transparency under a light microscope a quality known to as its crystal nature.

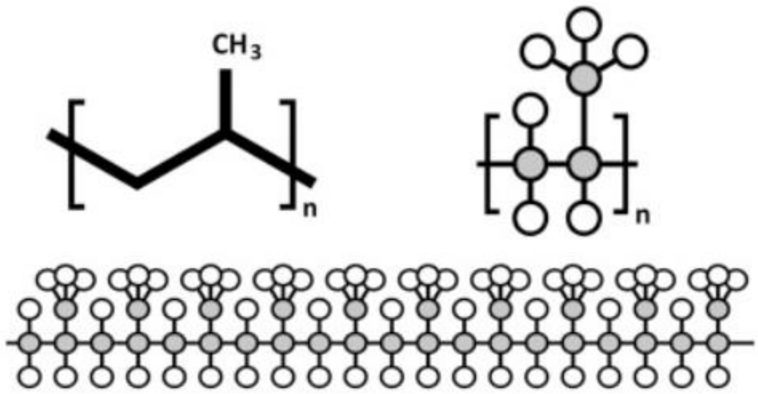

Figure 2.2: Structure of Polypropylene (Christopher Blair Crawford & Quinn, 2017)

2.2.1 Application of Polypropylene (PP)

The Table 2.2.1 summarizes the applications of PP based on the specific areas of focus in previous studies, showcasing the versatility of PP across various industries.

Table 2.2.1: Application of PP based on the specific areas of focus in previous studies.

Application	Reference
Packaging: Polypropylene (PP) is widely used by the packaging industry in the manufacture of bottles, containers and flexible packaging.	(Raheem, 2013)
Textile: In the textile industry, non-woven fabrics made of polypropylene are often used in items like carpet backing, disposable medical clothing, and geotextiles.	(Rani et al., 2023)
Automobile Parts: Dashboards, door panels, and trims are among the interior parts made of PP utilized in the vehicle industry.	(Kumar et al., 2023)
Packaging for Medical Devices: Polypropylene is used in the fabrication of medical equipment, including needles, vials, and packaging for drugs.	(Sastri, Vinny R & Sastri, Vinny R, 2022)
Home Products: PP may be found in many home products, including furniture, kitchenware, and plastic containers.	(Rani et al., 2023)
Construction Materials: Polypropylene is used in the building industry for fittings, pipelines, and insulation.	(Tulane et al., 2021)
Office and stationery supplies: Use in the production of binders, folders, and other stationery products.	(Xia et al., 2019)
Sheets and Films: PP films and sheets are used in numerous industries, including as stationery, food packaging, and agriculture (for greenhouse films and transparent sheets).	(Calhoun & Wagner, 2010)
Battery casings: PP has been used in the production of battery casings.	(Sastri, Vinny R & Sastri, Vinny R, 2022)
Disposables product: Polypropylene is often used to make disposable items like cups, plates, and flatware.	(Raheem, 2013)

2.2.2 Advantages of Polypropylene (PP)

Polypropylene (PP) is used a lot in different industries because it has many advantages. One big advantage is its great ability to resist chemicals, making it a top pick for situations where spreadable harmful stuff often strikes. PP products are not heavy, making them easy to carry and move because they lightweight material (Unterweger et al., 2014). Also, PP stands out for its high temperature resistance. This means it can keep its shape even when there is too much heat around. They provide many types for a range of shapes in several application domains. Stiff substance PP reinforces and enhances stress absorption. In making boxes, a special kind of plastic called PP helps to make the colours seen better and keep things safe. This is good for seeing what's inside while keeping it stored properly. In addition, its cost-effectiveness makes it suitable for a wide range of applications, from household appliances to industrial applications (Cossu et al., 2019). Lastly, its recyclability is consistent with sustainability goals, while its inert nature under medical conditions ensures safer device and packaging choices (Alsabri et al., 2022).

2.2.3 Limitation of Polypropylene (PP)

Even though polypropylene has some good points, it does have downsides too. One big problem is that it’s not very strong against UV light. This can cause wear and colour loss over time, especially outdoors where things get exposed to the sun's powerful rays all day long (Maddah, H.A., 2016). PP can be damaged by heat, which might affect its strength. To fix this problem, most people use a stabilizer because it helps make things better at high temperatures. PP is good at handling heat, but it may not be perfect for applications that require a lot of heat. Next, the sticky substance might not attach well to things without proper treatments, which can cause problems when joining with other materials. Therefore, applications that need better protection against fire are not suitable. Sometimes, polypropylene PP is see-through, which makes it hard to use in places where being seen is very important. The Table 2.2 are shown the summarizes of disadvantages and advantages of PP.

Table 2.2.3.1: Advantages and disadvantages of Polypropylene (Maddah, H.A., 2016)

Advantages of PP		Disadvantages of PP
Homo-polymer	Copolymer	Degraded by UV (Ultraviolet)
Process ability, Good	Process ability, High	Flammable, but retarded grades available
Impact resistance, Good	Impact resistance, High	Attacked by chlorinated solvents and aromatics
Stiffness, Good	Stiffness, High	Difficult to bond
Food contact, Acceptable	Food contact, Not preferable	Several metals accelerate oxidative degrading
		Low temperature impact strength is poor

2.3 Low Density Polyethylene (LDPE)

LDPE was the first plastic widely used in packaging in the late 1940s, which was a big deal for the plastics industry. It's made from ethylene molecules and has a structure with lots of branches shown in the Figure 2.3, unlike HDPE (Frączak, D.,2022). Because of all these branches, LDPE doesn't crystallize as much as HDPE, which makes it look a bit foggy, even though it's clearer than HDPE. This lack of crystal stuff also makes LDPE less dense, softer, and more flexible (Zhang et al., 2020). LDPE is great for flexible packaging because it can resist oils and chemicals. When it comes to sealing things with heat, LDPE melts at a lower temperature than HDPE. People use LDPE a lot, along with its mixtures, because it's so flexible, tough, and resistant to chemicals. Combined modification of LDPE composites by the addition of fillers such metals, carbon fibers, and ceramics improves mechanical strength, wear resistance, thermal stability, and flame retardancy.

Figure 2.3: Structures of polyethylene and polypropylene (Frączak, D.,2022).

2.3.1 Application of Low-Density Polyethylene (LDPE)

In engineering applications, plastics, including LDPE composites, are gradually taking over from traditional materials like glass, wood, and metals because of their advantageous properties. The wear resistance of LDPE composites is influenced by the characteristics of both the filler and the base material. By reinforcing the material and increasing its hardness, fillers such as carbon fibers, glass fibers, and ceramics can enhance wear resistance (Zhang et al., 2020). Additionally, lubricants and other additives can reduce friction, further improving wear resistance. The Table 2.3.1 gives insights into the different usage of LDPE, as shown by prior researcher.

Table 2.3.1: Application of LDPE in Previous Study

Application	Reference
LDPE in food packaging for extending shelf life.	(Giannakas et al., 2023)
LDPE films and bags in the packaging industry.	(Barros et al., 2023)
LDPE geomembranes in landfill liners.	(Halake et al., 2023)
Use of LDPE protective sheeting in construction.	(Szlachetka et al., 2021)
LDPE in pharmaceutical packaging.	(Sabee et al., 2022)
Utilization of LDPE in medical device components.	(An et al., 2022)
Household items made from LDPE.	(Prasad & Nandi, 2017)
LDPE agricultural films for mulching and greenhouse covers.	(Esposito et al., 2023)
LDPE in electrical cable insulation.	(Wang Chuan-Bo et al., 2022)

2.3.2 Advantages of LDPE

Low-density polyethylene (LDPE) is a vital material in polymer research due to its exceptional flexibility and broad range of applications. Its notable flexibility and durability make it perfect for producing various flexible packaging materials, such as plastic bags, shrink wrap, and squeeze bottles. The LDPE's resistance to impact and punctures ensures longevity in packaging applications where durability is crucial. Its ability to withstand moisture, chemicals, and corrosion enhances its suitability for numerous commercial and industrial uses, including agricultural films and medical packaging (He et al., 2022). Additionally, LDPE is widely used across industries due to its ease of processing through methods like extrusion and blow molding, demonstrating its cost-effectiveness in manufacturing. The lightweight nature of LDPE reduces material and energy consumption, making transportation more economical and supporting modern ecological efforts. Moreover, LDPE's recyclability offers a sustainable solution to the environmental challenges posed by plastic waste (Balu et al., 2022). Therefore, LDPE is a key material that embodies environmental responsibility, versatility, and functionality in contemporary polymer applications.

2.3.3 Limitation of LDPE

Low-Density Polyethylene (LDPE) is widely used for its flexibility, transparency, and ease of processing, yet it has several limitations that affect its suitability for various applications. Its lower tensile strength and rigidity, compared to High-Density Polyethylene (HDPE), make it less appropriate for structural uses requiring high strength (Kida et al., 2022). The material's low melting point (around 105-115°C) restricts its application in high-temperature environments, as it can deform or melt under relatively low heat. Additionally, LDPE exhibits higher permeability to gases and moisture, limiting its effectiveness as a barrier in packaging applications that require strict protection. The LDPE is also prone to environmental stress cracking and has limited chemical resistance to strong oxidizing agents and hydrocarbons (Cruz & Jansen, 2022). It degrades upon prolonged exposure to ultraviolet (UV) light, leading to embrittlement and loss of mechanical properties unless UV stabilizers are added, which increases costs. While LDPE is recyclable, the process can be challenging due to contamination and the need for thorough separation and cleaning, compounded by a less developed recycling infrastructure compared to other plastics. These limitations necessitate careful consideration to ensure LDPE meets the specific performance requirements of intended applications.

2.4 Repurpose Of Manufacturing Scrap

Repurposing manufacturing scrap has several benefits for resource efficiency and sustainability. First, recycling is a crucial strategy that minimizes waste and reduces the need for virgin resources by gathering and processing old materials to make new goods or raw material (Huysman et al., 2017). Another important factor is material recovery, which supports a circular economy by allowing valuable components like metals or polymers to be retrieved from the scrap and used again in different applications. Energy recovery is another possibility, especially for organic or combustible waste, since it enables to generate energy from the heat created during operations like burning, which helps develop a more sustainable energy mix (Shen & Qi, 2012). By remanufacturing useable components from manufacturing scrap, remanufacturing helps extend the life cycle of products. Furthermore, creative repurposing reduces the environmental impact of typical production by allowing the recycling of scrap into creative and unique items (Huysman et al., 2017). Continuous investigation and application of these repurposing techniques lead to more ecologically friendly and sustainable production methods.

2.4.1 Circular Economy

The circular economy idea, which encourages sustainable economic development, is based on a universal approach to resource management. This idea is to move away from the traditional linear economic model and toward a more complete circular one. Products are made to be long-lasting, repairable, and durable under this optimized system, breaking from the traditional which are take-make-dispose mentality (Korhonen et al., 2018). Throughout the product life cycle, the focus changes to resource optimization, waste minimization, and maximizing material usefulness. The key component of this strategy is waste reduction due to effective conservation and reuse. By separating economic growth from resource depletion, this ecologically conscious model aims to bring prosperity and responsible resource use into balance (Huysman et al., 2017). On the other side, the linear economy, a traditional resource consumption model, consumes natural resources to produce goods that eventually end up in landfills as in illustration of Figure 2.4. This straight line generates plenty of trash, harms the environment, and wastes a lot of resources.

Figure 2.4.1.1: Linear economy flow diagram (Upadhayay & Alqassimi, 2018)

In contrast, the closed-loop circular economy is specifically designed to increase resource efficiency and reduce waste. This model underscores the benefits of closed-loop systems, emphasizing the sustainability of the environment and responsible resource management. The closed-loop approach envisions products created with the intention of being reused, refurbished, or recycled, creating a self-sustaining system that minimizes the demand for new raw materials. This focus on circularity not only addresses environmental concerns but also ensures that materials remain within a closed system, contributing to a more sustainable and regenerative economic framework (Ellen MacArthur Foundation, 2013). On the other hand, materials are recycled in the open-loop circular economy, sometimes referred to as the cradle-to-grave method, but it also free to enter new product or industry cycles. The close loop concept can be understood by the illustration in the Figure of 2.5.

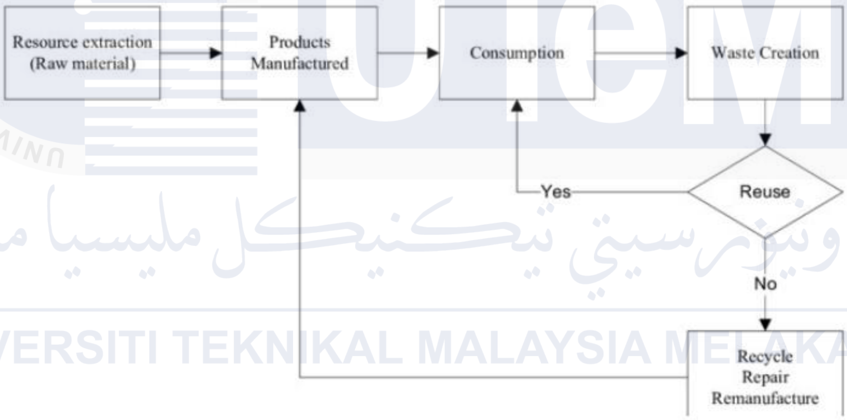

Figure 2.2.1.2: Circular economy flow diagram (Upadhayay & Alqassimi, 2018)

2.4.2 Environmental sustainability

Environmental sustainability means using nature in a smart way to meet the needs now without hurting what future people will need. This approach aims to make ecosystems last long, reduce harm to nature and support a healthy environment (Shen & Qi, 2012). Choosing ways that are good for the environment means taking on a completely new way to deal with issues that hurt nature and make it healthier in time. The first strategy is focusing on using natural energy sources like sun, wind, and river power instead of burning oil or coal (Nazish Huma Khan et al., 2021). This strategy will reduce heating up the planet due to gases released into the air by also making sure electricity can keep going in a lasting way without running out quickly. Next strategy is to reduce waste and increase recycle materials. This works by cutting down on scrap that are being produce from industries, encouraging company to use same items again or turn materials into new things. The idea of a circle-based economy places importance on how this helps save resources, reduces public waste grounds, and lessens harm to nature (Bocken et al., 2016).

2.5 Partial Replacement of Industrial Waste

In the industrial sector, partial waste replacement refers to a planned shift from using traditional raw materials to using waste generated during industrial processes. Reducing waste disposal, promoting responsible resource management, and minimizing the harmful effects of industrial activities on the environment are the three main objectives of this sustainable approach (Neli Babekova, 2023). Rather of treating industrial waste as a burden, this strategy turns it into a valuable resource that may be used in manufacturing, construction, and other industrial activities. One example of this tactic in action is the replacement of recycled plastic for virgin plastic during manufacture. This is a workable solution to the crucial issue of plastic pollution, and it follows as well to the circular economy's core values, which emphasize material reuse (Huysman et al., 2017). Recycled plastic is an important resource that keeps waste out of landfills and reduces the need to produce new plastic. It comes from post-consumer or post-industrial sources. The use of recycled plastic is one example of how businesses implementing such practices actively address environmental issues and waste reduction, highlighting the benefits of this shift to a more sustainable and responsible industrial ecosystem for the benefit of the economy and the environment.

2.5.1 Concept of Partial Replacement

Partial replacement refers to the practice of substituting a portion of a substance with another material in each application or process. This notion is commonly applied in numerous sectors like as construction, manufacturing, and materials engineering. The objective of partial replacement is to achieve certain goals or benefits without totally substituting the entire material. This method is often applied to enhance particular properties, minimize expenses, or solve environmental concerns (Md. Jahidul Islam & Md. Shahjalal, 2021).

In construction, a common example of partial replacement is the substitution of a portion of cement with supplementary cementitious materials (SCMs) such fly ash, silica fume, or slag in concrete mixtures. This partial replacement can lead to enhanced durability, less environmental impact, and cost savings. Partial replacement can also be used in manufacturing processes, where components of a material may be changed with alternatives to obtain desired features or maximize performance (Tiong et al., 2020). The decision to employ partial replacement is often impacted by considerations such as material availability, cost-effectiveness, and the unique needs of the intended application (Smith et al., 2019).

2.5.2 Partial Replacement as Cost Reduction Strategy

Partial replacement is a good way to cut costs in many fields, specially building and making things. This is important because industries spend huge amounts on their materials which make up their total expenses. It aims to save money without changing the important parts in products. This way is often used in building materials. For example, when making concrete industries can save money by using less cement and mixing it with stuff like ash from burning coal or slag left. Manufacturers regularly look into the substitution of raw materials, additives, or components with cost-effective alternatives without affecting product quality (Stanek et al., 2023). This may involve utilizing locally obtained materials to save shipping costs or adding recycled and repurposed materials into the production process.

Additionally, optimizing material combinations and applying waste reduction methods add to overall cost-effectiveness. By selectively replacing specific materials with more cost-efficient options, enterprises can establish a balance between economic considerations and product performance (Tiong et al., 2020). A lot of consideration is necessary when adopting partial replacement to ensure that the substituted materials fulfil required performance standards and do not affect the integrity or safety of the final product. Furthermore, examining the environmental and sustainability impacts of such substitutions is critical to line with broader company aims. Overall, partial replacement stands as a unique and successful cost reduction technique, offering enterprises with opportunity to boost efficiency, cut prices, and contribute to more sustainable practices.

2.5.3 Application on Partial Replacement

Partial replacement shows a wide range of uses, and its overall usefulness is usually created by previous study projects focused on increasing certain attributes. The Table 2.5.3.1 below gives insights into the varied applications of partial replacement (PR) as revealed by previous studies.

Table 2.5.3: Application of partial replacement based on previous studies.

Application	Reference
Tiles: partially replace aggregates in tiles that combine with plastic and leftover ceramic components.	(Philipose et al., 2023)
3D filament application: filament produced from recycled/virgin ABS blends has the capability to replace commercially available ABS filaments for fabricating high-quality plastic parts through an additive manufacturing routine.	(Mishra et al., 2023)
Brake system: TPV of PP/EPDM compounds close to the rubber properties in the middle of Thermoplastic Elastomer (TPE) were applied to the rubber parts in the needs like durability. Properties were inferior to thermoset rubber, but products performance requirements were satisfied.	(Rahul Bhandary et al., 2023).
Household application: Partial replacement of sand in thermoplastic composites improves household durability.	(Soni et al., 2022)
Pallets and crates: waste plastic is ground up and mixed with other plastics in the correct proportions	(Maja Dahlbom et al.,2023)

then injected under pressure into a pallet-shaped mould with the European dimensions of 80×120.	
Base and subbase for road constructions: PW has been proven to increase the shear, stiffness.	(Choudhary et al., 2014)
Door panels: mixing PW in pellets or powder form with cellulose fibre or wood flour to generate a thermoformable wood plastic matrix that can be used for door panels.	(Yang et al., 2012)
Insulation material: PW in the form of expanded polystyrene (EPS) can be utilized as insulation material during the development process.	(Awoyera et al., 2019)
Wood replacement: It was made of mixed polymers and may be treated like wood (cut, sawn, nailed, etc.) after recycling.	(Awoyera & Adesina, 2020)

2.5.4 Plastic Waste Issue

Plastic waste problem means an issue for nature because of the massive consumption of the plastic and the method of the disposal are wrong (Letcher, 2020). This can harm plants, animals, and people's health in some bad ways. The world's plastic waste problem gets worse because of the increase in one use plastics, bad recycling methods and not enough ways to manage trash (Niyitanga Evode et al., 2021). Plastic trash, especially small pieces of plastic called microplastics can dirty waterways. This harms sea creatures, and they stay in nature for a long time which keeps causing problems with the environment or health over many years. The extraordinary extent of this environmental crisis is estimated to be between 4.8 and 12.7 million metric tons of plastic garbage entering the seas in 2010, demonstrating the startling magnitude of this environmental challenge (Gonzalez-Paredes & Estrades, 2021).

2.5.5 The r-PP Utilization in Manufacturing

The r-PP is a term for recycled polypropylene, a form of plastic material. The use of recycled polypropylene as a raw material in different industrial processes is referred to as r-PP usage. Polypropylene recycling requires collecting post-consumer or post-industrial trash, processing it, and transforming it into recycled polypropylene. PP can be blended with different types of biodegradable polymers such as polylactic acid (PLA) and thermoplastic starch (TPS). It was proven that during the recycling process of PP, the presence of several biodegradable polymers could be detected as impurities that affect the thermal and mechanical properties of the recycled PP (Samper et al., 2018). Moreover, the elimination process of the impurities in the recycled PP requires further techniques followed by undesired environmental impacts. It is much harder to be recycled or separated than recycling pure PP (Samper et al., 2018) The use of recycled polypropylene (PP) in manufacturing is an important component of sustainable waste management (Ved Prakash Ranjan and Goel, 2021).

2.6 Carbon Nanomaterial

Carbon nanomaterials are various structures of carbon atoms at the nano level that pose unique features arising from their size and pattern. Nanomaterials are materials with a minimum of one exterior dimension in the size range of 1 to 100 nanometres, whereas nanoparticles are objects with three external dimensions at a specific nanoscale (Musa, N.2023). These materials include graphene, carbon nanotubes, fullerenes, carbon nanodots, carbon nanofibers, and carbon nanoribbons. The structural foundation of carbon materials underpins their exceptional properties. In the case of graphene, it takes the form of a single layer of carbon atoms arranged in a hexagonal lattice, creating a two-dimensional structure. Carbon nanotubes, on the other hand, manifest as cylindrical structures, composed of rolled-up graphene sheets, showcasing excellent mechanical, thermal, and electrical properties.

Carbon materials, exemplified by graphene and carbon nanotubes, bring forth exceptional properties, yet practical challenges temper their broad application. The large-scale production of high-quality carbon nanomaterials remains an expensive and complex endeavour. The functionalization of their surfaces, critical for diverse applications, proves intricate and can alter their intrinsic properties (Alvaredo-Atienza et al., 2020). Concerns about the potential toxicity of certain carbon nanomaterials, especially in biomedical contexts, necessitate careful consideration. Achieving uniform dispersion of these materials in various matrices poses challenges, impacting their performance in composites and other applications (Alvaredo-Atienza et al., 2020). Additionally, the lack of standardized production processes and characterization methods impedes widespread adoption in certain industries. The Figure 2.5.1 shows the different dimensions of crystal structure of carbon nanomaterials. In this study, the dimensions of carbon nanomaterials is graphene were the graphene nanoplatelets will be loaded to the thermoplastic blend.

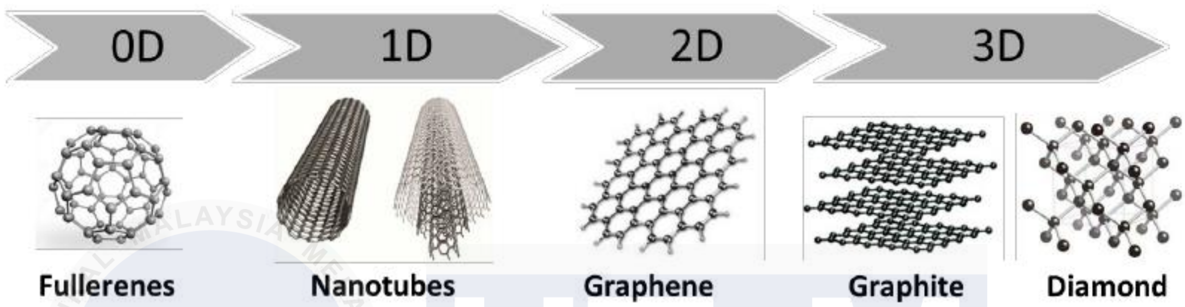

Figure 2.6: Crystal structure of carbon nanomaterials with different dimensions (Asha & Narain, 2020)

2.6.1 Graphene nanoplatelets

Graphene is a monolayer of hexagonally arranged carbon atoms that form the structure. It is an extraordinary material with great strength, electrical conductivity and a thermal one which places it as the game-changer in many industries. The fundamental two-dimensional structure of graphene plays a huge role in electronics, paving the way for high tech gadgets. Graphene's conductivity can enhance the efficiency of batteries and supercapacitors for energy storage (Lamastra et al., 2021). In materials research, graphene is used to reinforce composites, giving them better mechanical strength. A single-walled carbon nanotube, a structure close to graphene with its Young's modulus at approximately 1 TPA tonnes per annum (He et al., 2022). Additionally, graphene's surface could be functionalized to yield a new generation of reagents usable in completely different applications such as composite materials. These properties highlight graphene's versatility and can point out many technological breakthroughs influenced by it.

2.6.2 Advantages & Limitation GNPs

Graphene nanoplatelets has several industrial uses. It may be utilized in energy harvesting, strain sensors technology, steel industry, building and construction sectors. Graphene nanoplate can also be used in the fabrication of composites such as polyetheretherketone (PEEK)/graphene nanoplate (GNP) composites. Additionally, graphene-based materials have been used widely in different application fields such as in the fields of energy, wearable technology, agricultural, medical, and wastewater management (Al Faruque et al., 2021).

As stated in previous study, the use of GNPs improves several characteristics, and the strength of this improvement is highly dependent on the sheet size of GNPs (Jun et al., 2018). For example, when lightweight GNPs-reinforced composites are being explored for automobile parts for better fuel economy in the future, relatively tiny-sized GNPs should be added. High-barrier performance packaging materials for chemical, solvent, and fuel containers can also be made with GNPs. Relatively large GNPs can be used to increase electrical conductivity and reduce electrostatic discharge in safety-related situations (Alasvand Zarasvand & Golestanian, 2017b). Therefore, when the composites are made using traditional industrial machinery, it is crucial to understand how the physical characteristics of the GNPs affect the performance of the composites from a manufacturing perspective.

Beside that the benefit is their cost-effectiveness in comparison to carbon nanotubes, owing to reduced production expenses. Graphene nanoplatelets are also rigid, have a two-dimensional structure, and low thermal interface resistance, making them an effective filler to produce composite materials with better thermal conductivity (Lamastra et al., 2021b). Nevertheless, the primary constraints are the poor production rates and costly marketing expenses. Graphene nanoplatelets, particularly those formed from graphene with carboxyl group function, are not capable of being broken down by natural processes. Additionally, some nanomaterials belonging to the graphene family may have limitations when it comes to their use in biomedical applications (S.G. Prolongo et al., 2014).

2.7 Mechanical and physical properties testing

Mechanical and physical properties testing are procedures used to analyse the physical and mechanical qualities of materials (Wei, W. Bill., 2021). Physical property testing is performed to guarantee that a material or product obeys health and safety regulations in a particular industry or application. These tests measure the physical and mechanical qualities of a certain material, such as tensile strength, density, hardness, and flexibility, to mention a few. Mechanical testing, on the other hand, determines the mechanical qualities of a material or final product, such as tensile, fracture, fatigue, creep, impact, hardness, and non-destructive testing. These tests enable engineers to determine the most suitable mechanical test for their purposes. Mechanical characteristics testing offers information on strength, ductility, impact resistance, hardness, and fracture toughness (Zhang et al., 2022). Testing for mechanical qualities is conducted under different situations such as tension, increased temperature, stress, elongation, compression, load, impact, and fatigue. These tests are critical in product design and component manufacture for material characterisation, selection, and validation of products (Alvaredo-Atienza et al., 2020).

2.7.1 Mechanical Tensile Properties of Thermoplastic Blend Nano Composite

The mechanical tensile characteristics of thermoplastic mix nanocomposites may be dramatically modified by the inclusion of nanoparticles or nanofillers. These nanoparticles may increase the mechanical characteristics such as tensile strength, modulus, and elongation (Akhoundi and Behravesh., 2019). The tensile test is being conducted to evaluate material strength and resistance to stretching. A result from a case study which investigates the effect of filling pattern on the tensile and flexural mechanical properties of FDM 3D printed product shown that increase in elongation of breaks (Akhoundi and Behravesh., 2019).

2.7.2 Physical tensile properties of thermoplastic blend nano composite

The physical tensile properties of the thermoplastic blend with nano composite are increase from the traditional thermoplastic (Feldman, 2015). The tensile strength of traditional thermoplastics might vary based on the particular material and its composition. For example, the tensile strength of polypropylene (PP) can range from 100-600 psi, while the tensile strength of polyamide (nylon) 6/6 can range from 15-300 psi. Several studies shows that it appears that the tensile strength of thermoplastic composites can be improve by adding graphene nanoplatelets (GNPs). A study on PA66/thermoplastic copolyester elastomer composite found that the addition of GNPs improves the tensile property of the composite due to the substantial filler dispersion and firm interfacial adhesion between the reinforcement and matrix (Suresha et al., 2020). Similarly, tensile strength increased as GNPs loading increased. This integration of GNPs also resulted in an increase in Young's modulus. GNPs worked as space fillers at lower percentages of GNPs loading, and property was increased by a tiny amount. Tensile strength and modulus were improved by GNPs loading. Even with a 3 wt.% loading of GNPs, the results show a minor improvement in the characteristics.

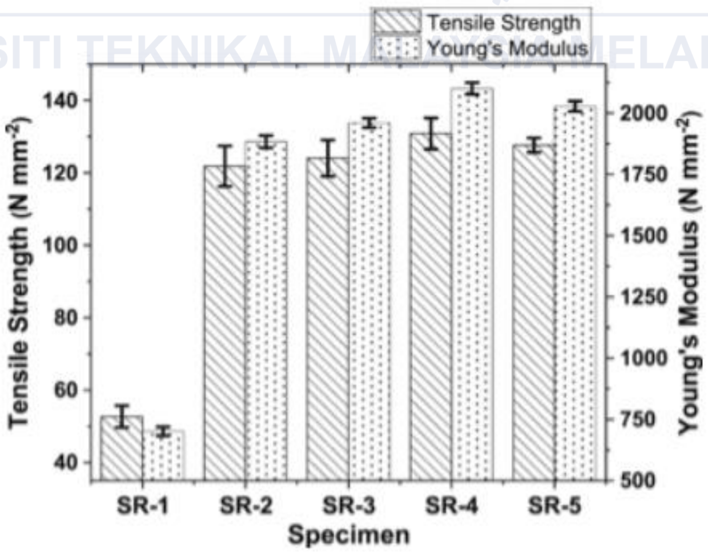

Figure 2.7.2: Tensile property of the PA66/TCE composites (Suresha et al., 2020).

2.8 Design of experiment

Design of Experiment (DoE) is a systematic technique used to examine the impact of several factors on a certain result in different fields, including physical property testing of materials. DOE is using in numerous sectors to discover the optimum parameter from multiple variables or factors to improve process output, minimize variance, and lower overall cost (Montgomery, 2013). DOE also enables the firms to evaluate several elements or variables simultaneously with a more accurate result that may lead to quicker experiments than the old technique, such as One Factor at a Time (OFAT). Hence, it makes DOE utilize less expense (Roy, 2001).

The core concepts of DOE include factor identification, factor level selection, experiment design, experiment conduct, data analysis, and optimization (Antony, 2023). Employing DOE may assist the effectively examining the impacts of numerous variables on mechanical characteristics and gain a better knowledge of the material's behaviour under varied situations (Sonebi & Yahia, 2020). This technique may assist in influencing the creation of new materials to improve the design and performance of current items. DOE as a scientific experimental technique has increased dramatically in the last 20 years in manufacturing and non–non-manufacturing businesses worldwide (Durakovic, 2017). DOE effectively determines the most significant component or variable to regulate to obtain optimum process performance (Kazemain, Ebrahimi-Nejad, & Jaafarian, 2018).

2.8.1 Two Level Full Factorial Design

The two-level full factorial design is a robust experimental methodology employed to investigate the influence of multiple variables on a response variable. In this design, each factor is manipulated at two levels, typically high and low, enabling a comprehensive analysis of individual factor effects and interactions between factors (Antony, 2023a). By testing all possible combinations of component values, this approach yields highly efficient and unbiased estimates, explaining the impacts of factors on the response variable. Widely applied in fields like physical and mechanical testing, the full factorial design accommodates both continuous and categorical factors with up to nine degrees of differentiation. Especially, when limited to two-level factors, the sample size is a power of two (2^f, where f is the number of factors), while for three factors, a sample size of three is employed.

$$N = L^k$$

Where k is the number of variables,

L is the number of variable levels

N is the number of experimental trials

In scenarios involving two-level variables or binary variables, a fractional factorial design, as described by (Gujral et al., 2018), offers a strategic approach. This design permits the exploration of numerous design variables through fewer experiments than a full factorial design. Specifically, fractional factorial designs are generated by selecting a fraction of the original design's trial runs. As an illustration, consider a fractional factorial design with four design variables (A, B, C, and D) denoted by '-' and '+', representing lower and upper levels, respectively. Initially, a complete factorial design is formed using three variables (A, B, and C), expressed as 2^3. This enables a comprehensive examination of the variable interactions while significantly reducing the number of experimental runs. This is the most secure design technique, but it is also the most expensive in terms of experimental resources.

Table 2.8.1: Description of full factorial 2^3

Experiment	A	B	C	AB	AC	BC	ABC
1	-	-	-	+	+	+	-
2	+	-	-	-	-	+	+
3	-	+	-	-	+	-	+
4	+	+	-	+	-	-	-
5	-	-	+	+	-	-	+
6	+	-	+	-	+	-	-
7	-	+	+	-	-	+	-
8	+	+	+	+	+	+	+

2.8.2 Past study on thermoplastic blend composite using DOE approach.

A study from Arak Petrochemical Company in Iran provided the polypropylene (PP-Z30S, MFR-25, 230 °C, 2.16 kg) and linear low-density polyethylene (LLDPE-0209, MFR-0.9, 190 °C, 2.16 kg, density 0.920 g/ml). Adding nano TiO_2 rutile structure from Iranian Nano-materials Pioneers (INP), which has an average size of 30 nm and a density of 4.23 g/cm3. Furthermore, styrene–ethylene/butylene–styrene (SEBS) grade 6110 from Dynasol Company, a KRATON polymer type G, was used as a coupling agent.

Experiments were done based on Box–Behnken response surface approach. The statistical program Minitab® 17 was used to build the design matrix and evaluate the experimental data. The input parameters, namely LLDPE, TiO_2, and SEBS, were examined at three levels as provided in Table 1. According to the Box–Behnken design of experiment, 15 trials containing three center points were carried out as stated in Table 2. For the statistical computation, the link between the coded values and real values was stated according to the following equation:

$$x_i = \frac{x_i - x_0}{\Delta X} \quad (1)$$

where ΔX is the variable's step change, xi is the variable's real value, X0 is the variable's actual value at the center point, and xi is the variable's coded value [17]. In order to minimize error resulting from the experimental procedure, the experiments in this research were conducted at random. The link between the independent variables (X1, X2, and X3) and the response (Y), which may be stated by the following equation, was thought to be correlated by a polynomial model:

$$Y = \beta_0 + \beta_1 X_1 + \beta_2 X_2 + \beta_3 X_3 + \beta_{11} x_1^2 + \beta_{22} x_2^2 + \beta_{33} x_3^2 + \beta_{12} X_1 X_2 + \beta_{13} X_1 X_3 + \beta_{23} X_2 X_3 \quad (2)$$

where the coefficients for the polynomial for linear effects are β1 and β2, the coefficients for the polynomial for the interaction effect are β12, β13, and β23, and the response is Y. The variables are X1, X2, and X3. The constant term is β0.

Table 2.8.2: Variable in Box- Behnken experiment design.

Parameters	**Levels used**		
	Low (−1)	**Middle (0)**	**High (+1)**
LLDPE (wt%)	20	40	60
TiO_2 (wt%)	0	2	4
SEBS (wt%)	0	3	6

Table 2.8.3: The Box-Behnken experiment design.

Experiment run	**1**	**2**	**3**	**4**	**5**	**6**	**7**	**8**	**9**	**10**	**11**	**12**	**13**	**14**	**15**
LLDPE (wt%)	20	20	60	60	40	40	40	40	20	60	20	60	40	40	40
TiO_2 (wt%)	0	4	0	4	0	4	0	4	2	2	2	2	2	2	2
SEBS (wt%)	3	3	3	3	0	0	6	6	0	0	6	6	3	3	3

2.9 Research Gap & Summary

The Table 2.9 provides a comprehensive summary of the several polymer blend composites that have been researched in the past, emphasizing the range of formulas and combinations that have been investigated. A critical evaluation, however, highlights the need for further research in these unknown regions by pointing out a significant gap in the study of certain combinations that may open unexpected features or uses.

Table 2.9: Polymer blend from previous study

Author	Type of polymer blend composites	Study/ Results
(Dikobe & Luyt, 2010)	PP/LLDPE/wood powder	The research investigated polypropylene (PP)/linear low-density polyethylene (LLDPE) and maleic anhydride grafted polypropylene (MAPP)/LLDPE blend systems. It tested compatibility and miscibility of the two polymers. Composites using wood powder (WP) were made and examined. The MAPP/LLDPE mix, and composites demonstrated superior characteristics owing to increased interfacial contact. The PP/LLDPE/WP mix composites had WP more in the LLDPE phase, whereas the MAPP/LLDPE/WP composites had WP in contact with both polymers. TGA studies indicated MAPP/LLDPE blends were more thermally stable.
(Jun, Um, Jiang, Lui, et al., 2018)	PP/GNPs	This review will cover the development of polymer/GNP nanocomposites, including fabrication, processing, viscoelastic, mechanical, electrical, dielectric, thermal conductivity, thermal stability, and the reinforcing effect. The synergy of GNPs with other carbon nanofillers as hybrid reinforcing systems shows great potential.
(Homkhiew et al., 2014)	r-PP/RWF	The study aimed to determine the optimal combination of rubberwood flour and reinforced recycled polypropylene for composites. The best formulation (50.3 wt% r-PP, 44.5 wt% RWF, 3.9 wt% MAPP, 0.2 wt% UV stabilizer, and 1.0 wt% lubricant) produced a composite with excellent mechanical characteristics.
(Mariam Atiqah et al.,2014)	r-PP/r-HDPE	The research explored how r-PP/rHDPE geo-composites tensile characteristics were affected by mixes. Results revealed that increasing rHDPE ratios reduced tensile strength and elongation at break but improved the modulus of elasticity. r-PP/rHDPE geo-composites showed better tensile strength and modulus of elasticity compared to rHDPE/r-PP geo-composites.
(Satya & Sreekanth, 2020)	r-PP/r-HDPE	The study about the mechanical characteristics of r-PP and r-HDPE comparing them with the virgin materials. The result reveal rHDPE demonstrates greater impact resistance and tensile strength, making it appropriate for construction, military, and industrial uses. r-PP displays excellent results in hardness and Young's modulus, making it appropriate for aerospace, automotive, and engineering applications.
(Daneshpayeh et al., 2016b)	PP/LLDPE/TiO_2	The study examines the mechanical properties of ternary nano-composites made from polypropylene/linear low-density polyethylene/nano-titanium dioxide (PP/LLDPE/TiO_2) using response surface methodology (RSM). Experiments show that LLDPE concentration significantly affects the nanocomposites' shape and mechanical properties. The optimal nano-particle values

		were 24.85 wt% for LLDPE, 3.02 wt% for TiO2, and 6 wt% for SEBS.
(Wang et al., 2004)	PP/LLDPE	Dynamic packing injection molding was utilized to make orientated pure polypropylene (PP) and its blends with linear low-density polyethylene (LLDPE). Pure PP has a significantly oriented structure in the sheared layer, whereas less oriented structure was identified in the core. The skin layer had a shish-kebab structure, whereas the core had an orientated spherulits structure. LLDPE showed a unique crystal shape and lamellar orientation, either perpendicularly or 45-508 away from the shear flow direction.

CHAPTER 3

METHODOLOGY

3.1 Overview of Methodology

Figure 3.1 illustrates the flow chart showing the approach used in this study, comprising both the preparation and experimental stages. The Design of Experiments (DOE) technique was applied to identify the best number of experiments. The combination of Result A (r-PP and LDPE) was loaded with graphene nanoplatelets (GNPs) during the single extrusion process. Subsequently, five samples of A+GNPs underwent mechanical and physical property tests. Three samples from Result B, representing the best, control, and worst instances, were chosen for the field emission scanning electron microscopy (FE-SEM) study. Lastly, FE-SEM was applied to investigate the morphologies of the samples, seeking to establish connections between the observed morphologies, tensile strength performance, and physico-mechanical evaluations.

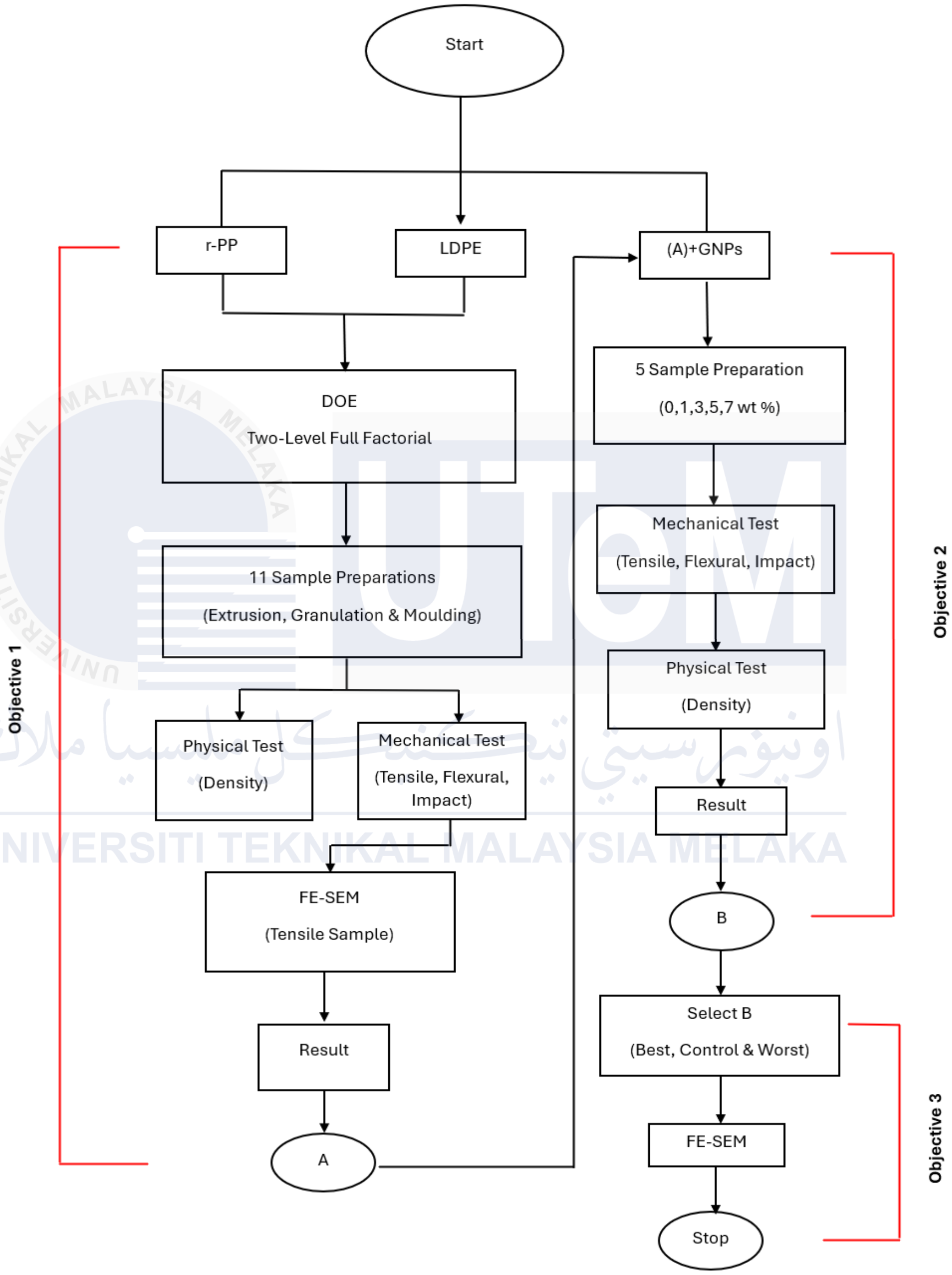

Figure 3.1: Flowchart of Methodology

3.2 Raw Materials and Characterization

This research consists of three main type of raw materials which recycle Polypropylene (r-PP), Low Density Polyethylene (LDPE) and Graphene Nanoplatelets (GNPs). Details of each classification of raw materials used were specified and characterized in this work. This explanation is then followed by the materials preparation which are basically based on their previous method established by various researchers where some of it was designed for others application and developed from this study.

3.2.1 Recycle Polypropylene and Low-Density Polyethylene

In this research, the r-PP (recycled polypropylene) wastes are supplied by the company in the form of pellets, which are generated as waste, as shown in Figure 3.2. These r-PP pellets are free from clay and water, ensuring their purity and suitability for the extrusion process. The absence of contaminants like clay and moisture is crucial to maintain the mechanical properties and quality of the final extruded product. The clean r-PP pellets ensure a smooth extrusion process and help in achieving consistent and reliable results in the material testing.

The LDPE (low-density polyethylene) used in this study is provided by UTeM and serves as the second material to be blended with r-PP, as shown in Figure 3.3. The two materials are manually mixed in plastic zip lock bags to ensure an even distribution before they undergo the single screw extrusion process. This manual mixing process helps to ensure that the LDPE and r-PP pellets are evenly distributed, minimizing the occurrence of isolated spots of either material. The LDPE pellets, characterized by their high flexibility, toughness, and chemical resistance, contribute significantly to the overall properties of the blended material. Ensuring a well-distributed mix of LDPE and r-PP before extrusion enhances the final product's performance, making it suitable for various applications requiring durability and resilience.

Figure 3.2.1.1: Pellets of r-PP

Figure 3.2.1.2: Pellets of LDPE

3.2.2 Graphene Nanoplatelets (GNPs)

Graphene nanoplatelets (GNPs) are a form of graphene-based nanomaterial made up of many layers of graphene sheets layered on top of one another. Graphene is a single layer of carbon atoms organized in a hexagonal lattice; when numerous layers are layered, they create graphene nanoplatelets. In this study GNPs are being use in the objective 2 and the properties are shown in the Table 3.2.2 and the Figure 3.2.2 shown the form of graphene nanoplatelets (GNPs).

Table 3.2.2: Details of Graphene Nanoplatelets (Hafeez et al., 2019)

Appearance	Black/Grey Powder
Diameter	2-7 µm
Thickness	2-10 nm

Specific surface area	20-40 m^2/g
Electrical conductivity	80,000 S/m
Carbon content	>99%
Apparent density	0.06-0.09 g/ml
Water content	<2 wt.%
Residual impurities	<1 wt.%

Figure 3.2.2: Graphene nanoplatelets

3.3 Design of Experiment: Two-Level Full Factorial Design

To conduct the formulation of r-PP/LDPE, the number of the experiment must be known earlier. The design of the experiment was done by using Design Expert software 6.0.8. Two level full factorial was utilized in this study which involved three factors named are speed of extrusion (rpm), ratio of r-PP/LDPE and temperature as shown in the Table 3.3.1. This 2^3 factorial design for three types of variable repetition at the center point and one block executed to produce 11 sample of experiment. Table 3.3 summarized the variables value used in the experiment.

Table 3.3.1: 3 Independent variables

	Min (-)	0	Max (+)
Temperature	160	170	180
rpm	300	400	500
ratio	30/70	50/50	70/30

Table 3.3.2: Parametric combination for r-PP/LLDPE preparation

Sample	Temperature	Speed of extrusion (rpm)	r-PP/LLDPE ratio	Response in Tensile strength (MPa)	Response in Flexural Strength (MPa)	Response in Impact Strength (MPa)
1	-	+	+			
2	-	-	+			
3	+	+	+			
4	0	0	0			
5	+	-	-			
6	-	+	-			
7	0	0	0			
8	-	-	-			
9	+	+	-			
10	0	0	0			
11	+	-	+			

3.4 The r-PP/LDPE Blend Preparation (11 sample)

Generally, the r-PP and LDPE blend are being studied by setting 11 samples corresponding to 3 independent variables which are temperature, rotation of extrusion and the ratio of r-PP/LDPE. By using single screw extrusion 11 sample of r-PP/LDPE are being created and undergoes Mechanical testing, Density test and FESEM.

3.4.1 Weight the r-PP and LDPE

Both r-PP and LDPE materials were precisely weighed to 200 grams using a digital weight scale. The digital scale was first calibrated, and stainless-steel bowls were cleaned and dried to prevent contamination. Each bowl was then tared separately to zero scale before adding the materials. r-PP was gradually added to one tared bowl until the scale read exactly 200 grams, ensuring an even distribution for accurate measurement, as shown in Figure

3.4.1.1. The weight was recorded, and the procedure was repeated for LDPE with a second tared bowl, achieving an exact weight of 200 grams, as depicted in the Figure 3.4.1.2. This careful weighing process ensures the reliability and reproducibility of the experimental results.

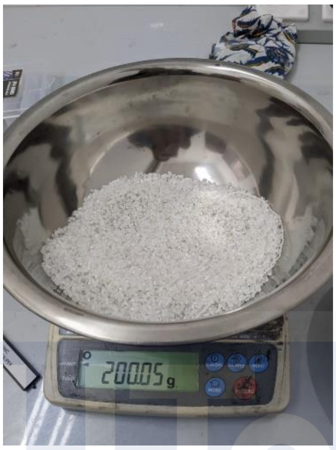

Figure 3.4.1.1: Weight of r-PP

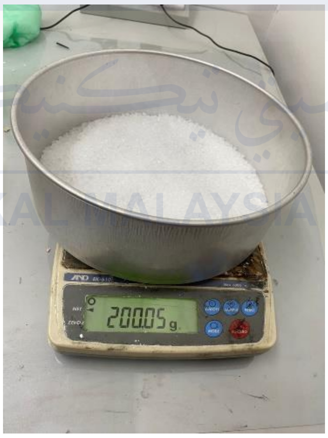

Figure 3.4.1.2: Weight of LDPE

3.4.2 Oven Drying

To ensure the absence of moisture and prevent bubble formation during the molding process, both r-PP and LDPE materials were dried in an oven at 80°C for 24 hours. The materials were placed in stainless steel bowls inside the oven, as shown in Figure 3.4.2, which illustrates the setup with bowls on the oven racks. This step is critical as retained moisture can lead to defects such as voids or bubbles, adversely affecting the mechanical properties and quality of the samples. The chosen drying conditions were based on the properties of r-PP and LDPE to ensure thorough drying without material degradation. This careful drying process ensures the samples are moisture-free, enhancing the accuracy and reliability of subsequent impact testing results.

Figure 3.4.2: Dry the materials

3.4.3 Mix sample in zip bag

To prepare samples for the extruder in single extrusion, the materials needed to be mixed manually in zip lock bags. Eleven samples were made according to the ratios specified in Table 2.8.1, with each plastic zip lock bag labeled with the corresponding ratio of r-PP and LDPE. The materials were added to the bags based on these labels and then manually mixed by shaking to ensure a uniform distribution. After mixing, the 11 samples in zip lock bags were put in containers to keep them free from contamination and moisture. Figure 3.4.3 illustrates a zip lock bag containing a mixture of r-PP and LDPE, clearly labeled with the specific ratio and ready for the next phase.

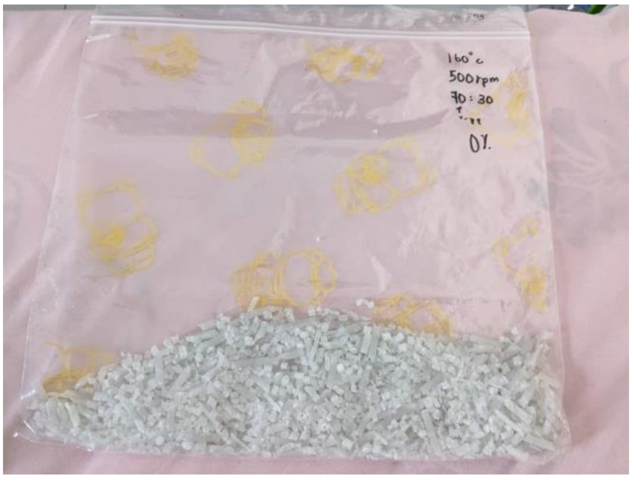

Figure 3.4.3: Mix manually

3.4.4 Single Screw Extrusion

The single-screw extrusion technique for manufacturing a mix of recycled polypropylene (r-PP) and low-density polyethylene (LDPE) requires careful procedures in the Figure 3.4.4.1. First, pure and contaminant-free r-PP and LDPE are prepared according to the required blend ratio. These materials are then fed into the hopper of a single-screw extruder. Inside the extruder, the polymers melt and are conveyed by the rotating screw, which generates heat through friction. Controlling the temperature is crucial, with different zones optimized for feeding, compression, melting, and metering. The screw design, aimed at efficient conveyance, compression, and mixing, affects the uniformity of the molten mixture. As the molten material exits the extruder die, it takes the desired shape, usually as a filament, which is then cooled and solidified shows in the Figure 3.4.4.2. The filament is crushed into small pellets, which are tested for mechanical strength for the first objective. For the second objective, r-PP and LDPE are mixed with graphene nanoplatelets (GNPs), forming five samples with different amounts of graphene. These samples undergo the same extrusion and crushing process, followed by molding for mechanical testing.

Figure 3.4.4.1: Single Screw Extrusion Machine

Figure 3.4.4.2: Sample Extrusion Process

3.4.5 Molding Hot Compression

To generate the ASTM Dog-bone and rectangular samples for the testing, a systematic set of operations is used in the hot compression molding technique for r-PP/LDPE samples from the extrusion process. First, extruded r-PP/LDPE samples are obtained from objectives 1 and 2. These samples are preheated to make them more malleable during the compression molding process. Next, the molding apparatus is prepared, with a clean and lubricated mould chamber to prevent material adhesion. Compression forces are then applied to the preheated r-PP/LLDPE loaded into the mould cavity, shaping the material to fit the mould. The process settings are 180°C and 100 MPa, with 5 minutes for preheating and cooling, and 10 minutes for molding. After molding, the r-PP/LDPE samples are carefully removed from the mould once the sample is release from the mould. These samples then undergo mechanical testing, density testing, and FESEM analysis.

Figure 3.4.5.1: Samples after the hot compression molding process

Figure 3.4.5.2: Hot Press Compression molding machine

3.5 Tensile Strength Test

ASTM D638 is the standard technique for doing tensile strength testing, which is important in evaluating the mechanical characteristics of materials. The goal of this study is to investigate the tensile characteristics of the r-PP/LDPE blend. For the tensile strength test, dog bone samples measuring as shown in Figure 3.5.1 were carefully manufactured. The specimens were firmly fixed in the testing apparatus's grips, guaranteeing accurate alignment for the examination. The test was carried out at a specified loading rate by ASTM D638 machine criteria as shown in Figure 3.5.2. The data on applied force for 11 samples are being collected to further analysis which is FE-SEM. Meanwhile for the objective 2, the sample are being loaded with GNPs nanofiller for 5 samples that are being conducted to this test and later be observe the surface morphology using SEM machine.

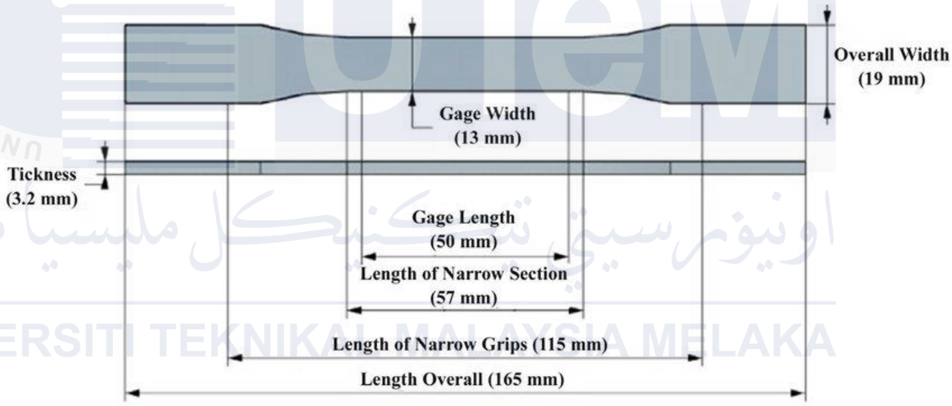

Figure 3.5.1: ASTM D638 Dimension for the tensile testing sample

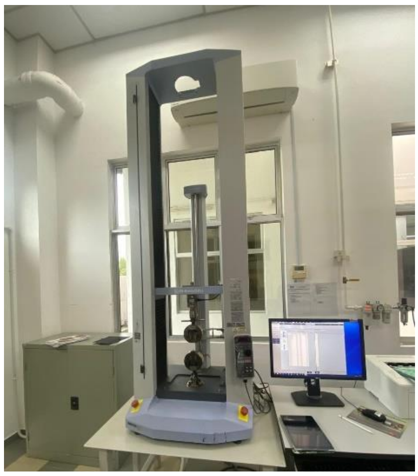

Figure 3.5.2: UTM Machine (Shimadzhu Autograph 20KN)

3.6 Flexural Test

The flexural testing of r-PP and LDPE samples using a Universal Testing Machine (UTM) follows a systematic procedure to ensure accurate results. Specimens are prepared according to ASTM D790 dimensions for the uniformity. The UTM machine, equipped with a flexural test fixture, was set up with two supporting pins and a central loading pin, adjusted to the relevant span. Specimens are centered and aligned on the supports, and a crosshead speed of 20 mm/min is applied. The UTM software inputs the specimen dimensions and support span, and data acquisition settings are verified. The UTM then applies a downward force, recording the load and deflection until specimen failure, generating a force-deflection curve. Key properties, including maximum force, deflection, flexural strength, and modulus, are recorded. Multiple specimens are tested for reliability, providing essential insights into the flexural properties of r-PP and LDPE for their mechanical performance evaluation.

Figure 3.6: ASTM D790 Dimension for the flexural testing sample

3.7 Impact Test

The impact testing of r-PP and LDPE samples by using an Izod impact tester follows a systematic procedure to ensure accurate results. Specimens are prepared according to ASTM D256 dimensions for uniformity. The Izod tester, equipped with a pendulum hammer and a vertical specimen holder, is set up with the appropriate settings. Specimens are clamped in the holder with the notch facing the pendulum. The Izod tester software inputs the specimen dimensions, and data acquisition settings are verified. The pendulum is then released, striking the specimen and recording the energy absorbed until fracture. Key properties, including impact energy, notch toughness, and fracture behavior, are recorded. Multiple specimens are tested for reliability, providing essential insights into the impact properties of r-PP and LDPE for their mechanical performance evaluation.

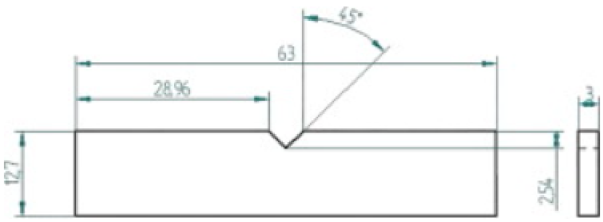

Figure 3.7.1: ASTM D256 Dimension for the impact testing sample

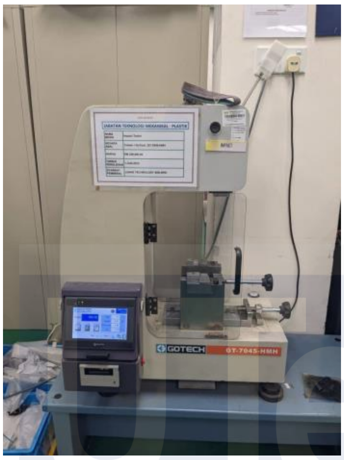

Figure 3.7.2: Impact Tester Machine

3.8 Density Test

The density analysis of r-PP/LDPE mix samples using a densimeter involves several precise steps. First, the samples are prepared and cleaned to ensure uniformity and prevent contamination. The densimeter is then calibrated using a standard reference material. Each sample's mass is measured using a precise balance, and the sample is carefully placed in the densimeter to determine its volume. The densimeter calculates the density based on these measurements. Multiple readings are taken for accuracy, and the results are recorded. The densimeter is cleaned and maintained after the measurements. This procedure provides reliable density data for the r-PP/LDPE samples, essential for evaluating their material properties. The densimeter used in this investigation is shown in Figure 3.8.

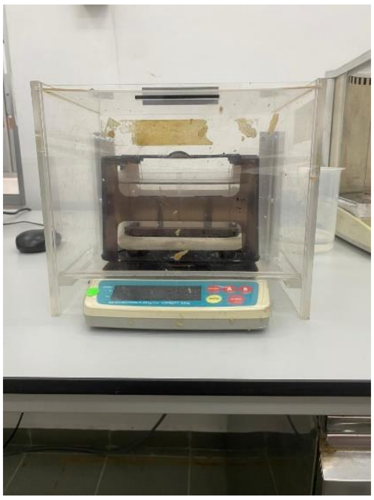

Figure 3.8: Densimeter

3.9 Field Emission Scanning Electron Microscopy

In addition to mechanical and physical testing, this study extensively utilizes a Field-Emission Scanning Electron Microscope (FESEM) to explore the surface morphology of r-PP/LDPE and the interface of r-PP/LDPE/GNPs. Observations are conducted at magnifications of 50X, 100X, 300X, and 500X to capture detailed images. The high-resolution capabilities of the FESEM facilitate the examination of aggregation and dispersion patterns with enhanced clarity. A powerful electron beam is employed to scan the samples, enabling comprehensive inspection, and understanding of surface characteristics and failures. The FESEM equipment utilized for this investigation is depicted in Figure 3.9.

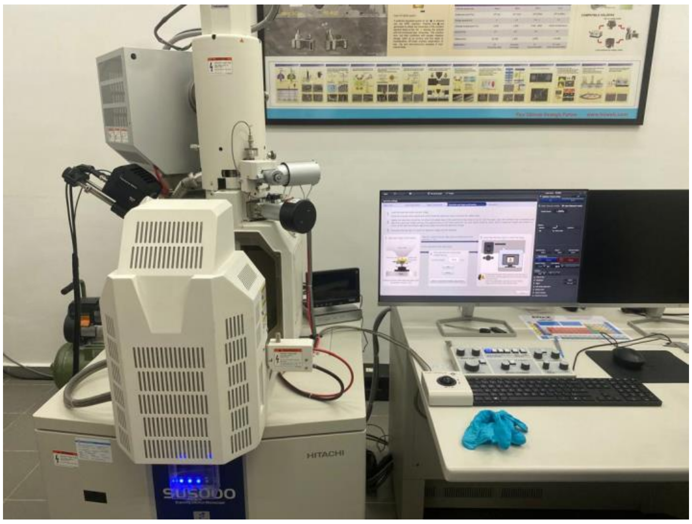

Figure 3.9: FESEM Machine

CHAPTER 4

RESULT AND DISCUSSION

4.1 Overview

A comprehensive overview of the tests that were performed and the analysis that went along with them are provided in this chapter. The primary aim of this study is to employ a melt mixing technique for the development of a novel sustainable material. Subsequently, the Design of Experiment (DOE) was utilized to optimize the experiment's parameters, focusing on three key responses which are tensile strength, flexural strength, and impact strength. A comprehensive discussion of these results was provided. Additionally, this chapter encompasses the findings obtained from the field emission scanning electron microscopy (FESEM) analysis and the density tests.

4.2 Design of experiment (DOE)

This method was performed by using the design expert software with screening utilisation of a two-level full factorial design experiment. About eleven (11) sets of experimental designs with different parametric combinations of temperature (°C) [A], rotor speed (rpm) [B], and r-PP/LDPE ratio[c] are tabulated in the Table 4.2.1. In order to prepare the r-PP/LDPE thermoplastic blend, the 2^3 two-level complete factorial design techniques were used to determine the blend ratio (%) [C]. The Design-Expert 13.0.5 software was used to create the experimental design. The analysis of the experimental design was primarily concerned with the tensile strengths, flexural properties, and impact of the resulting r-PP/LDPE thermoplastic blends. The coded factor's actual values are displayed in the Table 4.2.2. The shortest range for each parameter was represented by a negative one (-); the centre point was represented by a zero (0); and the largest range is represented by a positive one (+). Next, this design has to run eleven (11) sets of tests, as shown in the Table 4.2.2.

Table 4.2.1: Selected level of variables for r-PP/LDPE thermoplastic blend preparation

Temperature (°C) [A]	Rotor speed (rpm) [B]	r-PP/LDPE Blend Ratio (%) [C]
160(-)	300(-)	50(-)
170(0)	400(0)	60(0)
180(+)	500(+)	70(+)

Table 4.2.2: Parametric combination for r-PP/LDPE blend by using a 2^3 two-level full factorials

Std	**Run**	**Factor 1:** A: Temperature Deg. Celsius (°C)	**Factor 2:** B: Rotor Speed (rpm)	**Factor 3:** C: r-PP/LDPE	**r-PP Weight(g)**	**LDPE Weight (g)**	**Response 1 (R1) Tensile Strength (MPa)**	**Response 2 (R2) Flexural Strength (MPa)**	**Response 3 (R3) Impact Strength (J/m^2)**
6	1	160	500	70	105	45	13.9231	19.1953	0.12
11	2	160	300	70	105	45	9.74079	9.37695	0.795
9	3	180	500	70	105	45	12.5332	23.4916	0.127
8	4	170	400	60	90	60	13.3332	14.2337	0.181
5	5	180	300	50	75	75	9.89452	12.9634	0.196
4	6	160	500	50	75	75	12.7275	13.7291	0.115
3	7	170	400	60	90	60	13.211	10.2993	0.089
7	8	160	300	50	75	75	12.7067	13.609	0.1115
1	9	180	500	50	75	75	10.5684	11.243	0.11
2	10	170	400	60	90	60	13.1014	14.298	0.09
10	11	180	300	70	105	45	12.9407	18.3263	0.06

4.2.1 Tensile Strength Analysis of the r-PP/LDPE blend

The results were averaged from six (6) tested specimens from each experimental design at different parametric combinations. The results had revealed that, at the highest r-PP content of 70 wt. %, the lowest temperature at 160 °C, and the higher speed of the rotor at 500 rpm, the tensile strength response had a higher value compared to the other. This event has been proven by run 1, which has a 13.9231 MPa of the tensile strength value. Meanwhile, the tensile strength of run 2 was 9.74079 MPa, which has considerably the lowest among the other test run due to the lowest speed of rotor which was 300 rpm. The result shows that the lowest temperature and lowest speed of rotor in the blending leads to decreasing in the tensile strength value. It has been proven by Husseinsyah et al. (2015) that the tensile characteristics had decrease of with the lower temperature and speed of rotor. Table 4.2.1.1, below shows the parametric combination and the tensile response values for the r-PP/LDPE blends.

Table 4.2.1.1: Parametric combination for r-PP/LDPE blends tensile response values

Std	**Run**	**Factor 1:** A: Temperature Deg. Celsius (℃)	**Factor 2:** B: Rotor Speed (rpm)	**Factor 3:** C: r-PP/LDPE	**r-PP Weight(g)**	**LDPE Weight (g)**	**Response 1 (R1) Tensile Strength (MPa)**
6	1	160	500	70	105	45	13.9231
11	2	160	300	70	105	45	9.74079
9	3	180	500	70	105	45	12.5332
8	4	170	400	60	90	60	13.3332
5	5	180	300	50	75	75	9.89452
4	6	160	500	50	75	75	12.7275
3	7	170	400	60	90	60	13.211
7	8	160	300	50	75	75	12.7067
1	9	180	500	50	75	75	10.5684
2	10	170	400	60	90	60	13.1014
10	11	180	300	70	105	45	12.9407

The half-normal plot of tensile strength response that has generated from the two-level full factorial design of experiment approach was depicted in the following Figure 4.2.1.1. From the effects (factorials) result, factors A (temperature), B (screw speed), and C (blend ratio), as well as the interaction terms between AC, ABC, BC, and AB, were positioned away from the straight line, indicating the significant terms of this experiment (Winson Taam, 2014). The farther the term or interaction term from the half-normal plot, the higher the contribution of the term or interaction term towards the response studied. Next, all model terms were chosen to be analysed through the analysis of variance (ANOVA) test.

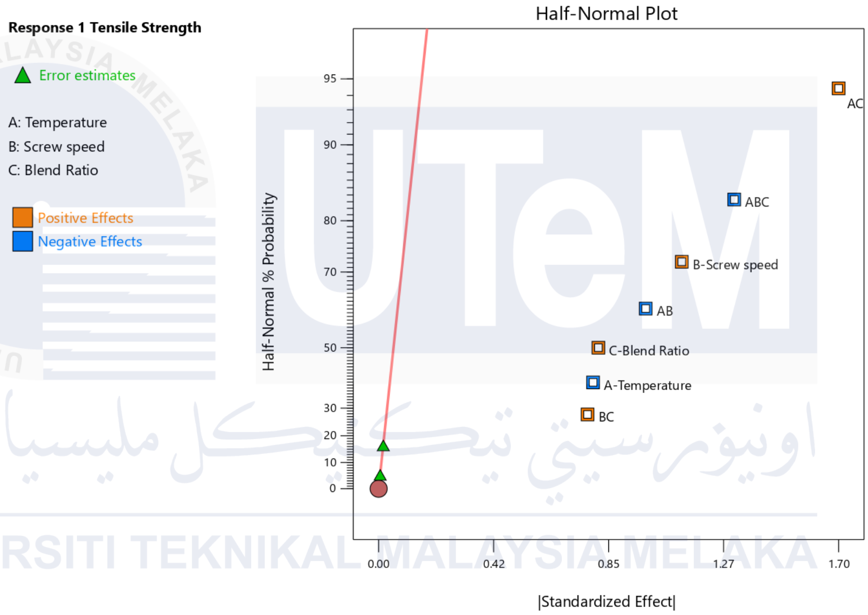

Figure 4.2.1.1: The Half normal plot of r-PP/LDPE blend for the Tensile Strength response

The Table 4.2.1.2 shows a standard deviation of 0.1160, which represents the estimated error of the design. In this case, a smaller standard deviation means a better design, indicating that the tensile strength results were closely aligned with the data set's mean, with a variation of ±12.24. The coefficient of variation (CV%) is 0.9474%, demonstrating the relative consistency and low variability of the results in relation to the mean. Adequate precision, which measures the signal-to-noise ratio, is considered good if it is above four. Here, the ratio is 39.8628, showing a strong signal-to-noise ratio. This have been proven by Oleg Chernoyarov et al., (2022) where precision above four for signal to noise ratio was considered good which indicate the error is small within a wide range of values. Additionally, the R-squared and adjusted R-squared values are 0.9985 and 0.9930, respectively, which are very close to one or unity. This means the data fit the regression model well and were accurately explained by it. Therefore, the experimental model is seen as accurate and effective for navigating the design space due to its high R-squared value.

Table 4.2.1.2: Fit Statistics for the tensile strength response

Std. Dev.	0.1160	**R^2**	0.9985
Mean	12.24	**Adjusted R^2**	0.9930
C.V. %	0.9474	**Predicted R^2**	NA[(1)]
		Adeq Precision	39.8628

Table 4.2.1.3 shows of an F-value of 184.40 for this model, indicating its significant impact, with a mere 0.54% probability of such a high value occurring by chance. Further reinforcing its significance, all p-values are below 0.05, confirming the importance of terms such as A (Temperature), B (Screw speed), C (Blend Ratio), AB, AC, BC, and ABC. Additionally, the curvature F-value of 289.38 highlights significant curvature within the design space, with a mere 0.34% chance of this occurrence being attributed to random noise. Furthermore, the low pure error of 0.0269 indicates minimal random measurement error, ensuring a high level of precision in the data. Moreover, the corrected total of 21.29 includes all the variability observed in the response data, making it an essential benchmark for assessing how well the model explains the data. Notably, the lack of a lack-of-fit value indicates that the experiment was conducted smoothly, without any errors identified by the DOE software. According to Goos and Gilmour (2017), state that the lack of lack of fit value indicates smooth experiment without errors and the DOE software identifies errors in experimental data.

Table 4.2.1.3: ANOVA of experimental data for r-PP/LDPE for tensile strength

Source	Sum of Squares	df	Mean Square	F-value	p-value	
Model	17.37	7	2.48	184.40	0.0054	significant
A-Temperature	1.25	1	1.25	92.84	0.0106	
B-Screw speed	2.50	1	2.50	185.60	0.0053	
C-Blend Ratio	1.31	1	1.31	97.58	0.0101	
AB	1.94	1	1.94	143.99	0.0069	
AC	5.75	1	5.75	427.25	0.0023	
BC	1.19	1	1.19	88.15	0.0112	
ABC	3.44	1	3.44	255.39	0.0039	
Curvature	3.89	1	3.89	289.38	0.0034	
Pure Error	0.0269	2	0.0135			
Cor Total	21.29	10				

The provided coded Equation 4.1 for the tensile strength helps to predict the impact of various factors (A, B, and C) on the tensile strength. The intercept (11.88) represents the baseline tensile strength. Factor A has a negative impact, while factors B and C positively influence tensile strength. Key interactions include a negative effect when both A and B are high, a strong positive effect between A and C, and a three-way interaction where high levels of all three factors reduce tensile strength. Optimizing tensile strength involves increasing factors B and C while carefully managing factor A and considering the significant interactions among the factors.

Tensile Strength = + 11.88 -0.3951 *A +0.5587*B +0.4051*C -0.4921*A*B +0.8477*A*C +0.3850*B*C -0.6554*A*B*C (Equation 4.1)

The provided Equation 4.2 uses actual factors to predict tensile strength based on Temperature, Screw Speed, and Blend Ratio. The analysis shows that increases in each factor individually decrease tensile strength, with coefficients of (-1.92413) for Temperature, (-0.602324) for Screw Speed, and (-6.01095) for Blend Ratio. Positive interaction terms, such as (+0.003440) for Temperature and Screw Speed and (+0.034691) for Temperature and Blend Ratio, indicate some beneficial combinations of factors that can mitigate the negative impacts. The very small negative three-way interaction term (-0.000066) suggests a minor decrease when all three factors increase together. In real-life experiments, actual equations are preferred over coded equations because it provide direct, practical predictions based on real-world measurements, making them more applicable and actionable in practical settings (Vuong et al., 2023).

Tensile Strength = +343.55698 -1.92413 *Temperature -0.602324* Screw Speed - 6.01095* Blend Ratio +0.003440 *Temperature* Screw Speed +0.034691*Temperature*Blend Ratio +0.011526* Screw Speed*Blend Ratio - 0.000066*Temperature*Screw Speed*Blend Ratio (Equation 4.2)

A three-dimensional response surface contour plot was utilised to interpret and evaluate the produced statistical model, as depicted in the following Figures 4.2.1.2, Figure 4.2.1.3 and Figure 4.2.1.4. The surface plot of the tensile strength response was based on the regresses of temperature (°C) [A], rotor speed (rpm) [B], and r-PP/LDPE blend ratio (%) [C]. The interaction of three (3) factors through the response surface plot has helped to understand and locate the optimum level between the results. In the Figure 4.2.1.2 from the tensile response surface plot indicate the results of the tensile strength are 13.3332 (MPa) in range for three control sample which are the sample 4,7 and 10. These control sample are being apply 170(°C), 400 rpm and ratio 60% of the r-pp.

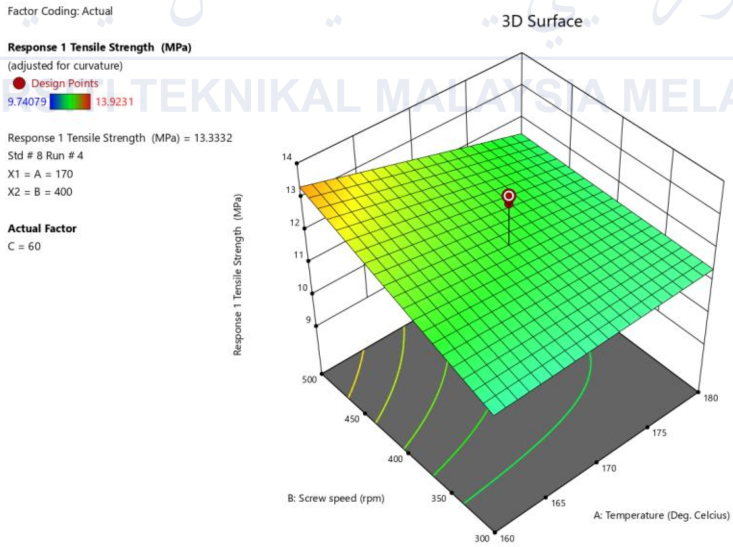

Figure 4.2.1.2: The AB interaction with 60 ratios of r-PP

In the Figure 4.2.1.3 these sample are being use ratio 50% of r-PP. The lowest tensile strength is 9.89452 (MPa) which are from sample 5 were at dark blue region. This sample undergoes high in temperature but use lower speed of the screw speed. This due to the most of both material of r-PP and the LDPE making incomplete bonding (Ding et al., 2022). Both r-PP and LDPE properties are being change since 50% are the portion of both materials. Meanwhile the highest tensile strength for this ratio of 50% r-PP is 12.7275 (MPa) which are from sample 6 which located at light green area. This sample undergoes low temperature but high in screw speed. Meanwhile, the speed of the screw gives increasing in tensile strength same for sample 9 which are 10.5684 (MPa) which located at light blue region even though using high temperature. This due to the tendency of shear forces inside the extruder are increased by high screw speeds. Therefore, it effects in a more homogenous mix by enhancing the polymer components' dispersion and distribution (Rahmat Saat and Rasid., 2022). Even though the screw speed contributed high in tensile strength, low temperature and low screw speed also give increasing in tensile strength which is 12.7067(MPa) proven by sample 8. This was due to the length and structure of the polymer chains are preserved at lower temperatures, which is essential for preserving high tensile strength. Lower processing temperatures are beneficial for heat-sensitive polymers because they better preserve their mechanical properties (Buzdugan et al., 2022).

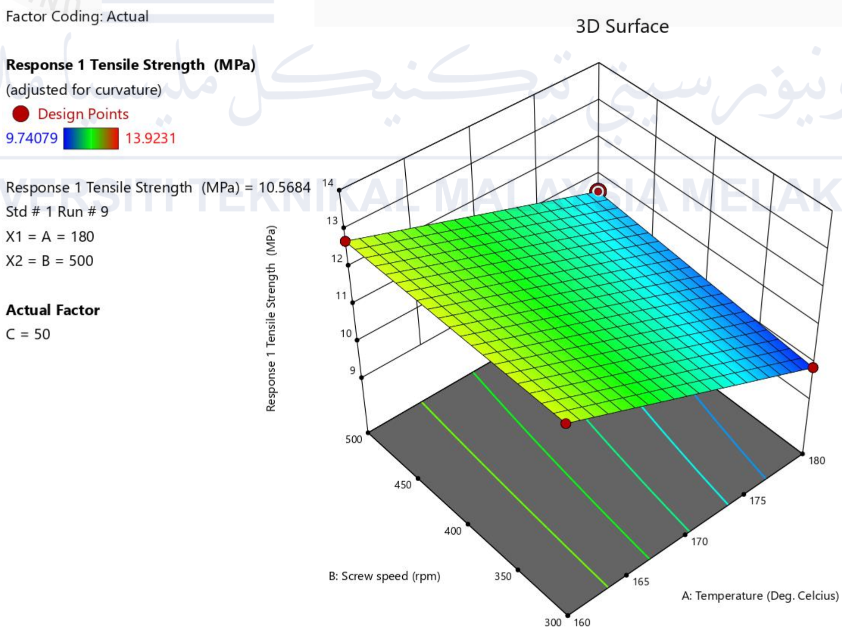

Figure 4.2.1.3: The AB interaction with 50 ratios of r-PP

In Figure 4.2.1.3, these 4 samples are use 70% contain r-pp in the thermoplastic blend. The highest tensile strength that can achieve from this blend ratio is 13.9231 MPa from sample 1 with low temperature and high-speed screw apply. Reduced processing temperatures reduce the possibility of the polymers degrading thermally. The material keeps its natural strength properties by preserving the polymers' molecular integrity (Krzysztof Pielichowski et al., 2023). The second highest in these studies are from sample 11 which are undergoes high temperature but low in screw speed which is 12.9407 MPa. High recycle PP Content led to increasing the proportion of r PP in the blend enhances the tensile strength due to r PP’s higher inherent tensile properties (Zhang et al., 2022). This makes the blend stiffer and stronger. Meanwhile sample 3 give 12.5332 MPa where this sample undergoes high in both temperature and screw speed. The result slightly below the control sample due to the high in 3 of parameters which are temperature, speed rate and ratio. The lowest tensile strength was from sample 2 which is 9.74079 MPa which are undergoes low in both temperature and speed rate.

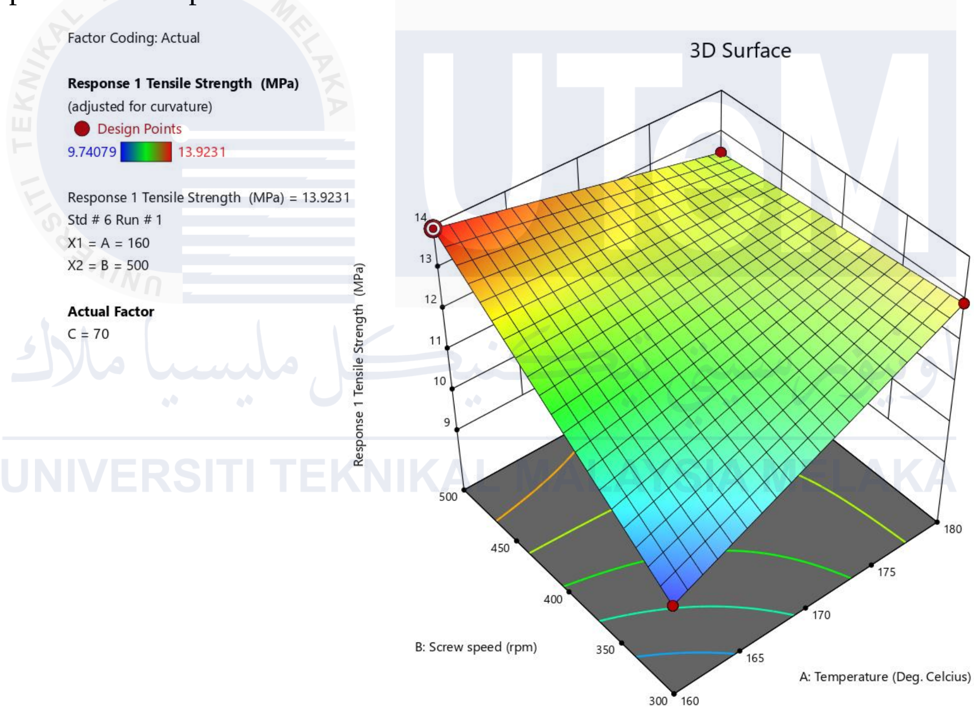

Figure 4.2.1.4: The AB interaction with 70 ratios of r-PP

In Figure 4.5, the cube graph provides a comprehensive visualization of the effects and interactions between the three factors in this DOE study which are temperature (A), screw speed rate (B), and blend ratio (C). Each axis of the cube represents one of these factors, with the corners indicating the combinations of their high and low levels. For instance, the back corner on the left representing (160°C, 300 rpm, 70%) corresponds to a tensile strength of 9.74079 MPa. Furthermore, the interaction between temperature, screw speed, and blend ratio significantly impacts the tensile strength. At low temperature (160°C), increasing the screw speed from 300 rpm to 500 rpm results in an increase in tensile strength. However, at low screw speed (300 rpm) and high temperature (180°C), this results in one of the lower tensile strengths, which was at 9.89452 MPa. These findings are critical for optimizing the extrusion process. By carefully selecting the temperature, screw speed, and blend ratio settings, it can maximize the tensile strength of the polymer blend, which was essential for improving product performance.

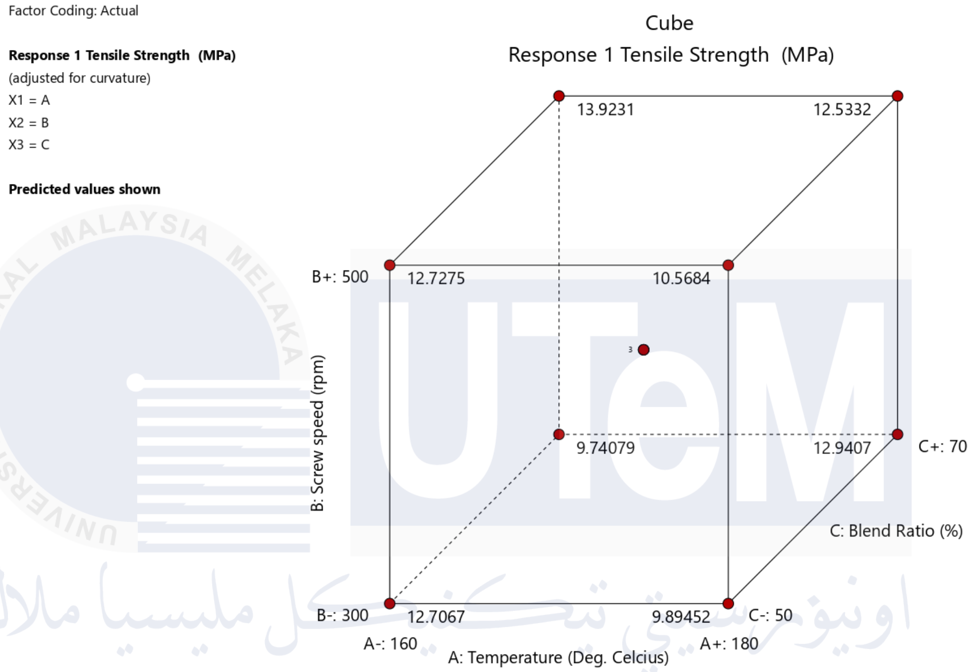

Figure 4.2.1.5: The 3D cube of tensile strength analysis

4.2.2 Flexural Strength Analysis on r-PP/LDPE blend

The findings were derived by calculating the average of four samples tested for each experimental design across various parametric combinations. The data derived from the studies on the effects of different factors on the flexural strength (R2) of the material. Upon examination, the highest flexural strength recorded was 23.4916 MPa, occurring in sample three (3) under the conditions of 180°C temperature, 500 rpm rotor speed, and an r-PP/LDPE blend ratio of 70. This have been proven by Muhammad Ariya Afif et al., (2022) which state that high ratio of r-PP, high temperature and high speed of rotor can enhance the flexural properties of the materials. Conversely, the lowest flexural strength observed was 9.37695 MPa, noted in sample 2 with a temperature of 160°C, rotor speed of 300 rpm, and the same blend ratio of 70. For the control samples (sample 4, 7, and 10), identical temperature, rotor speed, and r-PP blend ratio settings were implemented. This uniformity ensures the accuracy of the experiment. Table 4.6 below shows the parametric combination and flexural response values for r-PP/LDPE blends.

Table 4.2.2.1: Parametric combination for r-PP/LDPE blend flexural response values

Std	**Run**	**Factor 1:** A: Temperature Deg. Celsius (°C)	**Factor 2:** B: Rotor Speed (rpm)	**Factor 3:** C: r-PP/LDPE	**r-PP Weight(g)**	**LDPE Weight (g)**	**Response 2 (R2) Flexural Strength (MPa)**
6	1	160	500	70	105	45	19.1953
11	2	160	300	70	105	45	9.37695
9	3	180	500	70	105	45	23.4916
8	4	170	400	60	90	60	14.2337
5	5	180	300	50	75	75	12.9634
4	6	160	500	50	75	75	13.7291
3	7	170	400	60	90	60	10.2993
7	8	160	300	50	75	75	13.609
1	9	180	500	50	75	75	11.243
2	10	170	400	60	90	60	14.298
10	11	180	300	70	105	45	18.3263

The Figure 4.2.2.1 half-normal probability plot clearly shows which factors and interactions significantly influence flexural strength. The most important finding is that the C-Blend Ratio has the most substantial effect on flexural strength, indicating that the blend ratio is a key parameter to optimize. Additionally, interactions BC and AC, as well as B-Screw Speed, also play significant roles and should be considered in further experiments. On the other hand, factors like A-Temperature and the interaction AB are less impactful, meaning their optimization may not be as crucial. The factor ABC is near to the redline indicating it has a minimal effect on the experiment. Redline indicates factors with lower impact on the experiment (Winson Taam, 2014).

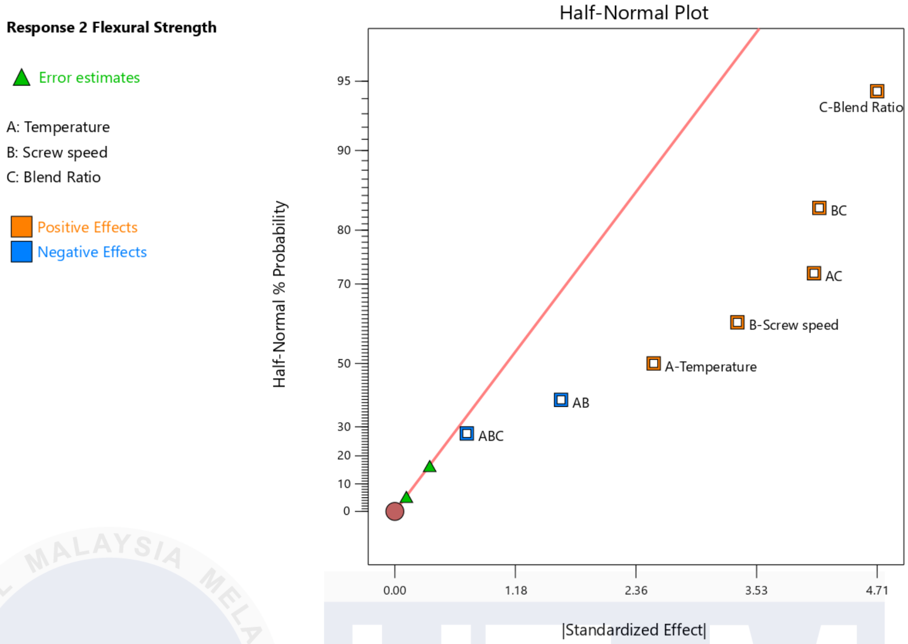

Figure 4.2.2.1: The Half normal plot of r-PP/LDPE blend flexural Strength response (R2)

The fit statistics Table 4.2.2.2 provide key insights into the model's performance. The standard deviation (2.29) and mean (14.62) highlight the dataset's variability and central tendency, respectively. The coefficient of variation (15.67%) indicates a moderate level of dispersion relative to the mean. The R^2 value of 0.9361 suggests that a significant proportion of the variance in the dependent variable is explained by the model. However, the adjusted R^2 value of 0.7125, which accounts for the number of predictors, indicates a moderate fit when considering the model's complexity. The Predicted R^2 is not defined due to case(s) with leverage of 1.0000, which suggests that the current model may not predict new data effectively, implying that the overall mean could be a better predictor. This suggests that the current model may benefit from refinement or the inclusion of higher-order terms to improve predictive accuracy. Nonetheless, the Adeq Precision value of 6.8131, which is above the desired threshold of 4, indicates a strong signal-to-noise ratio, signifying that the model is adequate for navigating the design space and can be used confidently in the experimental design process.

Table 4.2.2.2: Fit Statistics data for flexural strength

Std. Dev.	2.29	**R^2**	0.9361
Mean	14.62	**Adjusted R^2**	0.7125
C.V. %	15.67	**Predicted R^2**	NA(1)
		Adeq Precision	6.8131

Table 4.2.2.3 shows an F-value of 4.19 for this model, indicating its significant impact, with a mere 20.63% probability of such a high value occurring by chance. Further reinforcing its significance, all p-values are above 0.05, confirming the lack of importance of terms such as A (Temperature), B (Screw speed), C (Blend Ratio), AB, AC, BC, and ABC. Additionally, the curvature F-value of 2.20 highlights non-significant curvature within the design space, with a 27.65% chance of this occurrence being attributed to random noise. Furthermore, the low pure error of 5.25 indicates minimal random measurement error, ensuring a high level of precision in the data. Moreover, the corrected total of 175.75 includes all the variability observed in the response data, making it an essential benchmark for assessing how well the model explains the data. Notably, the lack of a lack-of-fit value indicates that the experiment was conducted smoothly, without any errors identified by the DOE software.

Table 4.2.2.3: ANOVA of experimental data for r-PP/LDPE for flexural strength

Source	Sum of Squares	df	Mean Square	F-value	p-value	
Model	153.73	7	21.96	4.19	0.2063	not significant
A-Temperature	12.79	1	12.79	2.44	0.2589	
B-Screw speed	22.39	1	22.39	4.27	0.1748	
C-Blend Ratio	44.39	1	44.39	8.46	0.1006	
AB	5.27	1	5.27	1.00	0.4217	
AC	33.53	1	33.53	6.39	0.1273	
BC	34.38	1	34.38	6.55	0.1247	
ABC	0.9888	1	0.9888	0.1885	0.7065	
Curvature	11.52	1	11.52	2.20	0.2765	
Pure Error	10.49	2	5.25			
Cor Total	175.75	10				

The Equation 4.3 in terms of coded factors serves as a predictive tool for assessing the impact of various factors on flexural strength in the r-PP/LDPE blend. The intercept coefficient of 15.24 indicates the average response, while positive coefficients for Temperature (1.26), Screw speed (1.67), and Blend Ratio (2.36) suggest their beneficial effects. Interaction terms such as AC (2.05) and BC (2.07) show significant positive impacts, whereas AB (-0.8117) and ABC (-0.3516) have less influence. The standard error for all coefficients is 0.8098, with 95% confidence intervals ensuring reliability. All VIF values are 1.0000, indicating no multicollinearity. This analysis underscores the significant contribution of individual and interaction factors to the flexural strength, guiding the optimization of process parameters.

Response 2

Flexural Strength= +15.24 +1.26*A+1.67*B+2.36*C 0.8117*AB+2.05*AC+2.07*BC-0.3516*ABC (Equation 4.3)

The relationship between numerous parameters and the flexural strength of the r-PP/LDPE blend is clarified by the presented regression equation. The Equation 4.4 states that the blend ratio, temperature, screw speed, and their interactions all affect the baseline flexural strength, which is 319.73152. Flexural strength decreases with decreasing temperature (-1.62096), screw speed (-0.328262), or blend ratio (-6.46448). Furthermore, the terms in the formula show how two factors working together can affect flexural strength: Temperature * Screw speed (+0.001298), Temperature * Blend Ratio (+0.034534), Screw speed * Blend Ratio (+0.008050), and Temperature * Screw speed * Blend Ratio (-0.000035). The response for a given level of each factor can be predicted using the equation when it is represented in terms of actual factors. For precise projections, it is important to provide the levels in the original units. Additionally, the intercept is not located at the centre of the design space instead, the coefficients in the equation are scaled to account for the units of each element. As a result, precaution should be taken when applying each factor's relative impact from its coefficient values alone.

Response 2

Flexural Strength= +319.73152-1.62096* Temperature-0.328262* Screw speed-6.46448*Blend Ratio +0.001298*Temperature*Screw speed +0.034534*Temperature * Blend Ratio+0.008050*Screw speed * Blend Ratio-0.000035*Temperature * Screw speed * Blend Ratio (Equation 4.4)

Figure 4.2.2.2 illustrates the interaction between Temperature (A) and Screw Speed (B) for a control sample with a 60 ratio of r-PP, focusing on sample 4, 7, and 10, all processed at a temperature of 170°C and a screw speed of 400 rpm. The flexural strength results are 14.2337 MPa for sample 4, 10.2993 MPa for sample 7, and 14.298 MPa for sample 10. Despite identical processing conditions, the flexural strengths vary, suggesting potential material property variability or slight differences in the processing environment. The average flexural strength across these runs is around 13 MPa, highlighting the need for consistent processing conditions and material homogeneity to achieve reliable mechanical properties in recycled polymer blends. This have been proven by Titone et al., (2023) were the inhomogeneity affects mechanical properties due to inconsistent dispersion.

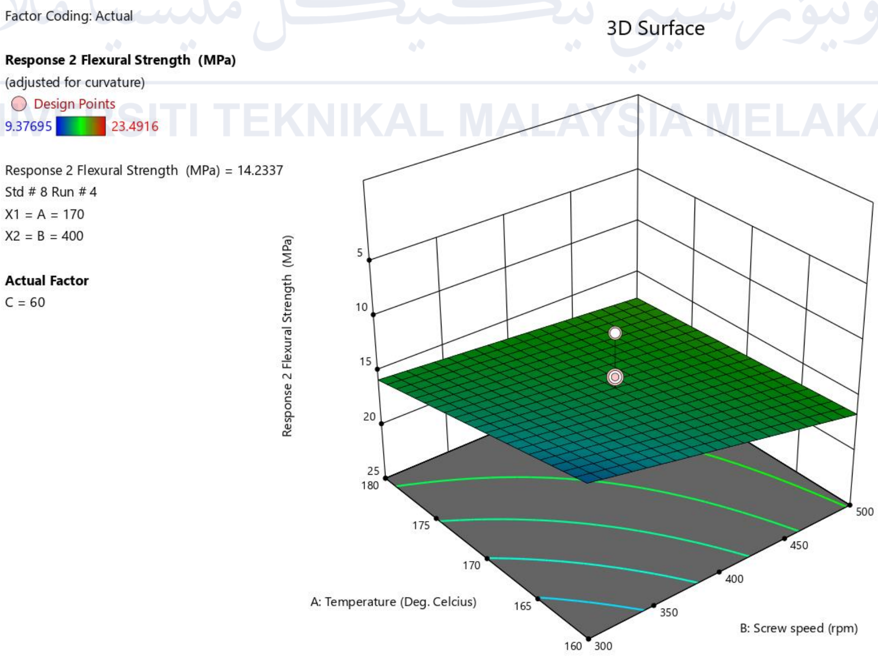

Figure 4.2.2.2: The AB interaction with 60 ratios of r-PP

Figure 4.2.2.3 illustrates the interaction between Temperature (A) and Screw Speed (B) for a 50 ratio of r-PP, applied to sample 9, 6, 8, and 5. The lowest flexural strength is observed in sample 9, with a value of 11.243 MPa, occurring at high temperature and high screw speed. The highest flexural strength, 13.7291 MPa, is sample in run 6, achieved with low temperature and high screw speed. This is because lower processing temperatures can lead to a higher degree of crystallinity in the polymer matrix. Higher crystallinity often results in improved stiffness and strength, contributing to higher flexural strength (SalakhovSs et al., 2021). Other notable results include 13.609 MPa in sample 8 and 12.9634 MPa in sample 5. This graph demonstrates that within this ratio, varying Temperature and Screw Speed impacts the flexural strength, with high screw speeds generally resulting in higher flexural strengths.

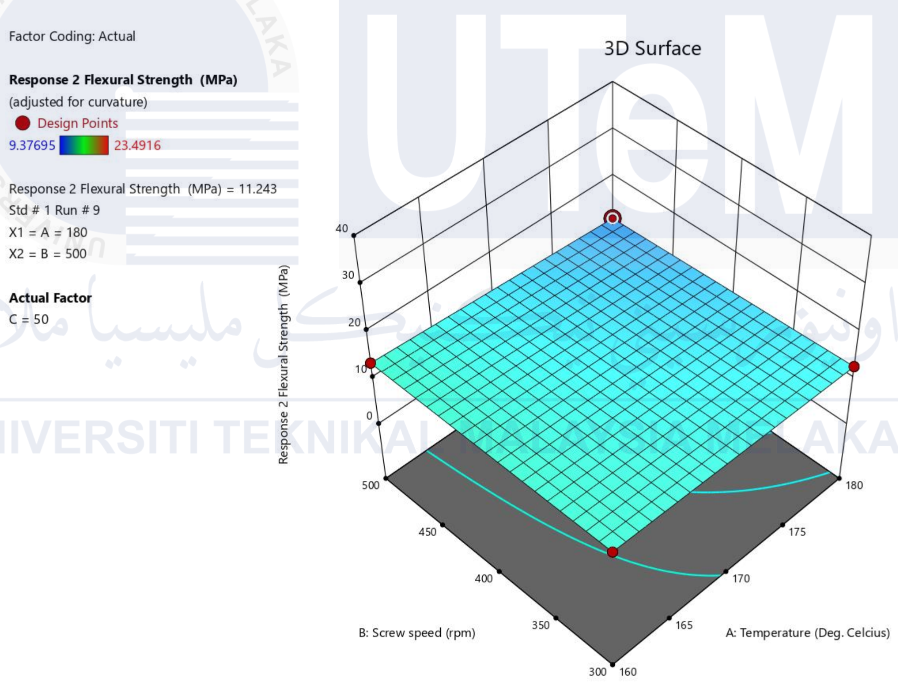

Figure 4.2.2.3: The AB interaction with 50 ratios of r-PP

Figure 4.2.2.4 depicts the interaction between Temperature (A) and Screw Speed (B) with a 70 ratio of r-PP on flexural strength. The highest flexural strength, 23.4916 MPa, occurs in the orange region, corresponding to high temperature and screw speed (sample 3). The blue region shows the lowest flexural strength of 9.37695 MPa, resulting from low temperature and screw speed (sample 2). Intermediate flexural strengths are represented in the greenish region, with values of 18.3263 MPa and 19.1953 MPa from sample 11 and 1, respectively. This graph had effectively illustrates how varying these factors impacts the material's flexural strength, demonstrating that higher temperature and screw speed enhance strength, while lower settings reduce it (Khamis et al., 2017). The experimental setup involved adjusting these factors during the extrusion process to observe their effects on the flexural strength of the r-PP blend.

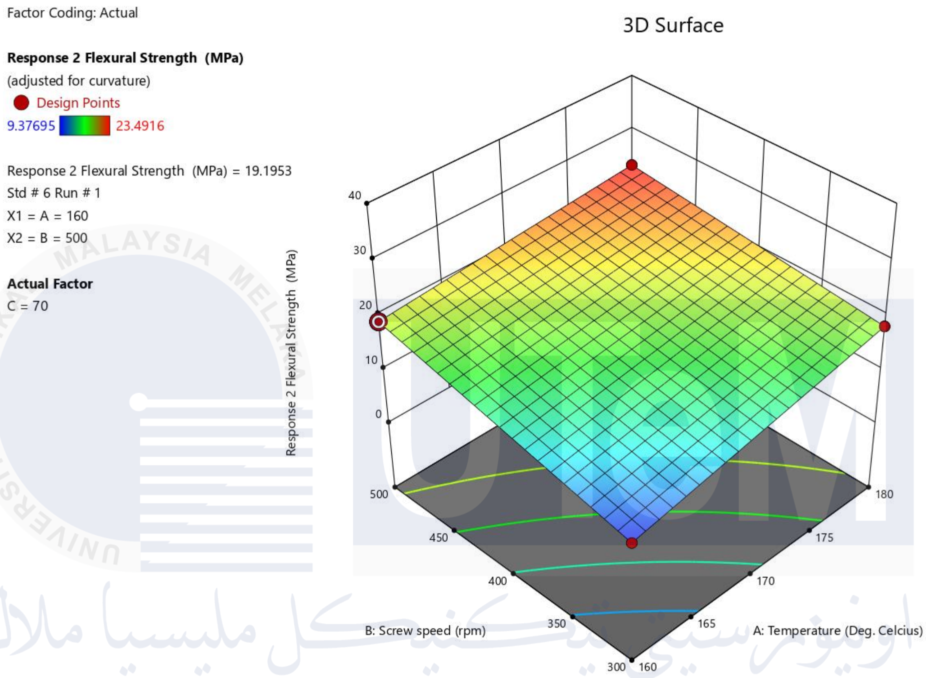

Figure 4.2.2.4: The AB interaction with 70 ratios of r-PP

The Figure 4.2.2.5 illustrates the significant interactions between temperature (A), screw speed (B), and blend ratio (C) on flexural strength in this DOE study. Notably, increasing the screw speed from 300 rpm to 500 rpm at both low (160°C) and high temperatures (180°C) results in increased flexural strength, with the highest observed strength of 23.4916 MPa at 180°C, 500 rpm, and a 70% blend ratio. Conversely, the lowest strength of 9.37695 MPa occurs at 160°C, 300 rpm, and a 50% blend ratio. This have been proven by previous studies which low ratio of r-PP and LDPE leads to low flexural strength (S. Ray Chowdhury et al., 2015). These findings highlight the importance of optimizing temperature, screw speed, and blend ratio to maximize the flexural strength of the polymer blend, crucial for enhancing product performance.

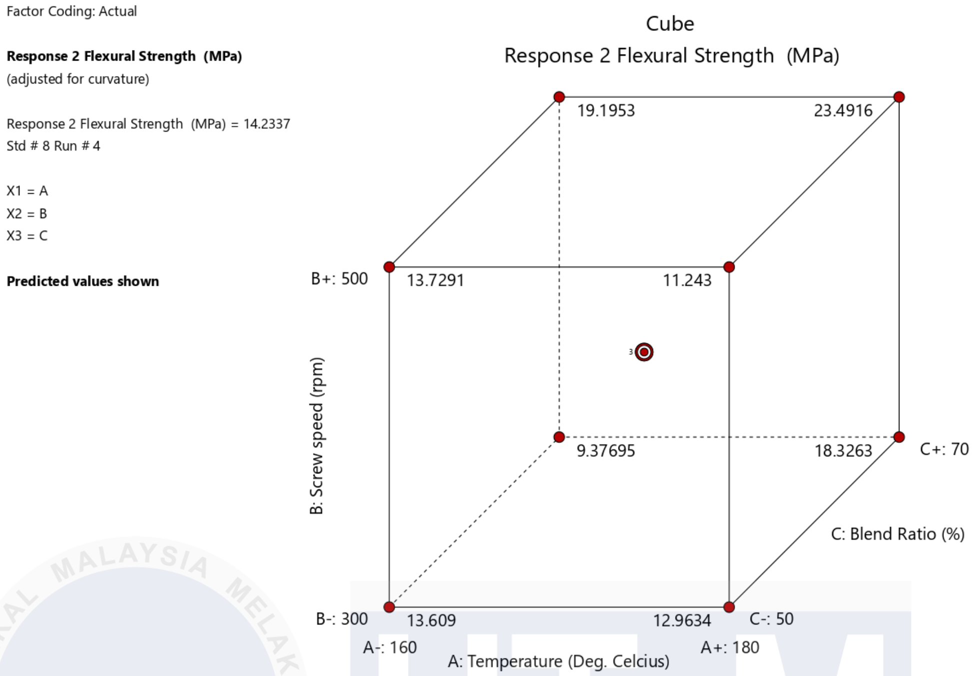

Figure 4.2.2.5: The 3D cube of flexural strength analysis

4.2.3 Impact Strength Analysis on r-PP/LDPE blend

The impact strength analysis of the r-PP/LDPE blend, averaged from four tested samples for each experimental design, shows that the highest impact strength of 0.795 J/m² is achieved at a lower temperature of 160°C, a rotor speed of 300 rpm, and a blend ratio of 70% r-PP, highlighting the significance of these parameters in enhancing mechanical properties. This is because better polymer blending, at lower speeds and temperatures, the mixing might be gentler, allowing for better blending and dispersion of the recycled PP (r-PP) and LDPE without causing phase separation or agglomeration (Barati et al., 2023). A well-dispersed blend typically shows improved mechanical properties, including impact strength. In contrast, the lowest impact strength of 0.06 J/m² occurs at a higher temperature of 180°C, the same rotor speed, and a balanced blend ratio of 50% r-PP to 50% LDPE, indicating that higher temperatures and less optimal blend ratios reduce impact strength. These results, as summarized in Table 4.2.3.1, underscore the necessity of optimizing processing conditions to improve the mechanical performance of polymer blends.

Table 4.2.3.1: Parametric combination for r-PP/LDPE blend impact strength response values (R3)

Std	**Run**	**Factor 1:** A: Temperature Deg. Celsius (℃)	**Factor 2:** B: Rotor Speed (rpm)	**Factor 3:** C: r-PP/LDPE	**r-PP Weight(g)**	**LDPE Weight (g)**	**Response 3 (R3) Impact Strength (J/m^2)**
6	1	160	500	70	105	45	0.12
11	2	160	300	70	105	45	0.795
9	3	180	500	70	105	45	0.127
8	4	170	400	60	90	60	0.181
5	5	180	300	50	75	75	0.196
4	6	160	500	50	75	75	0.115
3	7	170	400	60	90	60	0.089
7	8	160	300	50	75	75	0.1115
1	9	180	500	50	75	75	0.11
2	10	170	400	60	90	60	0.09
10	11	180	300	70	105	45	0.06

The Half-Normal Probability Plot in Figure 4.2.3.1 provides a clear visualization of which factors and interactions have a significant impact on the impact strength of the r-PP/LDPE blend. The plot reveals that the interaction between the three factors (ABC) has the most substantial effect, highlighting its critical role in determining the impact strength. The interactions AC and BC, along with the main effect of B-Screw Speed, also show significant influence and should be prioritized in optimization efforts. Conversely, the main effects of A-Temperature and C-Blend Ratio, as well as the interaction AB, appear to have lesser impacts, suggesting that their optimization may not be as crucial. This analysis underscores the importance of considering multiple factors and their interactions to enhance the impact strength of the polymer blend. The redline in the plot indicates factors with lower impact on the experiment, guiding further experimental design and process adjustments to focus on the most influential parameters.

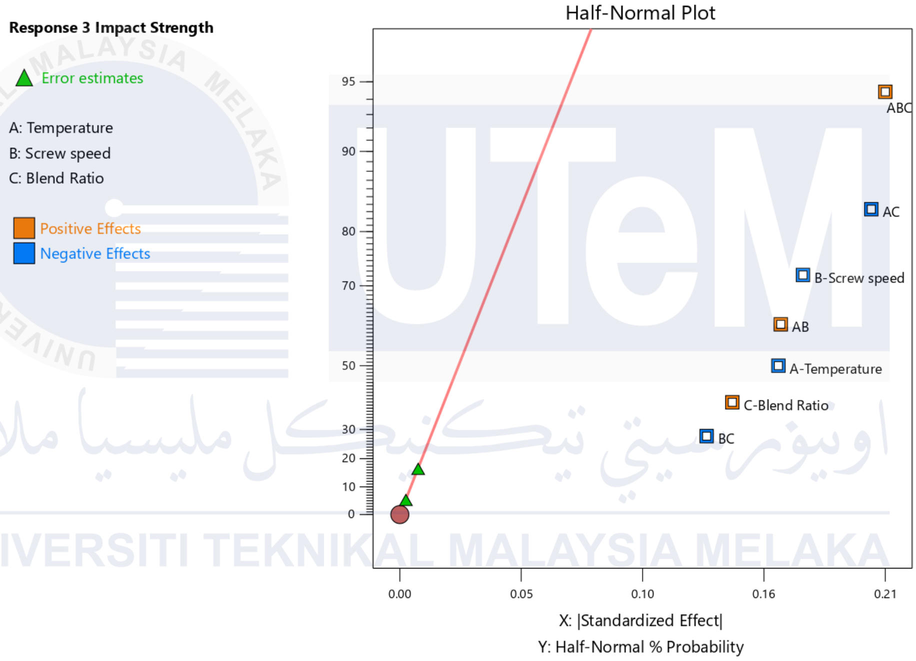

Figure 4.2.3.1: The Half normal plot of r-PP/LDPE blend impact strength response (R3)

Table 4.2.3.2 presents the fit statistics for the flexural strength model, indicating its strong reliability and predictive capability. The model shows a high R^2 value of 0.9865, meaning it explains 98.65% of the variability in flexural strength. The Adjusted R^2 value of 0.9393 supports the accuracy of the model, accounting for the number of predictors. The standard deviation of 0.0528 and mean of 0.1813 reflect precise measurements with low variability. The coefficient of variation (C.V.) of 29.14% indicates a moderate level of dispersion. The Adequate Precision ratio of 15.3809, well above the desirable threshold of 4, confirms a strong signal-to-noise ratio, making the model suitable for navigating the design space. Overall, these statistics validate the model's effectiveness in predicting flexural strength, resulting from carefully chosen parameters and controlled experimental conditions.

Table 4.2.3.2: Fit Statistics data for impact strength (R3)

Std. Dev.	0.0528	**R^2**	0.9865
Mean	0.1813	**Adjusted R^2**	0.9393
C.V. %	29.14	**Predicted R^2**	NA(1)
		Adeq Precision	15.3809

Table 4.2.3.3 presents the ANOVA results for the impact strength of the r-PP/LDPE blend, revealing a significant model with an F-value of 20.90 and a p-value of 0.0464, indicating a very low probability (4.64%) that this result is due to random noise. The significant factors identified include A-Temperature, B-Screw Speed, AB, AC, and ABC interactions, all with p-values less than 0.05. This suggests these factors and interactions significantly influence the impact strength. Specifically, the ABC interaction has the most substantial effect with a sum of squares of 0.0864 and an F-value of 30.97. Conversely, factors like C-Blend Ratio and BC interactions show higher p-values, indicating a lesser impact. The model's curvature F-value of 5.56, though not highly significant, suggests some degree of curvature in the design space. The low pure error sum of squares (0.0056) reflects minimal random measurement error, underscoring the precision of the data (Mellenbergh, 2019). The corrected total sum of squares (0.4295) encompasses all observed variability, serving as a comprehensive benchmark for model assessment. This analysis confirms the critical parameters and interactions that need optimization to enhance the impact strength of the polymer blend.

Table 4.2.3.3: ANOVA of experimental data for r-PP/LDPE for impact strength

Source	Sum of Squares	df	Mean Square	F-value	p-value	
Model	0.4084	7	0.0583	20.90	0.0464	significant
A-Temperature	0.0526	1	0.0526	18.84	0.0492	
B-Screw speed	0.0596	1	0.0596	21.35	0.0438	
C-Blend Ratio	0.0405	1	0.0405	14.53	0.0625	
AB	0.0532	1	0.0532	19.07	0.0486	
AC	0.0815	1	0.0815	29.20	0.0326	

BC	0.0345	1	0.0345	12.37	0.0722	
ABC	0.0864	1	0.0864	30.97	0.0308	
Curvature	0.0155	1	0.0155	5.56	0.1425	
Pure Error	0.0056	2	0.0028			
Cor Total	0.4295	10				

The final equation for Response 3 Impact Strength as shown in the Equation 4.5. The intercept (0.2043) represents the baseline impact strength when all factors are at their centre points. Factors A (temperature) and B (screw speed) negatively impact strength, decreasing it by 0.0811 and 0.0863 units, respectively, while factor C (blend ratio) positively affects it, increasing the strength by 0.0712 units. The interaction between factors A and B slightly increases impact strength by 0.0816 units, whereas interactions between A and C, and B and C, reduce it by 0.1009 and 0.0657 units, respectively. The three-way interaction among A, B, and C results in a positive effect, increasing impact strength by 0.1039 units. This equation highlights the complex interplay between temperature, screw speed, and blend ratio, with careful adjustments needed to optimize impact strength in recycled PP and LDPE blends during the extrusion process.

Response 3

Impact Strength= +0.2043 -0.0811*A -0.0863*B+0.0712*C+0.0816 *AB

-0.1009*AC -0.0657* BC +0.1039*ABC (Equation 4.5)

The final equation in terms of actual factors provides a comprehensive model for predicting the impact strength of the r-PP/LDPE blend based on specific levels of temperature, screw speed, and blend ratio shown in the Equation 4.6. The equation shows that the baseline impact strength is -47.23188 when all factors are at zero. The impact strength increases with temperature (+0.269281), screw speed (+0.095229), and blend ratio (+0.911763), indicating their positive contributions. However, interactions such as Temperature * Screw speed (-0.000542), Temperature * Blend Ratio (-0.005167), and Screw speed * Blend Ratio (-0.001833) exhibit negative effects, while the three-way interaction (Temperature * Screw speed * Blend Ratio) has a minimal positive effect (+0.000010). These coefficients help predict the impact strength for different levels of each factor when specified in their original units. It is important to note that the coefficients are scaled for the units of each factor, and the intercept is not at the design space's center, so the equation should not be used to determine the relative impact of each factor directly.

Response 3

Impact Strength=-47.23188 +0.269281*Temperature +0.095229* Screw speed +0.911763*Blend Ratio -0.000542*Temperature * Screw speed -0.005167 *Temperature * Blend Ratio -0.001833*Screw speed * Blend Ratio +0.000010*Temperature * Screw speed * Blend Ratio (Equation 4.6)

Figure 4.2.3.2 shows the impact strength for three control samples with a 60 ratio of r-PP, all processed at 170°C and 400 rpm, resulting in values of 0.181 J/m² for run 4, 0.089 J/m² for run 7, and 0.09 J/m² for run 10. Despite identical processing parameters, variations in impact strength occur due to factors such as material inhomogeneity, slight processing variations, measurement errors, microstructural differences, and aging or degradation of the recycled polymers. These findings highlight the need for stringent control over material quality and processing conditions to achieve consistent mechanical properties in the recycled polymer blends.

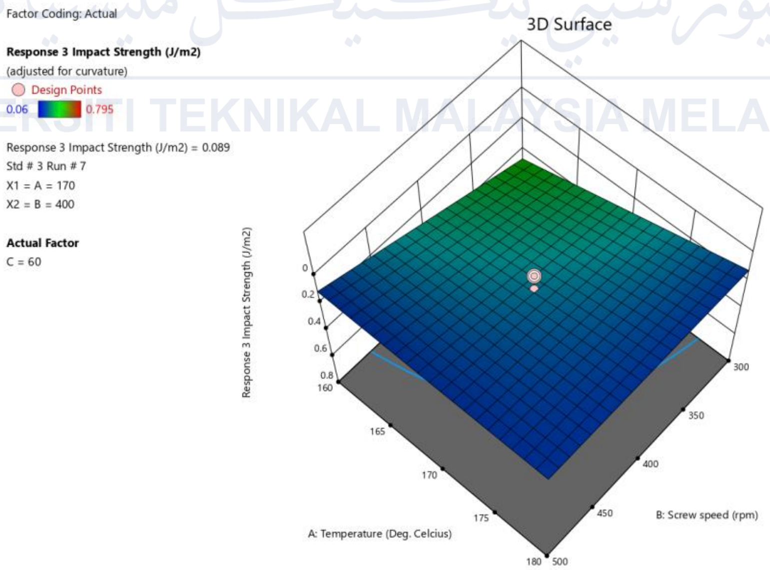

Figure 4.2.3.2: The AB interaction with 60 ratios of r-PP

Figure 4.2.3.3 demonstrates the interaction between Temperature (A) and Screw Speed (B) for a 50 ratio of r-PP on impact strength. The highest impact strength value, 0.196

J/m², is observed in run 5, which employed low temperature and low screw speed. This indicates that these conditions are favourable for maximizing impact strength in this specific blend ratio. This have been proven by Rosales et al. (2022) at previous studies which state r-PP in high ratio blend has high impact strength. Conversely, the lowest impact strength of 0.11 J/m² is seen in run 9, which used high temperature and high screw speed, suggesting that these conditions are detrimental to impact strength. Other runs, such as run 6 and run 8, show intermediate impact strengths of 0.115 J/m² and 0.1115 J/m², respectively, highlighting the influence of different combinations of temperature and screw speed on the material's performance. These results suggest that lower temperatures and screw speeds tend to enhance impact strength, likely due to reduced thermal degradation and better polymer blend homogeneity.

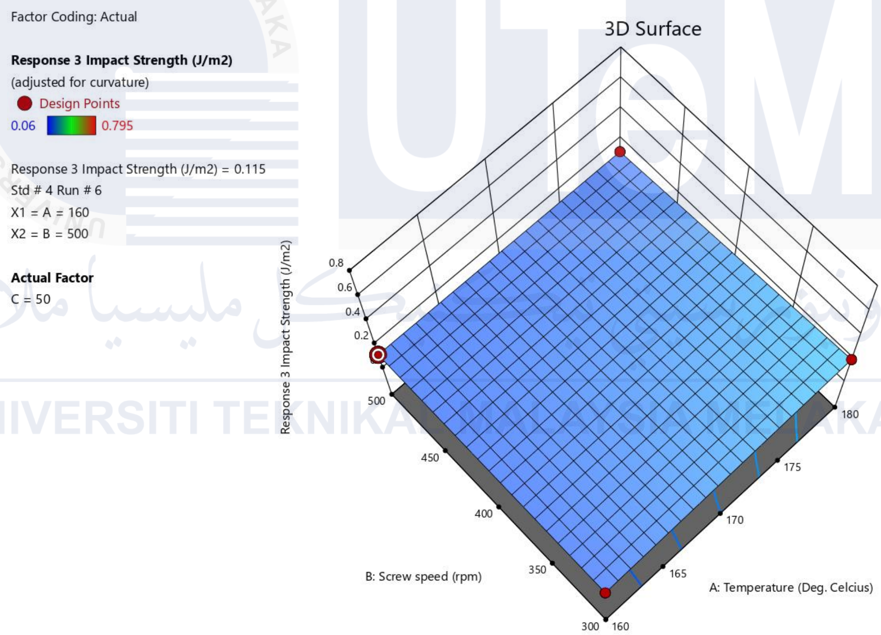

Figure 4.2.3.3: The AB interaction with 50 ratios of r-PP

Figure 4.2.3.4 illustrates the interaction between Temperature (A) and Screw Speed (B) for a 70 ratio of r-PP on impact strength. The highest impact strength, 0.795 J/m², is observed in run 2, which used the lowest temperature (160°C) and the lowest screw speed (300 rpm). The lowest impact strength, 0.06 J/m², is seen in run 11, which applied the highest temperature (180°C) and the lowest screw speed (300 rpm). Applying high temperatures causes microstructural changes within the polymer blend, such as the formation of larger spherulites or phase separation between r-PP and LDPE, which can weaken the material (Fomicheva & Serenko, 2023). These changes can create weak points in the material, leading to reduced impact strength. Runs 1 and 3, which also used a 70 ratio of r-PP, show intermediate impact strengths of 0.12 J/m² and 0.127 J/m², respectively. This data suggests that lower temperatures and screw speeds tend to enhance the impact strength of the r-PP blend, while higher temperatures reduce it.

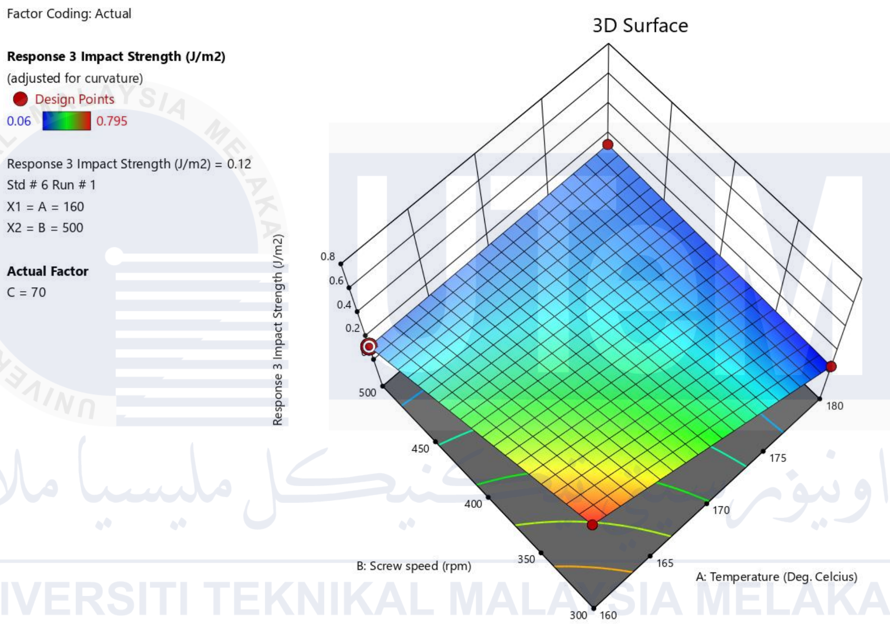

Figure 4.2.3.4: The AB interaction with 70 ratios of r-PP

The 3D cube graph illustrates in the Figure 4.2.3.5 the significant interactions between temperature (Factor A), screw speed (Factor B), and blend ratio (Factor C) on flexural strength in this DOE study. The cube shows that increasing the screw speed from 300 rpm to 500 rpm at both low (160°C) and high temperatures (180°C) results in increased impact strength. The highest observed impact strength is 0.127 J/m² at the combination of 180°C, 500 rpm, and a 70% blend ratio, while the lowest impact strength of 0.06 J/m² occurs at 160°C, 300 rpm, and a 50% blend ratio. These findings highlight the importance of optimizing temperature, screw speed, and blend ratio to maximize the impact strength of the polymer blend, which is crucial for enhancing product performance. This detailed analysis of the interaction effects underscores the necessity of a strategic approach in adjusting the processing parameters to achieve the desired mechanical properties in polymeric materials.

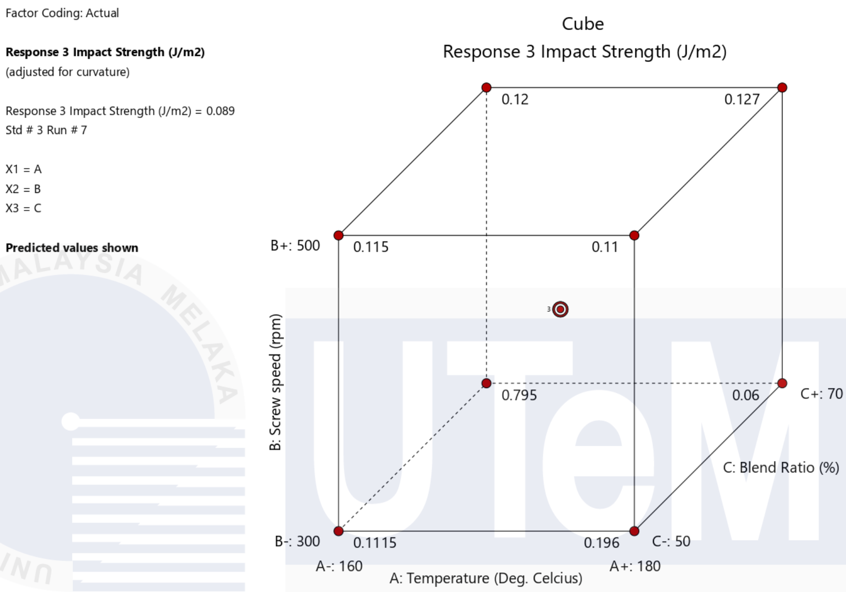

Figure 4.2.3.5: The 3D cube of impact strength analysis

4.2.4 Optimisation Results on r-PP/LDPE blend

The optimization strategies recommended by the Design of Experiments (DOE) software are compiled and presented in the Table 4.2.4.1. The objective of the optimization was to maintain the blend ratio within a specified range, minimize temperature, and maximize screw speed for the independent variables. These adjustments aimed to optimize the dependent responses of tensile strength, flexural strength, and impact strength. Simultaneously, the Table 4.2.4.2 outlines ten (10) potential optimisation recommendations, each associated with desirability for the corresponding tensile, flexural and impact strength response.

The initial recommendation characterised by a desirability score of one (unity), was selected for additional validation testing due to its representation of the most desirable solution for achieving maximum tensile strength response and flexural strength response. This chosen solution comprises a blend ratio of 70%, a temperature of 160℃, a rotor speed of 445.170 rpm, a tensile strength of 12.777 MPa, a flexural strength of 16.504 MPa and a impact strength of 0.305 J. The desirability result, approaching a value of one, signifies that all assessed elements are pertinent and should not be overlooked. While alternative recommended solutions exist to attain a similar outcome, they come with lower desirability values and the presence of residue. However, in this analysis, emphasis was placed on validating and further investigating the first solution proposed by the software.

Table 4.2.4.1: Optimisation results of RSM on r-PP/LDPE polymer blends

Name	Goal	Lower Limit	Upper Limit	Lower Weight	Upper Weight	Importance
A: Temperature	is in range	160	180	1	1	3
B: Screw speed	is in range	300	500	1	1	3
C: Blend Ratio	is in range	50	70	1	1	3
Response 1 Tensile Strength	maximize	9.74079	13.9231	1	1	3
Response 2 Flexural Strength	maximize	9.37695	23.4916	1	1	3
Response 3 Impact Strength	maximize	0.06	0.795	1	1	3

Table 4.2.4.2: Optimisation recommendations of r-PP/LDPE polymer blend solution

Number	Temperature	Screw speed	Blend Ratio	Response 1 Tensile Strength	Response 2 Flexural Strength	Response 3 Impact Strength	Desirability	
1	**160.000**	**445.170**	**70.000**	**12.777**	**16.504**	**0.305**	**0.496**	**Selected**
2	160.000	445.112	70.000	12.775	16.501	0.305	0.496	
3	160.000	444.311	70.000	12.759	16.461	0.308	0.496	
4	160.000	446.214	70.000	12.798	16.555	0.302	0.496	
5	160.103	445.285	70.000	12.778	16.538	0.304	0.496	
6	160.000	447.638	70.000	12.828	16.625	0.297	0.496	
7	160.278	444.885	70.000	12.769	16.567	0.303	0.496	
8	160.529	443.850	70.000	12.746	16.587	0.304	0.496	
9	160.742	443.781	70.000	12.744	16.643	0.302	0.496	
10	160.826	443.443	70.000	12.737	16.650	0.303	0.496	

As illustrated in the Figure 4.2.4.1, the ramps indicate that the optimal temperature parameters, rotor speed and blend ratio are in the highest range, and tensile strength, flexural strength and impact strength responses are near the highest range (highlighted by the red bullet). In the Figure 4.2.4.2, the bar graph depicts the desirability of each factor, specifically the tensile strength response, flexural strength and impact strength separately. The optimal factor settings are shown with orange bars, and the Optimal response prediction values are displayed in blue. Other than that, the bottom bar graph illustrates the combined attractiveness of all parameters for the tensile and flexural strength responses. The proposed solution from the Design of Experiments (DOE) suggests a blend ratio of 70% r-PP/LDPE, a temperature of 160 °C, a rotor speed of 445.170 rpm, a tensile strength of 12.777 MPa, a flexural strength of 16.504 MPa and a impact strength 0.305J. These values resulted in a desirability score of unity, signifying a flawless interaction between the involved parameters. This indicates that the recommended combination of factors can optimise the polymer blend to achieve the desired properties effectively.

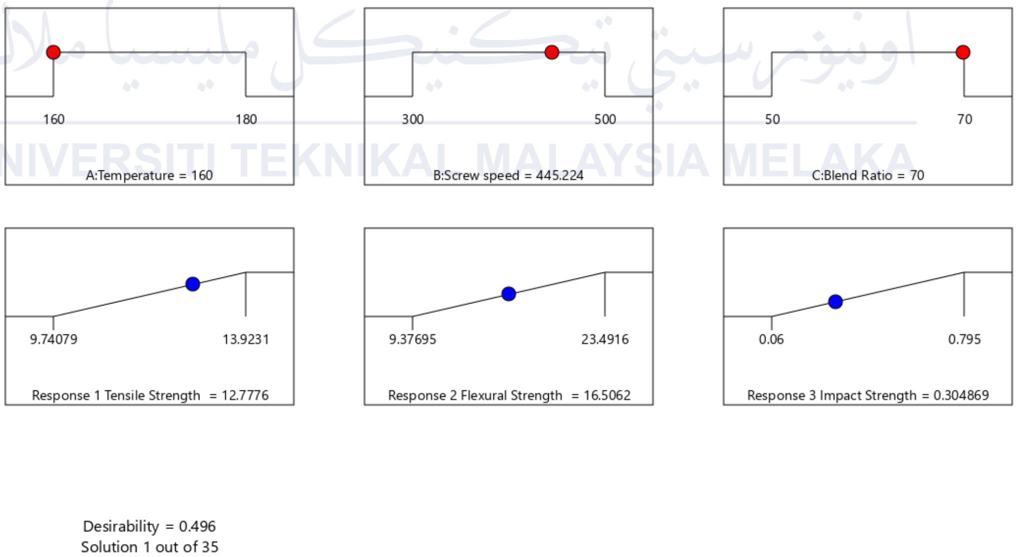

Figure 4.2.4.1: Optimisation result of r-PP/LDPE blend in ramps graphical view

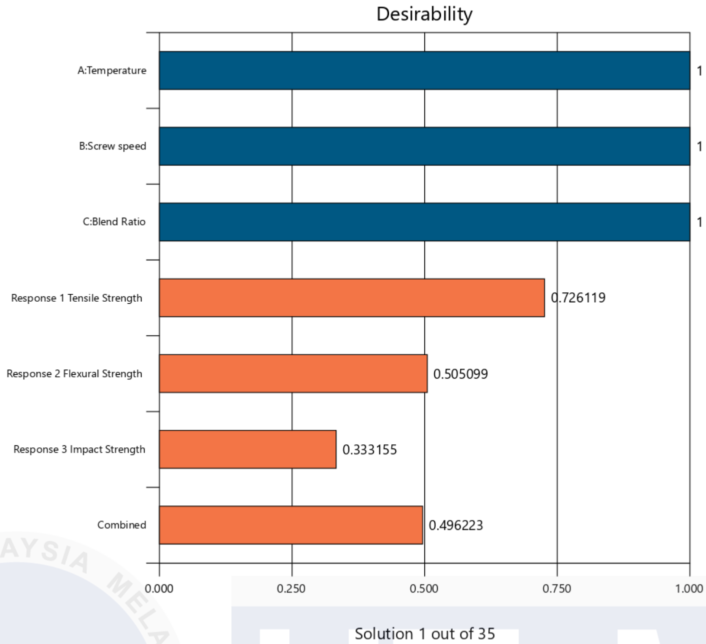

Figure 4.2.4.2: Optimisation result of r-PP/LDPE blend in bar graphical view

4.3 Density Analysis on r-PP/LDPE blend

Figure 4.3 in the graph shows the density changes detected across multiple samples, which include blends of recycled polypropylene (r-PP) and low-density polyethylene (LDPE), as well as pure LDPE and pure r-PP. The horizontal axis is indicative of the different samples (S1 to S11, LDPE, and r-PP), while the vertical axis denotes density measured in grams per cubic centimetre (g/cm³). The utilization of colour schemes serves to represent the r-PP ratio: 70% is depicted in yellow, 60% in green, 50% in blue, LDPE in red, and pure r-PP in yellow. As the proportion of r-PP increases, the density also rises, reaching its peak at 1.17975 g/cm³ for pure r-PP, attributed to its densely packed semi-crystalline configuration, further reinforced by the recycling procedure (Jamnongkan et al., 2022). PP has a higher degree of crystallinity and more regular molecular structure, leading to tighter packing of polymer chains and higher density (Luca Fambri & Luca Lutterotti, 2020). LDPE, registering at 1.0715 g/cm³, exhibits greater density than the r-PP compounds but falls short of the density level of pure r-PP. LDPE has a highly branched structure and lower degree of crystallinity, resulting in looser packing of polymer chains and lower density (Zhu et al., 2022). The densities of the r-PP mixtures, spanning from 0.882 to 0.917 g/cm³, are comparatively lower due to the incorporation of materials with lower density, thereby underscoring the substantial influence of material composition and manufacturing processes on the ultimate characteristics of these thermoplastic amalgams.

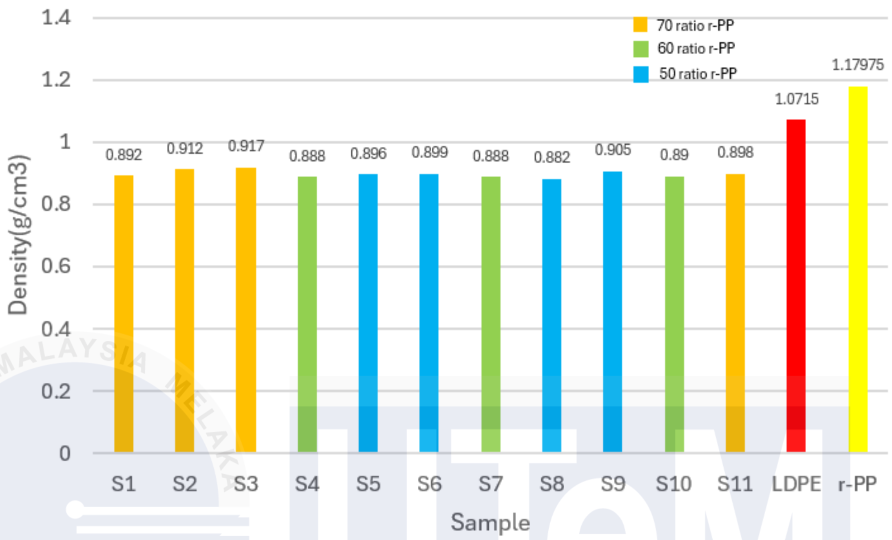

Figure 4.3: Bar chart on the density of r-PP/LDPE blend

4.4 Field Emission Scanning Electron Microscopes

Observation of the microstructure reveals a highly uniform and dense composition with well-aligned layers and minimal voids, which significantly enhances the tensile strength of the recycled PP shown in the Figure 4.4.1. The absence of blend interfaces and impurities ensures a continuous and uninterrupted matrix, allowing for better load-bearing capacity and greater resistance to deformation under tensile stress. The well-aligned layers facilitate efficient stress distribution, minimizing weak points and stress concentration areas, thereby improving the overall mechanical performance and durability of the blend (Sun et al., 2022). Additionally, the minimal presence of voids reduces the likelihood of crack initiation and propagation, while the dense packing of polymer chains enhances interfacial adhesion between different phases of the blend. This strong interfacial bonding ensures effective stress transfer and load distribution, enabling the material to withstand higher tensile loads without failure (Hao et al., 2022). Overall, these microstructural characteristics underscore the superior tensile properties of the recycled PP and provide a foundation for optimizing processing conditions to achieve even better performance in practical applications.

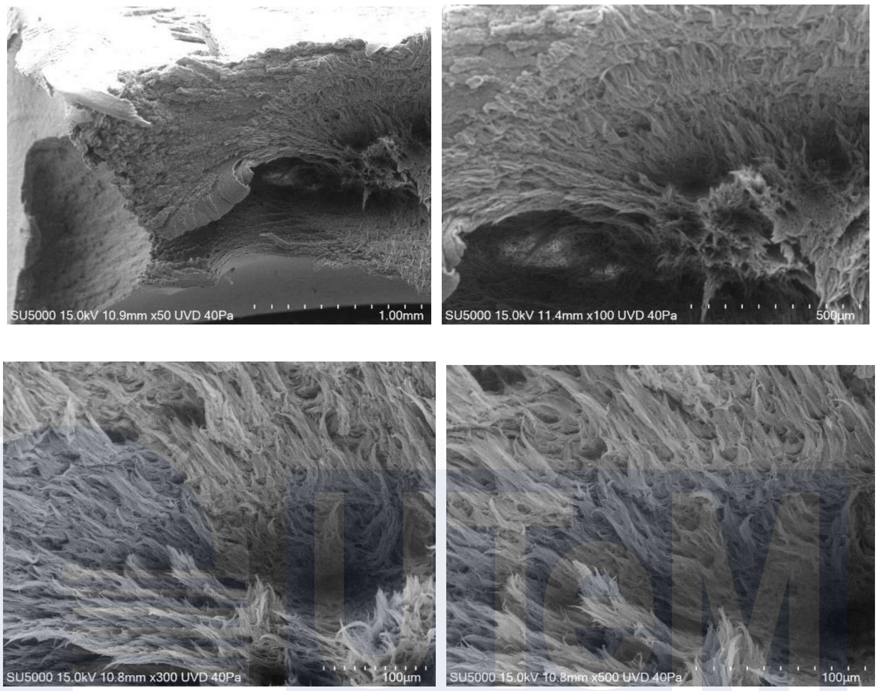

Figure 4.4.1: The Phase Morphology of neat r-PP Sample

The FE-SEM analysis of virgin LDPE unveiled several significant findings where it shown in the Figure 4.4.2. Firstly, the LDPE exhibited a uniform and layered structure, indicating consistency in composition and the presence of distinct layers influenced by manufacturing conditions. Additionally, clear lamellar structures with smooth surfaces were observed, suggesting well-defined boundaries between layers and minimal processing disruptions. This smoothness implies controlled manufacturing processes. The material appeared homogeneous, ensuring consistent properties across the observed area, which is crucial for uniform performance in different applications. Moreover, the LDPE demonstrated good structural integrity with minimal voids or cracks, indicative of robust manufacturing processes. Lastly, the well-organized layers and strong intermolecular bonding highlighted regular polymer chain alignment, contributing to mechanical strength and stability (Yusof et al., 2023). Overall, the analysis portrays the virgin LDPE as a well-processed material with essential characteristics for quality and performance across various applications.

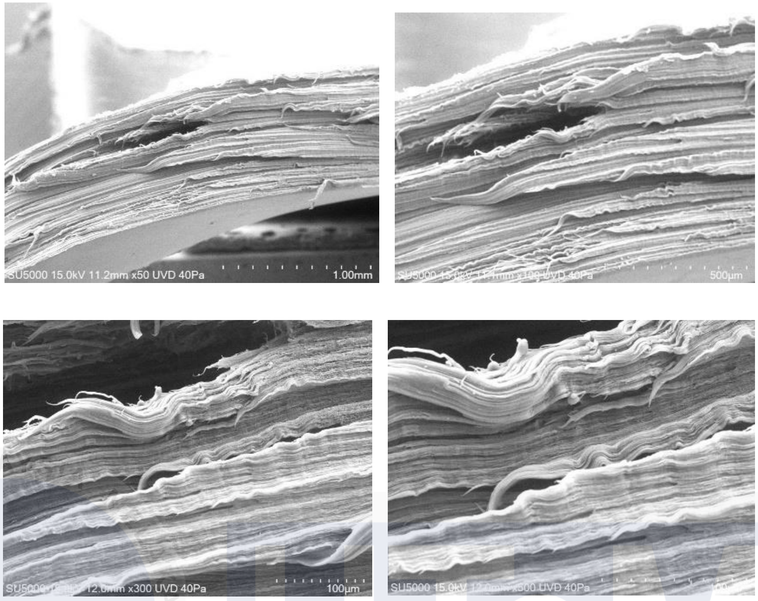

Figure 4.4.2: The Phase Morphology of neat LDPE Sample

The provided SEM image of a thermoplastic blend composed of 70% recycled polypropylene (r-PP) and 30% low-density polyethylene (LDPE), processed at 160°C with a screw speed of 500 rpm, shows a complex and heterogeneous surface morphology in the Figure 4.4.3. Key features include a homogeneous distribution of polymer phases, good interfacial adhesion, and the presence of fibrillar structures, all contributing to high tensile strength. The rough surface topology enhances mechanical interlocking between phases (Mu et al., 2022). The highlighted region in the SEM image demonstrates optimal interaction between r-PP and LDPE, supporting the blend's superior mechanical performance. This analysis justifies the sample 1 are the best sample in tensile strength.

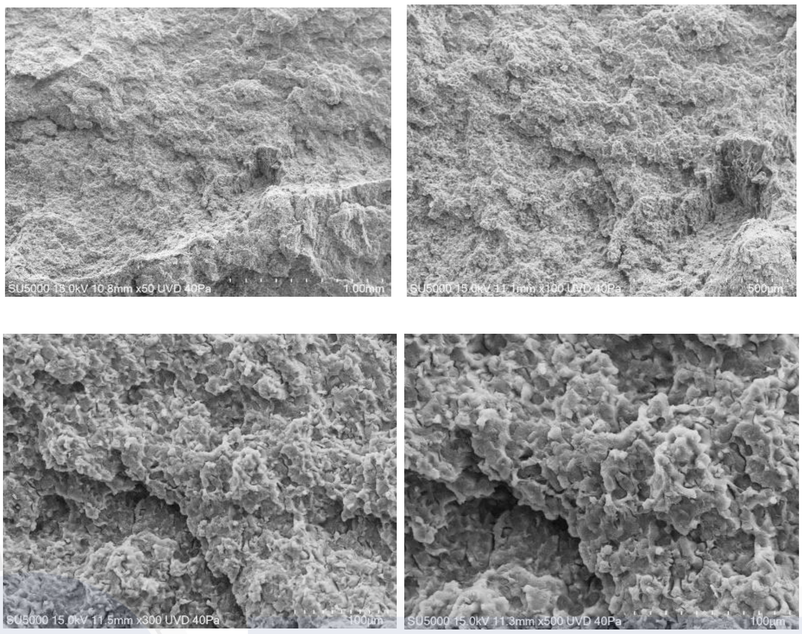

Figure 4.4.3: Phase Morphology of Sample 1; r-PP/LDPE (Best)

The observations shown in the Figure 4.4.4 are the worst sample in tensile strength value which is sample 5. Firstly, the structure appears highly irregular and rough, indicating significant deviations from expected uniformity. This irregularity is further emphasized by the presence of significant fragmentation and fibrillation, which point towards poor material integrity (Erdman et al., 2013). Moreover, the surface exhibits numerous voids and cracks, suggesting weak intermolecular bonding and phase separation between polypropylene (PP) and low-density polyethylene (LDPE). The morphology further indicates poor mixing and dispersion of the polymers, likely attributed to the high screw speed and processing temperature (Albareeki et al., 2019). These findings have several implications. The high temperature (180°C) and high screw speed (300 rpm) employed during processing may have caused thermal degradation and excessive shear forces, contributing to the observed rough and fragmented morphology. The inadequate mixing and dispersion result in a heterogeneous blend, which is expected to negatively impact mechanical properties and overall performance (Ferreira & Silva, 2023). Additionally, the presence of voids and cracks indicates poor integration of the recycled polymers, leading to weakened areas and potential failure points within the material.

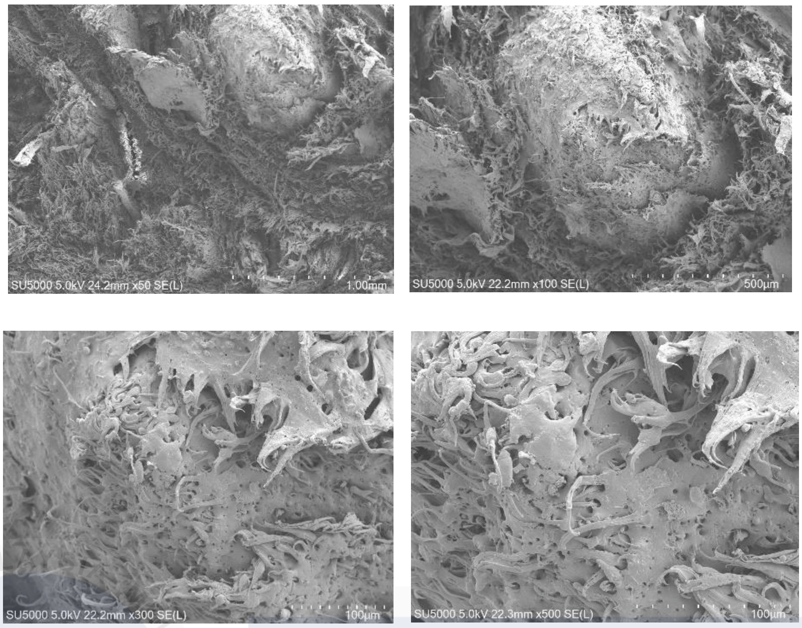

Figure 4.4.4: The Phase Morphology of Sample 5; r-PP/LDPE (Worst)

4.5 Mechanical Properties Evaluation of r-PP/LDPE/GNPs Blend

The next stage of this research was followed by the preparation and characterisation of r-PP/LDPE blend with the addition of graphene nanoplatelets (GNPs) at various loadings (0, 1, 3, 5, and 7 wt.%). At this point, the potential of GNPs addition to further improve the performance of the r-PP/LDPE blend was evaluated and investigated. The selected r-PP/LDPE blend sample, optimised from the recommended DOE experimental strategies and determined by the critical property of tensile strength analysis, was further characterised by various aspects of mechanical, physical, and morphological attributes. The discussions on various properties of the r-PP/LDPE/GNPs blend were elaborated further in the following section:

4.5.1 Tensile Properties Analysis

The graph in the Figure 4.5.1 shows the link between a composite material's tensile strength, expressed in megapascals (MPa), and the percentage of graphene added to it. Tensile strength is indicated by the Y-axis, and graphene percentage is represented by the X-axis. Measurements at 0%, 1%, 3%, 5%, and 7% graphene content are shown by data points. Tensile strength is 12.6003 MPa at 0% graphene and 13.7032 MPa at 1% graphene, demonstrating the initial reinforcing effect of graphene because of its superior mechanical characteristics. Tensile strength increases slightly to 13.72415 MPa at 3% graphene, suggesting a stage where the reinforcing effect persists but at a decreasing rate because of irregular graphene dispersion. With 5% graphene, the tensile strength peaks at 14.9424 MPa, indicating ideal graphene dispersion within the matrix and maximizing graphene's potential for reinforcement (Wang et al., 2021). However, due to graphene agglomeration, which produces stress concentration spots and weakens the composite, the tensile strength drops to 14.21215 MPa at 7% graphene (Madi & Ali Sadiq Alithari, 2022). Therefore, while adding graphene increases tensile strength, there is an ideal content (about 5%) beyond which the benefits decrease because of agglomeration and inadequate dispersion. This emphasizes the significance of appropriate concentration and dispersion in optimizing the reinforcement effect of graphene.

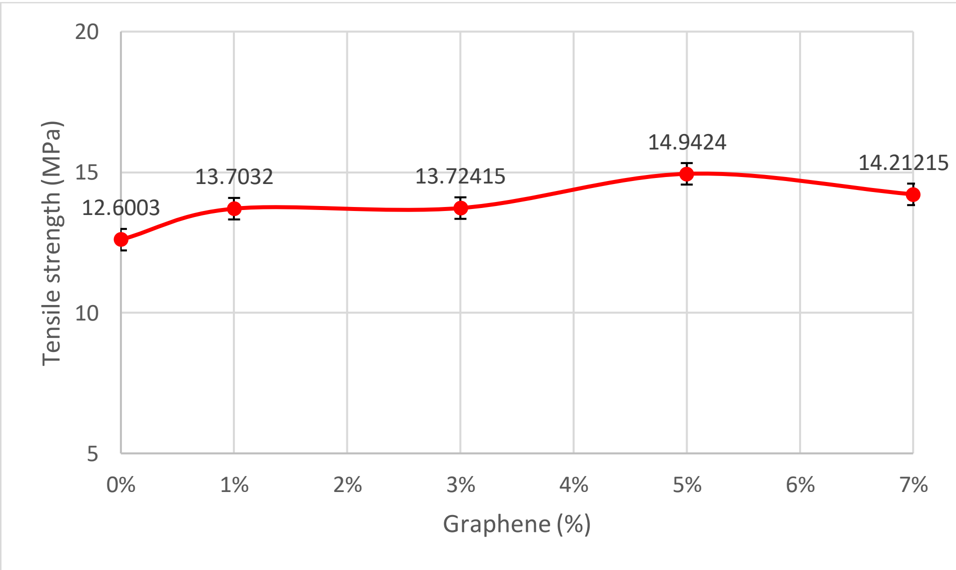

Figure 4.5.1: Tensile strength r-PP/LDPE/GNPs blend nanocomposite

4.5.2 Flexural Properties Analysis

The graph in the Figure 4.5.2 reveals how the amount of graphene in a composite material influences its flexural strength. At 0% graphene, the composite exhibits a flexural strength of 17.1941 MPa. Adding 1% graphene significantly boosts the strength to 22.9456 MPa, demonstrating graphene's reinforcing effect due to its high strength and stiffness. However, increasing the graphene content to 3% results in a drop to 21.1358 MPa due to poor dispersion and agglomeration of graphene particles, which reduces their reinforcing effectiveness. When the graphene content is increased to 5%, the flexural strength rises again to 23.2069 MPa, suggesting better dispersion of graphene within the composite. Improved graphene dispersion, enhanced interfacial bonding, and reaching a critical volume fraction led to this significant increase in flexural strength (Naebe et al., 2014). Beyond this point, increasing the graphene content further to 7% stabilizes the flexural strength around 23.2417 MPa, indicating that the composite has reached a saturation point where additional graphene does not significantly improve strength due to factors like agglomeration, reaching the mechanical percolation threshold, and matrix limitations (Sutar et al., 2021). This suggests that while graphene can enhance the mechanical properties of composites, careful control over its dispersion and concentration is essential to achieve optimal performance.

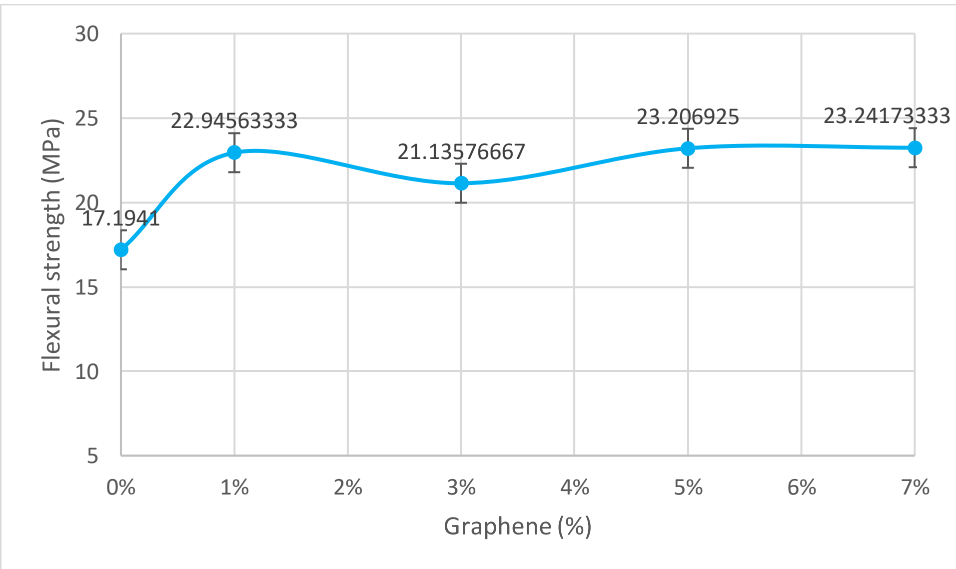

Figure 4.5.2: Flexural strength r-PP/LDPE/GNPs blend nanocomposite

4.5.3 Impact Properties Analysis

The graph shows in the Figure 4.5.3 is the relationship between the percentage of graphene added to the r-PP/LDPE blend and the amount of energy absorbed. It shows that energy absorption increases with graphene addition up to 5%, then decreases at 7%. A variety of reasons contribute to this trend. To begin, when modest amounts (1% to 5%) of graphene are added to the mixture, it works as a reinforcing agent, considerably enhancing the composite's ability to absorb and distribute impact energy. The graphene nanoparticles effectively transfer stress throughout the matrix, increasing the composite's overall toughness and impact resistance (Shao et al., 2022). At these concentrations, graphene can be well disseminated throughout the polymer matrix, resulting in a homogeneous distribution that improves mechanical characteristics. The interface between graphene and the polymer matrix is excellent, resulting in efficient load transmission and energy dissipation at impact. This enhanced bonding allows the composite to absorb more energy before failure. Furthermore, graphene can operate as a crack propagation barrier; when an impact occurs, graphene particles assist deflect and bridge cracks, enhancing the material's impact resistance and resulting in greater impact energy absorption (Wang et al., 2023). However, the benefits decrease significantly above 5% graphene, most likely due to agglomeration of graphene particles, which can affect the effectiveness of stress transfer and dispersion.

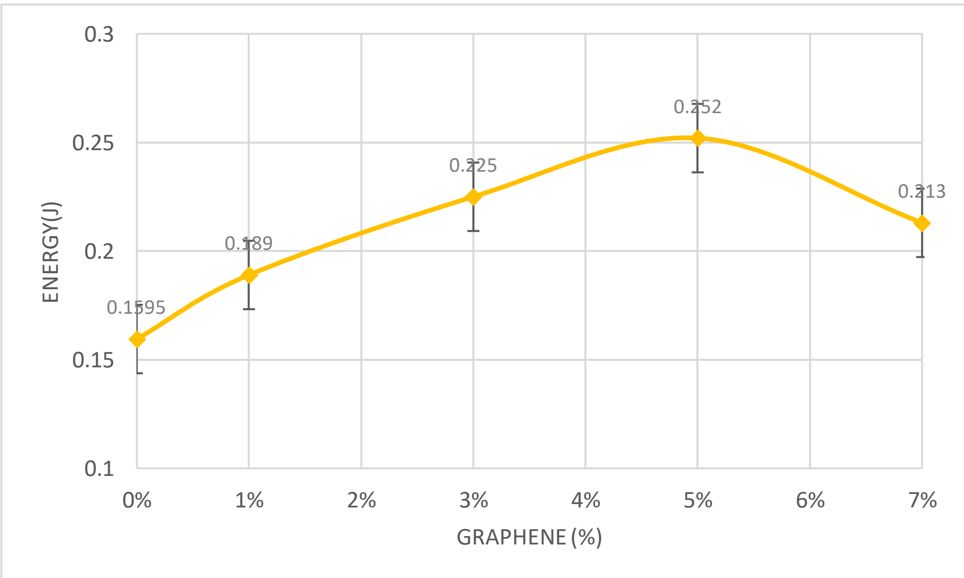

Figure 4.5.3: Impact strength r-PP/LDPE/GNPs blend nanocomposite

4.6 Density Properties Analysis

The graph shown in the Figure 4.6 has shown the percentage of graphene added to the r-PP/LDPE blend affects the composite's density. At lower percentages (0% and 1%), the density marginally increases compared to the basic material, showing that graphene has been incorporated into the blend. At 3% graphene, density decreases slightly due to the distribution and arrangement of graphene within the composite. As the graphene proportion rises to 5% and 7%, the density rises considerably. This rise is due to the blend's particles being packed more densely (Ravichandran et al., 2021). The density changes are influenced by particle packing efficiency, interactions between graphene and the matrix, and porosity variations. The presence of graphene affects the overall composite structure, causing density changes depending on how well it is incorporated and diffused throughout the matrix.

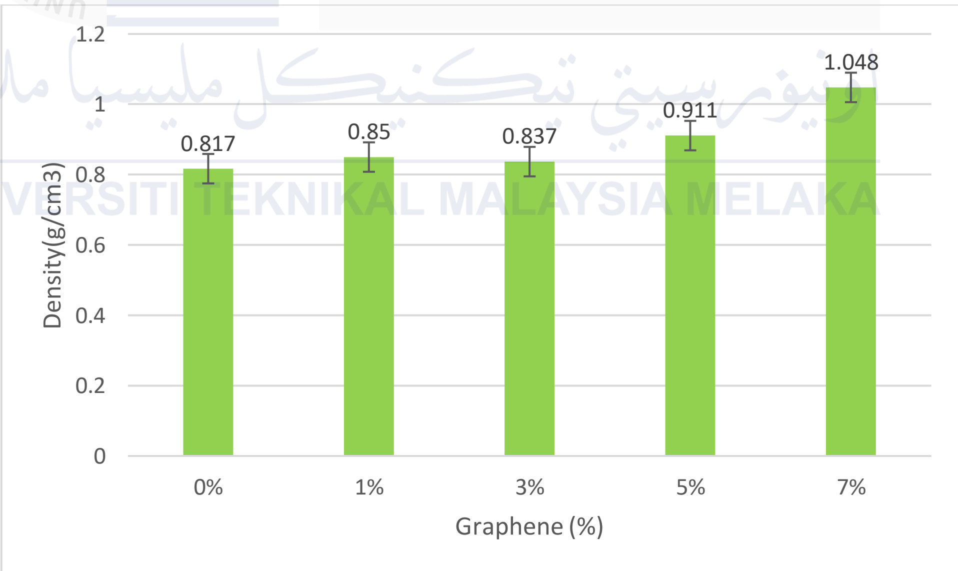

Figure 4.6: Density of r-PP/LDPE/GNPs blend

4.7 Field Emission Scanning Electron Microscope

Figure 4.7.1 illustares microstructure analysis of the r-PP (recycled polypropylene)/LDPE (low-density polyethylene) composite with added 5% carbon graphene nanoplatelets (GNPs) reveals significant improvements compared to the previous sample. The surface morphology appears more compact and less fibrous, indicating enhanced material distribution and reduced voids. This improvement is attributed to the introduction of GNPs, which enhance interfacial bonding between the r-PP and LDPE phases, promoting a more uniform microstructure (Ferreira & Silva, 2023). Additionally, the GNPs act as reinforcing agents, filling voids and reducing defects within the material. Consequently, the composite exhibits increased tensile strength and improved mechanical properties, demonstrating the beneficial effects of GNPs on the surface morphology and overall performance of the r-PP/LDPE blend.

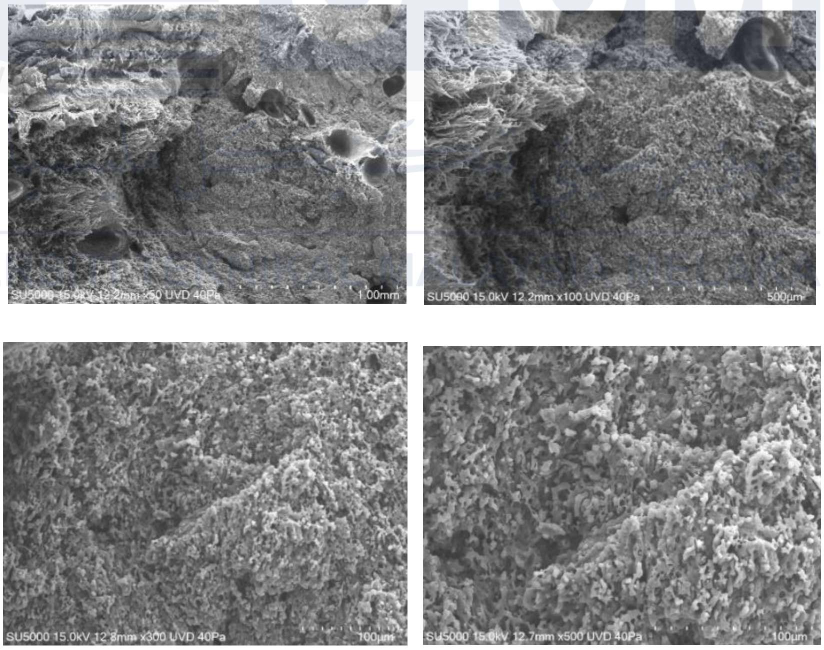

Figure 4.7.1: Phase Morphology of r-PP/LDPE-GNPs of 5% (Best) Blend nanocomposite

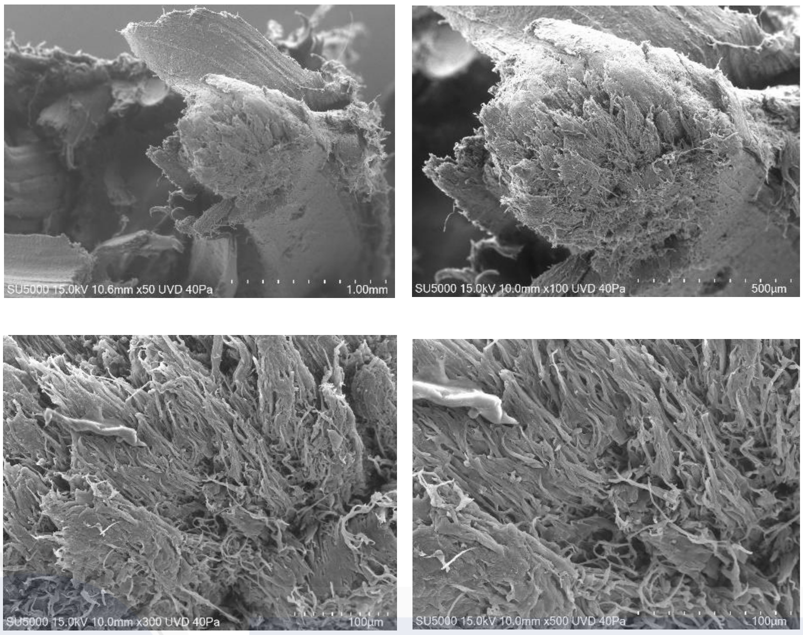

Figure 4.7.2: Phase Morphology of r-PP/LDPE-GNPs of 0% (Control & Worst) Blend nanocomposite

CHAPTER 5

CONCLUSION AND RECOMMENDATIONS

5.1 Conclusions

In conclusion, this study effectively optimized the formulation and processing parameters of the r-PP/LDPE blend by using the melt blending process and response surface methodology (RSM). Through a two-level, full-factorial statistical optimization technique, optimal conditions were identified the best parametric condition at 160°C temperature, 445.170 rpm rotor speed, and a 70 wt.% r-PP/LDPE blend ratio. These circumstances led to significant increases in mechanical parameters, such as higher tensile strength (12.777 MPa), flexural strength (16.504 MPa), and impact strength (0.305 J). The findings demonstrate the usefulness of response surface methodology in refining processing parameters to improve thermoplastic blend performance measures.

The second goal of this work was to look at the role of graphene nanoplatelets (GNPs) as a reinforcing filler in an r-PP/LDPE matrix blend. Results has indicated that the incorporating of GNPs nanofiller at loadings up to 5% has significantly bolstered the tensile, flexural, and impact strengths. However, a subsequent increase in GNPs loading to 7% resulted in a decline in these mechanical properties, suggesting an optimal effectiveness of GNPs at lower concentrations. This observation underscores the importance of balancing GNP content to achieve optimal mechanical enhancements in the blend, highlighting the critical role of GNPs as a compatibilizer in improving the overall performance of biodegradable thermoplastic hybrid materials.

The third objective aimed to characterize the fracture surface morphology of the r-PP/LDPE blend using Field Emission Scanning Electron Microscopy (FESEM). Analysis revealed well-dispersed GNPs within the r-PP matrix, indicative of effective blending and distribution of the nanofillers. This uniform dispersion has contributed significantly to the observed enhancements in mechanical properties, validating the role of GNPs in reinforcing the polymer matrix. Overall, the comprehensive characterization through the FESEM has corroborates the mechanical improvements observed in the presence of GNPs nanofiller, affirming their potential for enhancing the structural integrity and performance of the biodegradable thermoplastic blends processed via melt blending extrusion methods.

5.2 Recommendations for Future Study

Further research may be conducted to improve the interface between graphene and the composite mix by performing surface treatment to the graphene nanoplatelets. This treatment enhances graphene compatibility with the polymer matrix, resulting in enhanced the graphene dispersion throughout the blend material. As a result, the composite displays improved mechanical characteristics and overall performance. Next, converting recycled polypropylene (r-PP) and low-density polyethylene (LDPE) to powder form rather than pellets results in a more consistent and complete mixing procedure. Manually combining these powders produces a constant mixture, which improves extruder homogeneity and, as a result, the mechanical qualities and performance of the final extruded product. Miscibility studies utilizing Differential Scanning Calorimetry (DSC) are critical for further evaluating and optimizing the mix. These tests offer precise information on the blend's thermal properties, such as miscibility, phase transitions, crystallinity, and thermal stability. Understanding these features at the molecular level is critical for assuring the composite material's compatibility and efficacy, which will guide further optimization and industrial use.

5.3 Sustainable Design and Development

This research was motivated by the need to develop sustainable materials by optimizing recycled polypropylene (r-PP) and low-density polyethylene (LDPE) blends. Utilizing recycled polymers reduces plastic waste and dependence on virgin plastics. The in of graphene nanoplatelets (GNPs) enhances the mechanical properties of these blends, making them more durable and efficient. This approach not only promotes a circular economy but also demonstrates the potential of nanotechnology in creating high-performance, eco-friendly composites. By focusing on material efficiency and improved processing techniques, this study contributes to reducing the environmental impact of polymer manufacturing.

REFERENCES

Al Faruque, M. A., Syduzzaman, M., Sarkar, J., Bilisik, K., & Naebe, M. (2021). A Review on the Production Methods and Applications of Graphene-Based Materials. *Nanomaterials*, *11*(9), 2414.

Alasvand Zarasvand, K., & Golestanian, H. (2017). Investigating the effects of number and distribution of GNP layers on graphene reinforced polymer properties: Physical, numerical and micromechanical methods. *Composites Science and Technology*, *139*, 117–126.

Alsabri, A., Tahir, F., & AlGhamdi, S. G. (2022). Environmental impacts of polypropylene (PP) production and prospects of its recycling in the GCC region. *International Conference on Applied Research and Engineering 2021*, *56*, 2245–2251. https://doi.org/10.1016/j.matpr.2021.11.574

Alvaredo-Atienza, A., Fernández-Blázquez, J. P., Castell, P., & Guzman de Villoria, R. (2020). Production of graphene nanoplate/polyetheretherketone composites by semi-industrial melt-compounding. *Heliyon*, *6*(4), e03740. https://doi.org/10.1016/j.heliyon.2020.e03740

Antony, J. (2023a). *6 - Full factorial designs* (J. Antony, Ed.; Third Edition, pp. 65–87). Elsevier. https://doi.org/10.1016/B978-0-443-15173-6.00009-3

Antony, J. (2023b). *12 - Design of Experiments in the service industry: a critical literature review and future research directions* (J. Antony, Ed.; Third Edition, pp. 233–248). Elsevier. https://doi.org/10.1016/B978-0-443-15173-6.00005-6

Awoyera, P. O., & Adesina, A. (2020). Plastic wastes to construction products: Status, limitations and future perspective. *Case Studies in Construction Materials*, *12*, e00330. https://doi.org/10.1016/j.cscm.2020.e00330

Awoyera, P., Onoja, E., & Adesina, A. (2019). Fire resistance and thermal insulation properties of foamed concrete incorporating pulverized ceramics and mineral admixtures. *Asian Journal of Civil Engineering*, *21*(1), 147–156. https://doi.org/10.1007/s42107-019-00203-4

Bell, S. (2009). *Experimental design* (R. Kitchin & N. Thrift, Eds.; pp. 672–675). Elsevier. https://doi.org/10.1016/B978-008044910-4.00431-4

Benson, C. H., & Khire, M. V. (1994). Reinforcing Sand with Strips of Reclaimed High-Density Polyethylene. *Journal of Geotechnical Engineering*, *120*(5), 838–855. https://doi.org/10.1061/(asce)0733-9410(1994)120:5(838)

Calhoun, A. (2010). *Chapter 3 - polypropylene* (J. R. Wagner, Ed.; pp. 31–36). William Andrew Publishing. https://doi.org/10.1016/B978-0-8155-2021-4.10003-6

Calhoun, A., & Wagner, J. R. (2010). Chapter 3Polypropylene. In *Plastics Design Library* (pp. 31–36). William Andrew Publishing. https://doi.org/10.1016/B9780815520214.100036

Carlson, R. (Ed.). (1992). *Chapter 5 Two-level factorial designs* (Vol. 8, pp. 89–122). Elsevier. https://doi.org/10.1016/S0922-3487(08)70252-1

Choudhary, A., Jha, J. N., Gill, K., & Sanjay Kumar Shukla. (2014). *Utilization of Fly Ash and Waste Recycled Product Reinforced with Plastic Wastes as Construction Materials in Flexible Pavement*. https://doi.org/10.1061/9780784413272.377

Christopher Blair Crawford, & Quinn, B. (2017). *4 - Physiochemical properties and degradation* (Christopher Blair Crawford & B. Quinn, Eds.; pp. 57–100). Elsevier. https://doi.org/10.1016/B978-0-12-809406-8.00004-9

Chu, Z., Zhao, T., Li, L., Fan, J., & Qin, Y. (2017). Characterization of Antimicrobial Poly (Lactic Acid)/Nano-Composite Films with Silver and Zinc Oxide Nanoparticles. *Materials*, *10*(6), 659. https://doi.org/10.3390/ma10060659

Cossu, R., Stegmann, R., Cossu, R., Stegmann, R., Cossu, R., Stegmann, R., Cossu, R., Stegmann, R., Alibardi, L., Andreottola, G., Artuso, A., Ashwath, N., Astrup, T. F., Ayalon, O., Bakas, I., Barausse, A., Batarseh, E. S., Beaven, R., Benaud, P., & Beretta, G. P. (2019). List of Contributors. In *Solid Waste Landfilling* (p. xixviviii-xvi-xiv). Elsevier. https://doi.org/10.1016/B9780124077218.010020

Daneshpayeh, S., Ashenai Ghasemi, F., Ghasemi, I., & Ayaz, M. (2016). Predicting of mechanical properties of PP/LLDPE/TiO2 nano-composites by response surface methodology. *Composites Part B: Engineering*, *84*, 109–120. https://doi.org/10.1016/j.compositesb.2015.08.075

Dikobe, D. G., & Luyt, A. S. (2010). Comparative study of the morphology and properties of PP/LLDPE/wood powder and MAPP/LLDPE/wood powder polymer blend composites. *Express Polymer Letters*, *4*(11), 729–741. https://doi.org/10.3144/expresspolymlett.2010.88

E.K. Gamstedt, & Berglund, L. A. (2003). *11 - Fatigue of thermoplastic composites* (B. Harris, Ed.; pp. 314–338). Woodhead Publishing. https://doi.org/10.1533/9781855738577.3.314

Emblem, A., Emblem, H., Emblem, A., Emblem, H., Anne, Emblem, H., Emblem, A., Emblem, H., Emblem, A., Emblem, H., Emblem, A., Emblem, H., Emblem, A., Richard, I. G., Crompton, G., Emblem, H., Farmer, N., Grayhurst, P., Page, B., & Kerry, J. (2012). Contributor contact details. In *Packaging Technology* (p. xiiiixixxviiiv-iii-xv). Woodhead Publishing. https://doi.org/10.1016/B9781845696658.50024X

Feldman, D. (2015). Polyblend nanocomposites. *Journal of Macromolecular Science, Part A*, *52*, 8. https://doi.org/10.1080/10601325.2015.1050638

Ghalia, M. A., Hassan, A., & Yussuf, A. (2011). Mechanical and thermal properties of calcium carbonate-filled PP/LLDPE composite. *Journal of Applied Polymer Science*, *121*(4), 2413–2421. https://doi.org/10.1002/app.33570

Gonzalez-Paredes, D., & Estrades, A. (2021). *9 - plastics versus turtles: An overview of the uruguayan case* (B. Nahill, Ed.; pp. 83–92). Academic Press. https://doi.org/10.1016/B978-0-12-821029-1.00009-X

Goswami, T. K., & S. Mangaraj. (2011). *8 - Advances in polymeric materials for modified atmosphere packaging (MAP)* (José-María Lagarón, Ed.; pp. 163–242). Woodhead Publishing. https://doi.org/10.1533/9780857092786.1.163

Gujral, G., Kapoor, D., & Jaimini, M. (2018). AN UPDATED REVIEW ON DESIGN OF EXPERIMENT (DOE) IN PHARMACEUTICALS. *Journal of Drug Delivery and Therapeutics*, *8*(3). https://doi.org/10.22270/jddt.v8i3.1713

Hafeez, M., Ahmad, N., Kamal, M., Rafi, J., Haq, M., Jamal, Zaidi, S., & Nasir, M. (2019). Experimental Investigation into the Structural and Functional Performance of Graphene Nano-Platelet (GNP)-Doped Asphalt. *Applied Sciences*, *9*(4), 686. https://doi.org/10.3390/app9040686

He, J., Hu, W., Xiao, R., Wang, Y., Pawel Polaczyk, & Huang, B. (2022). A review on Graphene/GNPs/GO modified asphalt. *Construction and Building Materials*, *330*, 127222. https://doi.org/10.1016/j.conbuildmat.2022.127222

Homkhiew, C., Ratanawilai, T., & Thongruang, W. (2014). The optimal formulation of recycled polypropylene/rubberwood flour composites from experiments with mixture design. *Composites Part B: Engineering*, *56*, 350–357. https://doi.org/10.1016/j.compositesb.2013.08.041

Hu, Z. (2012). Heat-Resistant Steels, Microstructure Evolution and Life Assessment in Power Plants. *InTech EBooks*. https://doi.org/10.5772/26766

Huysman, S., De Schaepmeester, J., Ragaert, K., Dewulf, J., & De Meester, S. (2017). Performance indicators for a circular economy: A case study on post-industrial plastic waste. *Resources, Conservation and Recycling*, *120*, 46–54. https://doi.org/10.1016/j.resconrec.2017.01.013

Jun, Y-S., Um, J. G., Jiang, G., & Yu, A. (2018). A study on the effects of graphene nano-platelets (GnPs) sheet sizes from a few to hundred microns on the thermal, mechanical, and electrical properties of polypropylene (PP)/GnPs composites. *Express Polymer Letters*, *12*(10), 885–897. https://doi.org/10.3144/expresspolymlett.2018.76

Koerner, G. R., Y.G. Hsuan, & Koerner, R. M. (2007). *3 - The durability of geosynthetics* (R.W. Sarsby, Ed.; pp. 36–65). Woodhead Publishing. https://doi.org/10.1533/9781845692490.1.36

Korhonen, J., Honkasalo, A., & Seppälä, J. (2018). Circular Economy: the Concept and Its Limitations. *Ecological Economics*, *143*(1), 37–46. https://doi.org/10.1016/j.ecolecon.2017.06.041

Kumar, L., Saha, A., Khushbu, Warkar, Sudhir G, Sarkar, A., Sharma, B., & Shekhar, S. (2023). Chapter 11Biodegradability of automotive plastics and composites. In *Biodegradability of Conventional Plastics* (pp. 221–242). Elsevier. https://doi.org/10.1016/B9780323898584.000075

Lamastra, F. R., Mehdi Chougan, Marotta, E., Samuele Ciattini, Seyed Hamidreza Ghaffar, Caporali, S., Vivio, F., Giampiero Montesperelli, Ugo Ianniruberto, Al-Kheetan, M. J., & Bianco, A. (2021a). Toward a better understanding of multifunctional cement-based materials: The impact of graphite nanoplatelets (GNPs). *Ceramics International*, *47*, 14. https://doi.org/10.1016/j.ceramint.2021.04.012

Lamastra, F. R., Mehdi Chougan, Marotta, E., Samuele Ciattini, Seyed Hamidreza Ghaffar, Caporali, S., Vivio, F., Giampiero Montesperelli, Ugo Ianniruberto, Al-Kheetan, M. J., & Bianco, A. (2021b). Toward a better understanding of multifunctional cement-based materials: The impact of graphite nanoplatelets (GNPs). *Ceramics International*, *47*, 14. https://doi.org/10.1016/j.ceramint.2021.04.012

Letcher, T. M. (2020). *Plastic waste and recycling : environmental impact, societal issues, prevention, and solutions*. Academic Press. https://www.elsevier.com/books/plastic-waste-and-recycling/letcher/978-0-12-817880-5

Li, J., Shanks, R. A., Olley, R. H., & Greenway, G. R. (2001). Miscibility and isothermal crystallisation of polypropylene in polyethylene melts. *Polymer*, *42*, 18. https://doi.org/10.1016/S0032-3861(01)00248-8

Md. Jahidul Islam, & Md. Shahjalal. (2021). Effect of polypropylene plastic on concrete properties as a partial replacement of stone and brick aggregate. *Case Studies in Construction Materials*, *15*, e00627. https://doi.org/10.1016/j.cscm.2021.e00627

Md. Tanvir Hossain, Shahid, A., Mahmud, N., Habib, A., Md. Masud Rana, Khan, S., & Md. Delwar Hossain. (2024). Research and application of polypropylene: a review. *Discover Nano*, *19*(1). https://doi.org/10.1186/s11671-023-03952-z

Musa, N. (2023). Carbon Nanomaterials and Their Applications. *Emerging Nanomaterials and Their Impact on Society in the 21st Century*, 40–71. https://doi.org/10.21741/9781644902172-3

Nazish Huma Khan, Nafees, M., Amjad ur Rahman, & Saeed, T. (2021). *Chapter 22 - Ecodesigning for ecological sustainability* (T. Aftab & Khalid Rehman Hakeem, Eds.; pp. 589–616). Academic Press. https://doi.org/10.1016/B978-0-323-90943-3.00019-5

Niyitanga Evode, Sarmad Ahmad Qamar, Bilal, M., Damià Barceló, & Hafiz M.N. Iqbal. (2021). Plastic waste and its management strategies for environmental sustainability. *Case Studies in Chemical and Environmental Engineering*, *4*, 100142. https://doi.org/10.1016/j.cscee.2021.100142

Parimala Gnana Soundari Arockiam JeyaSundar, Ali, A., Guo, di, & Zhang, Z. (2020). *6 - Waste treatment approaches for environmental sustainability* (P. Chowdhary, A. Raj, D. Verma, & Y. Akhter, Eds.; pp. 119–135). Elsevier. https://doi.org/10.1016/B978-0-12-819001-2.00006-1

Philipose, M. C., Suresh, J., Shajan, S. P., P.R Dheeraj Kumar, & Suresh, A. (2023). Plastic and ceramic modified interlock tiles. *Materials Today: Proceedings*. https://doi.org/10.1016/j.matpr.2023.03.476

Raheem, D. (2013). Application of plastics and paper as food packaging materials ? An overview. *Emirates Journal of Food and Agriculture*, *25*(3), 177. https://doi.org/10.9755/ejfa.v25i3.11509

Rani, M., Meenu, & Shanker, U. (2023). *Chapter 14 - The role of nanomaterials in plastics biodegradability* (A. Sarkar, B. Sharma, & Shashank Shekhar, Eds.; pp. 283–308). Elsevier. https://doi.org/10.1016/B978-0-323-89858-4.00012-9

S.G. Prolongo, R. Moriche, A. Jiménez-Suárez, M. Sánchez, & A. Ureña. (2014). Advantages and disadvantages of the addition of graphene nanoplatelets to epoxy resins. *European Polymer Journal*, *61*, 206–214. https://doi.org/10.1016/j.eurpolymj.2014.09.022

Samper, M. D., Bertomeu, D., Arrieta, M. P., Ferri, J. M., & López-Martínez, J. (2018). Interference of Biodegradable Plastics in the Polypropylene Recycling Process. *Materials*, *11*(10). https://doi.org/10.3390/ma11101886

Samuel, C. O. U., Crangle, A., Mather, R. R., Samuel, C. O. U., Sadiku, E. R., Kim, Y. K., Patel, R. M., Martin, J., Claasen, G., Allgeuer, T., Kotek, R., Afshari, M., Harbison, V., Gupta, A., Sun, G., Badrossamay, M. R., Malkan, S. R., Fan, Q., Shamey, R., & Ugbolue, S. C. O. (2009). Preface. In *Woodhead Publishing Series in Textiles* (pp. xixxiiiifc1iviiixixii–xviixx). Woodhead Publishing. https://doi.org/10.1016/B9781845692070.500172

Sarat Chandra Patra, Swain, S., Pragyan Senapati, Sahu, H., Rabiranjan Murmu, & Harekrushna Sutar. (2022). Polypropylene and Graphene Nanocomposites: Effects of Selected 2D-Nanofiller's Plate Sizes on Fundamental Physicochemical Properties. *Inventions*, *8*(1), 8–8. https://doi.org/10.3390/inventions8010008

Sastri, Vinny R, & Sastri, Vinny R. (2022). 2Regulations for Medical Devices and Application to Plastics Suppliers. In *Plastics Design Library* (pp. 13–40). William Andrew Publishing. https://doi.org/10.1016/B9780323851268.000102

Satya, S. K., & Sreekanth, P. S. R. (2020). An experimental study on recycled polypropylene and high-density polyethylene and evaluation of their mechanical properties. *Materials Today: Proceedings*, *27*, 920–924. https://doi.org/10.1016/j.matpr.2020.01.259

Shen, X., & Qi, C. (2012). Countermeasures towards Circular Economy Development in West Regions. *Energy Procedia*, *16*, 927–932. https://doi.org/10.1016/j.egypro.2012.01.148

Sonebi, M., & Yahia, A. (2020). *1 - Mix design procedure, tests, and standards* (R. Siddique, Ed.; pp. 1–30). Woodhead Publishing. https://doi.org/10.1016/B978-0-12-817369-5.00001-5

Stanek, B., Wang, W., & Łukasz Bartela. (2023). A potential solution in reducing the parabolic trough based solar industrial process heat system cost by partially replacing absorbers coatings with non-selective ones in initial loop sections. *Applied Energy*, *331*, 120472. https://doi.org/10.1016/j.apenergy.2022.120472

Suresha, B., Hemanth, G., Hemanth, R., & Lalla, N. P. (2020). Role of graphene nanoplatelets and carbon fiber on mechanical properties of PA66/thermoplastic copolyester elastomer composites. *Materials Research Express*, *7*(1), 015325. https://doi.org/10.1088/2053-1591/ab648d

Tiong, H. Y., Lim, S. K., Lee, Y. L., Ong, C. F., & Yew, M. K. (2020). Environmental impact and quality assessment of using eggshell powder incorporated in lightweight foamed concrete. *Construction and Building Materials*, *244*, 118341. https://doi.org/10.1016/j.conbuildmat.2020.118341

Tulane, S., de, Cecchin, D., Marvila, Markssuel T, Amran, M., Fediuk, R., Vatin, N., Karelina, M., Klyuev, S., & Szelag, M. (2021). Application of Plastic Wastes in Construction Materials: A Review Using the Concept of LifeCycle Assessment in the Context of Recent Research for Future Perspectives. *Materials*, *14*(13). https://doi.org/10.3390/ma14133549

Upadhayay, S., & Alqassimi, O. (2018). Transition from Linear to Circular Economy. *Westcliff International Journal of Applied Research*, *2*(2), 62–74. https://doi.org/10.47670/wuwijar201822oasu

Valerio, O., Misra, M., & Mohanty, A. K. (2018). Statistical design of sustainable thermoplastic blends of poly(glycerol succinate-co-maleate) (PGSMA), poly(lactic acid) (PLA) and poly(butylene succinate) (PBS). *Polymer Testing*, *65*, 420–428. https://doi.org/10.1016/j.polymertesting.2017.12.018

Ved Prakash Ranjan, & Goel, S. (2021). Recyclability of polypropylene after exposure to four different environmental conditions. *Resources, Conservation and Recycling*, *169*, 105494. https://doi.org/10.1016/j.resconrec.2021.105494

Wang, Y., Na, B., Fu, Q., & Men, Y. (2004). Shear induced shish–kebab structure in PP and its blends with LLDPE. *Polymer*, *45*(1), 207–215. https://doi.org/10.1016/j.polymer.2003.10.020

Yang, Y., Boom, R., Irion, B., Heerden, van, Kuiper, P., & Wit, de. (2012). Recycling of composite materials. *Delft Skyline Debate*, *51*, 53–68. https://doi.org/10.1016/j.cep.2011.09.007

APPENDIX A

TENSILE STRESS-STRAIN CURVE ON r-PP/LDPE BLEND

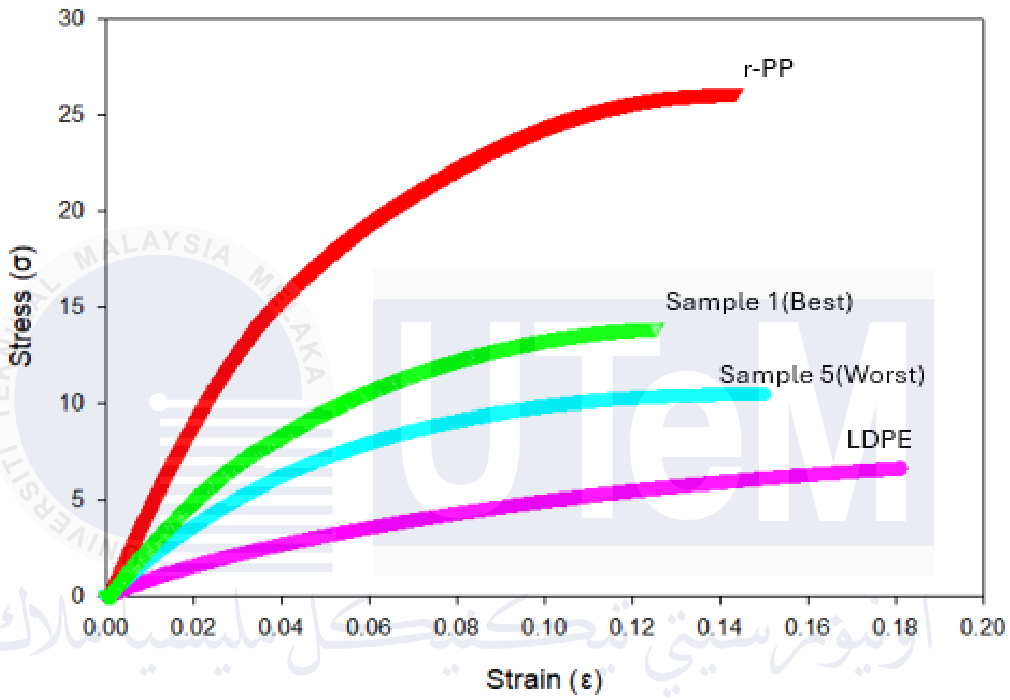

APPENDIX B

TENSILE STRESS-STRAIN CURVE ON r-PP/LDPE/GNPs BLEND

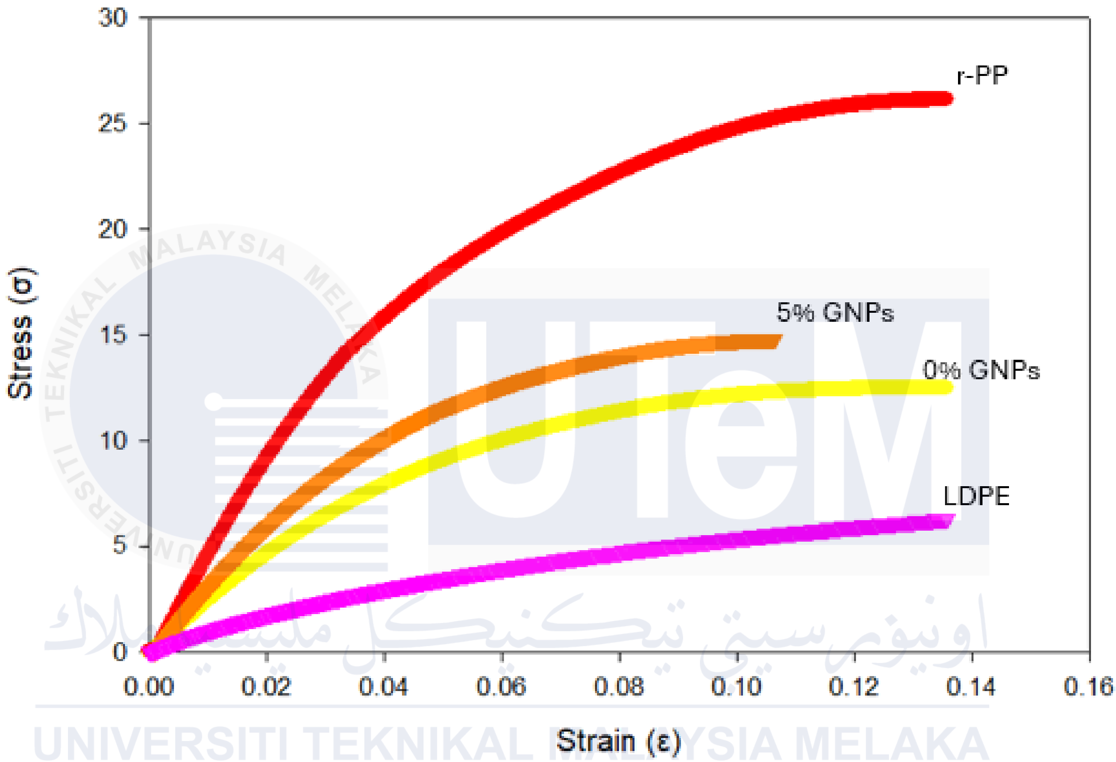

APPENDIX C

GANTT CHART PSM 1

No	Task Description		Week 1	Week 2	Week 3	Week 4	Week 5	Week 6	Week 7	Week 8	Week 9	Week 10	Week 11	Week 12	Week 13
1	Registration	Planned													
		Actual													
2	Briefing of Final Year Project 1	Planned													
		Actual													
3	Collecting data from journals, articles and other sources	Planned													
		Actual													
4	Chapter 1: Introduction	Planned													
		Actual													
5	Chapter 2: Literature Review	Planned													
		Actual													
6	Chapter 3: Methodology	Planned													
		Actual													
7	Draft submission	Planned													
		Actual													
8	Presentation	Planned													
		Actual													
9	Final report submission	Planned													
		Actual													

APPENDIX D

GANTT CHART PSM 2

No	Task Description		Week 1	Week 2	Week 3	Week 4	Week 5	Week 6	Week 7	Week 8	Week 9	Week 10	Week 11	Week 12	Week 13	Week 14	Week 15
1	Project title exchange registration	Planned															
		Actual															
2	Briefing of Final Year Project 2	Planned															
		Actual															
3	Experimenting and Characterization	Planned															
		Actual															
4	Chapter 4: Result and Discussion	Planned															
		Actual															
5	Chapter 5: Conclusion and Recommendation	Planned															
		Actual															
6	Presentation	Planned															
		Actual															
7	Draft Submission	Planned															
		Actual															
8	Final report submission	Planned															
		Actual															
9	Technical report	Planned															
		Actual															